ELECTRON PARAMAGNETIC RESONANCE STUDIES OF FERRIC IONS IN MYOGLOBIN

by

R.H. FARROW, M.Sc.

Being a thesis submitted to the University of Keele for the Degree of Doctor of Philosophy.

- - - -

Department of Physics,
University of Keele,
Keele, Staffordshire.

March, 1971.

ABSTRACT

This thesis reports investigations of the protein molecule myoglobin by means of electron paramagnetic resonance and supplemented by optical absorption measurements.

Certain ions can be attached to the sixth coordination point of the iron atom in the haem site of the myoglobin molecule. Attachment of these ions causes the iron ion to be in either the ferric or ferrous state. Several ferric types (or derivatives) of myoglobin are studied at microwave frequencies of 35 GHz and 70 GHz.

The spin state of the iron can be either low ($S = \frac{1}{2}$) or high ($S = \frac{5}{2}$). It is found that the angular dependance of the 'high spin derivative' spectra can be described by the spin Hamiltonian :

$$= \beta \bar{B}.\bar{\bar{g}}.\bar{S} + D\,(S_z^2 - \tfrac{1}{3} S(S+1)) + E(S_x^2 - S_y^2)$$

where D is very large $\sim 5\ cm^{-1}$

and E is very small $\sim 0.01\ cm^{-1}$

Since D is very large only the transition between the energy levels of the lowest Kramer's doublet is observed using normal microwave frequencies. It is possible to use a simplified spin Hamiltonian to describe the angular variation of the spectra. This is :

$$= \beta \bar{B}.\bar{\bar{g}}_{eff}.\bar{S}$$

where g_{eff} is the effective g-value.

Angular variation measurements of single crystals of the fluoride derivative (F^-) yield effective g-values

$$g_x = 5.85, \quad g_y = 5.98, \quad g_z = 2.00, \pm 0.005$$

and the z axis of the g-tensor system is found to be 5^o away from the normal to the haem plane. Measurements on the paste spectrum of the fluoride derivative at Q-band determined g-values $g_x = 5.85$, $g_y = 6.03$, ± 0.01.

Myoglobin formate HCO_2^- was found to produce two separate spectra whose effective g-values were $g_x = 5.52$, $g_y = 5.94$ and $g_x = 5.87$, $g_y = 6.06$. Other derivatives studied in paste form at Q-band were acid-met (H_2O) and cyanate (OCN^-) and their respective effective g-values were $g_x = 5.87$, $g_y = 5.99$ and $g_x = 5.72$, $g_y = 5.98$. The cyanate derivative when studied at 4.2^oK appeared to exist in two forms, one being high spin and the other low spin. Yet optical absorption measurements at room temperature show that it is essentially in the low spin state.

Two methods were used to determine the zero field splitting parameter D. Firstly, from the variation of the intensity of the g = 6 absorption line with temperature, and secondly, the dependance of the effective g-values on microwave frequency. The values found are significantly lower than those determined by other workers. It was found that the intrinsic linewidth of the e.p.r. signal in the case of a paste spectrum increased linearly with microwave frequency.

ACKNOWLEDGMENTS

The author wishes to express his gratitude to the following :

Professor D.J.E. Ingram for providing research facilities in his department.

Dr E.F. Slade for guidance and supervision throughout the course of this work.

Dr. P. Weightman and Mr B.J. Munday for their assistance with computation and for use of their computer programmes.

Mrs B. Haywood for her care and patience in typing this thesis.

Mr. W. Brearley for undertaking the photographic work and, together with the technical staff of the Physics Department, for general assistance.

Mr. G. Dudley and other members of the Department Workshop for their aid with the construction of apparatus.

Other members of the Magnetic Resonance Group for helpful discussions.

The Science Research Council for kindly providing a maintenance grant during the two years in which the research was undertaken.

CONTENTS

CHAPTER I

INTRODUCTION

This thesis is a study of the active centre (haem group) in the protein molecule myoglobin by electron paramagnetic resonance and supplemented by optical absorption measurements. Electron paramagnetic resonance (e.p.r.) discovered in 1945[1], has now reached a highly sophisticated level. It is essentially high resolution spectroscopy using microwave frequencies between 10 and 100 GH_z. Microwave power incident on a paramagnetic system can stimulate transitions between the Zeeman levels, the splittings of which are altered by the magnitude of an applied magnetic field. From detection of the absorption of microwave power it is possible to obtain important information concerning the paramagnetic system.

Myoglobin is a protein molecule of molecular weight 17000. Its function is to act as a temporary store of oxygen in the muscles of vertibrate animals. Diving birds and sea mammals contain large amounts of myoglobin and these investigations were made on myoglobin from sperm whale. Oxygen is transported around the body in the blood by haemoglobin. A myoglobin molecule will accept one oxygen molecule from haemoglobin which it will hold until the oxygen partial pressure in the muscle tissues descends to a certain level. It will then release the oxygen molecule as the affinity for oxygen is affected by the ambient partial pressure of oxygen.

Chromatography and X-ray studies have shown that the myoglobin molecule is composed of a single polypeptide chain of 153 amino acids. Extensive X-ray diffraction studies have been made by J.C. Kendrew et al[2-6] down to 1.4 Å resolution. Extreme difficulties were encountered in the analysis of the Laue diffraction pattern from a single crystal of myoglobin. The problem was in determining the phase of the radiation diffracted from atoms within the molecule which contributed to a Laue fringe pattern. The solution to the problem was a modification of a technique devised by Perutz, that was later used for the analysis of haemoglobin, called isomorphous replacement. This technique involves attaching a heavy atom, such as mercury, to certain known atoms of the protein molecule. Comparison of the Laue fringes with and without the heavy atom attached give unambiguous values for the phase. By this method three dimensional fluctuations in electron density were plotted at a series of imaginary sections cut through the molecule. These electron densities were plotted on thin perspex sheeting and stacked on top of one another thus showing the electron density throughout the molecule. Initial investigations at 6 Å resolution revealed the presence of rods penetrating the structure and having a similar cross sectional dimension to Pauling's α - helix. These rods were interwoven throughout the molecule in a complex way. Later analysis at 2 Å resolution, involving analysis of 10,000 Laue diffraction spots, showed rods in the shape of a helix with side chains. The dimensions of this helix were found to be very similar to the

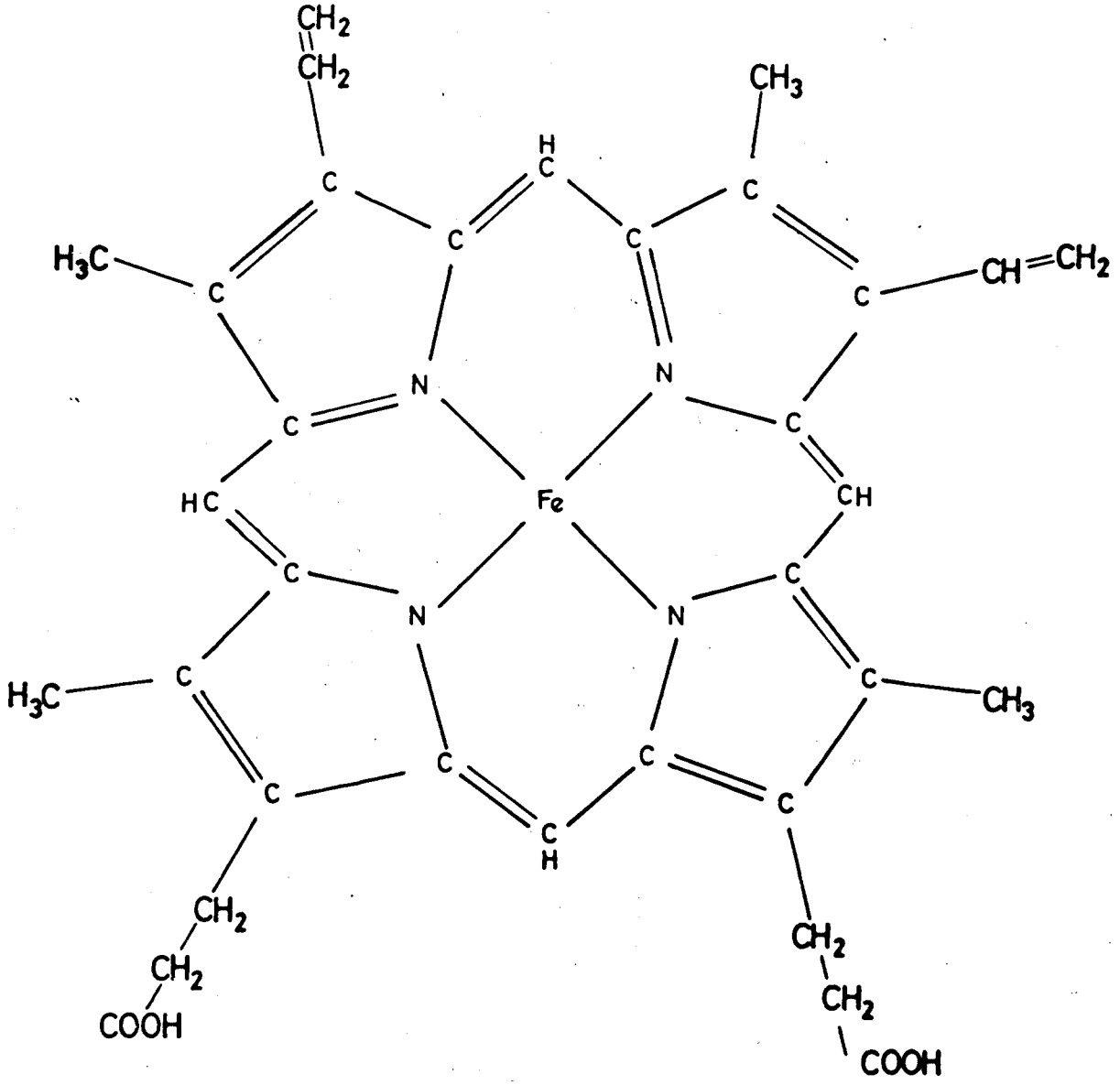

Fig 1.1. CHEMICAL FORMULA OF HAEM GROUP

α - helix. It was deduced that the α - helix is the basis of globular as well as fibrous proteins. Xray diffraction has been completed to 1.4 Å resolution which has revealed the positions of every atom in the molecule.

The haemoglobin molecule, the structure of which has been analysed by M.F. Perutz[7-10], is found to consist of two pairs of dissimilar helices all intertwined. One pair are similar in structure to myoglobin, being α helices, whilst the other pair are called β - helices. Therefore, knowledge of the structure and functional mechanisms of myoglobin is particularly useful as the molecule may be treated as a model for more complex haem proteins such as haemoglobin.

Each of the helices or chains in haemoglobin contain an iron atom, as does a myoglobin molecule and it is to this atom an oxygen molecule becomes attached. The iron atom is located in a porphyrin structure as shown in Fig. 1. In the haem plane four nitrogen atoms are seen to be attached to the iron atom. Below the haem plane a nitrogen atom of a histidine amino acid group and vertically above the plane an oxygen molecule form the fifth and sixth ligands of an octahedral complex. When deoxygenated, of course, the sixth coordination point is vacant. It is this small part of the molecule, the haem group, which forms the active centre of myoglobin that is of interest in e.p.r. studies. The remainder of the molecule can only be investigated, by this means, through its effect upon the environment of the iron ion in the porphyrin group.

Iron in myoglobin and haemoglobin is in a ferrous state (Fe^{2+}) when it is oxygenated or deoxygenated. The electron configuration is thus $(3d)^6$ but contrary to Hunds rules, the oxygenated form is diamagnetic[11]. In the deoxygenated state there is a resultant spin S = 2 but e.p.r. has not been observed from myoglobin in this state. Moreover it is possible to reduce the iron atom to the ferric state (Fe^{3+}) by attachment of various ions onto the haem group at the sixth coordination point in place of oxygen. The configuration is now $(3d)^5$ which results in a ground state of $^6S_{\frac{5}{2}}$ ($S = {}^5/_2$) when the sixth ligand is essentially ionically bound to the iron atom. If the bonding is more of a covalent nature a low spin form ($S = \frac{1}{2}$) results. The high spin form has a characteristic e.p.r. spectrum of a single resonance line resulting from a transition between the $m_s = \pm \frac{1}{2}$ levels, with a large g value variation between 2, when the magnetic field is parallel to the magnetic z axis, to 6, when the field is in the xy plane. In the low spin form the axial symmetry, inherent in the high spin case is lost. An angular variation of g values between approximately 1.5 and 2.8 is found. In a single crystal of myoglobin the linewidth varies with orientation of the magnetic axes with respect to the magnetic field being a minimum when the field is in the xy plane, which is found to be the haem plane. Linewidths are large as a result of inhomogeneous broadening due to misorientations of the haem planes within a crystal.

When the iron ion is changed to the ferric state the molecule is said to be in the met form. Met-myoglobin and

haemoglobin occur within the body when nitrites and nitrates combine reversibly with the haem group. Certain ions such as cyanide become so strongly attached that the process is irreversible. Molecules in the met form are incapable of transporting oxygen and they remain in the system, ineffectual in the respiratory process, until they either are naturally replaced or revert to the ferrous state. Congenital met haemoglobinae occurs in certain people where the amino acid sequence of the molecule is disturbed. Such a disease often causes cyanosis, a blue colouring of the skin.

It is comparatively easy to exchange the ligand at the sixth coordination point of the haem group in myoglobin in vitro and thus to study changes in the haem environment. From changes produced in the e.p.r. and optical spectra it is possible to investigate the symmetry of the iron atom and its immediate surroundings and hopefully to relate this to the function of the protein. The mechanism by which oxygen binds to myoglobin is still not understood nor even is the orientation of the O_2 molecule relative to the haem plane known. The strange phenomena in haemoglobin of cooperative ligand binding, in which the four haem groups in a molecule simultaneously attach an oxygen molecule and again simultaneously release them at the appropriate time, still remains unexplained.* Unfortunately the diamagnetic oxygen derivative cannot be studied by e.p.r. but there are many paramagnetic derivatives, which naturally can be investigated. Studies of the lowest lying energy levels of such derivatives as are available for spectroscopic investigations are very important

* since starting the writing of this thesis this mechanism has been explained by Perutz.

if the nature of this unique chemical bond between O_2 and Haemoglobin is to be understood.

The lowest lying energy levels of the ferric ion in the high spin form have an unusually large splitting in zero magnetic field and the mechanism for such splittings is not very well understood. Careful measurements of the exact magnitude of such splittings are essential if an effective theoretical explanation is to be developed. The establishment of a suitable theory for these large splittings would be one step nearer to an understanding of the function of these complex molecules.

Studies have been made on the angular variation of g values in single crystals of myoglobin and the directions of the magnetic axes have been determined for the fluoride derivative. Estimates of the large zero field splittings for certain high spin derivatives have been made by two methods. The first is by a measurement of the g value variation as a function of applied magnetic field, and the second method is an intensity variation study of the g = 6 signal as a function of temperature. Finally the optical spectra of various derivatives were measured which together with the e.p.r. spectra of the pastes of these derivatives indicate that high spin and low spin forms exist together in thermal equilibrium.

REFERENCES

1. E. Zavoiski, J. Phys. U.S.S.R. 9, 211, 1945.
2. J.C. Kendrew, Proc. Roy. Soc. A201, 62, 1949.
3. J.C. Kendrew, R.G. Parrish, Nature 174, 946, 1954.
4. J.C. Kendrew, P.J. Pauling, Proc. Roy. Soc. A237, 255, 1956.
5. J.C. Kendrew, R.G. Parrish, Proc. Roy. Soc. A238, 305, 1956.
6. J.C. Kendrew et al, Nature 185, 422, 1960.
7. M.F. Perutz, Proc. Roy. Soc. A195, 474, 1949.
8. J. Boyes-Watson, et al, Proc. Roy. Soc. A191, 83, 1947.
9. M.F. Perutz, et al, Nature 185, 416, 1960.
10. M.F. Perutz, Science, 140, May 1963.
11. J.S. Griffith, Proc. Roy. Soc. A235, 23, 1956.

CHAPTER II

BASIC THEORY AND TECHNIQUES OF ELECTRON PARAMAGNETIC RESONANCE.

2.1 Introduction

In order for e.p.r. to occur it is necessary for the electrons on the atoms being studied to have a resultant angular momentum. The angular momentum may arise from orbital motion of the electrons or from their intrinsic spin. When the electrons of a free atom or ion have resultant angular momentum then they possess a permanent magnetic dipole moment given by

$$\bar{\mu} = \gamma \bar{G} \qquad 2.1$$

where μ - magnetic dipole moment

G - angular momentum in units of h

γ - magnetogyric ratio

Using a classical picture it can be shown that[1], in the presence of an applied magnetic field, the magnetic moment will precess around the applied magnetic field with the Larmor frequency given by

$$\bar{\omega} = - \gamma \bar{B} \qquad 2.2.$$

Resonance will occur if an oscillating field is applied with a frequency the same as the Larmor frequency. If magnetic fields up to 1 tesla (10 Kg) are used then the corresponding frequencies of the applied radiation will be in the microwave range.

E.P.R. has been used to investigate many systems. Certain ions in crystals have partly filled orbital shells and hence have a permanent dipole moment due to either orbital or spin angular momentum or both. These ions are from the 3d, 4d, 4f, 5d and 5f transition groups and e.p.r. has yielded valuable information concerning the symmetry, valency and bonding of such ions. In free radicals the electrons are usually delocalised and therefore their dipole moment is due to spin angular momentum. Similar resonances occur in both conductors, due to conduction electrons, and unpaired electrons, associated with donor or acceptor atoms, in semiconductors where the orbital angular momentum can be considered to be zero.

2.2. Paramagnetism

The permanent magnetic dipoles associated with the resultant angular momentum of the electrons of an ion is given by

$$\bar{\mu} = \gamma \bar{G} \qquad 2.3.$$

where $$\gamma = - g \left(\frac{e}{2m_o}\right)$$

e, and m_o are the charge and mass of an electron and g is a pure number whose value depends on the relative contributions of orbit and spin to the total angular momentum.

If the only contribution to the angular momentum is from the orbital motion of the electrons then g = 1

and $$\bar{G} = \hbar \bar{L} \qquad 2.4$$

where $\bar{L}$ is the quantum number of the orbital momentum

If only spin angular momentum is present we can write

$$\bar{G} = \hbar \bar{S} \qquad \text{and} \quad g = 2 \qquad 2.5$$

$\bar{S}$ is the quantum number of the total spin momentum.

When both orbital and spin angular momentum are present then the value of g depends on the way in which the two are coupled. When LS coupling is applicable the resultant angular momentum is associated with quantum number $\bar{J}$, where $\bar{J} = \bar{L} + \bar{S}$ and g is given by the Lande g factor

$$g_J = {}^3/_2 + \frac{S(S+1) - L(L+1)}{2J(J+1)} \qquad 2.6$$

Then the resultant electronic magnetic dipole moment is

$$\bar{\mu}_J = - g_J \beta \bar{J} \qquad 2.7$$

where $\beta = \frac{e\hbar}{2m_o}$ is the Bohr magneton

$$\beta = 0.9273. \ 10^{-23} \text{ ampere - metre}^2$$

The units adopted throughout this thesis are the S.I. system which has gained international acceptance. The system is based on the six basic units metre, kilogramme, second, ampere, degree Kelvin and candela. The familiar unit for magnetic flux density, the gauss, is replaced by the tesla.

$$1 \text{ tesla} = 10^4 \text{ gauss}$$

Equation 2.7 is valid if we can ignore any interactions that would admix states of different $\bar{J}$. This means that the energy associated with interactions, such as the Zeeman interaction with an external field, must be small compared with the energy

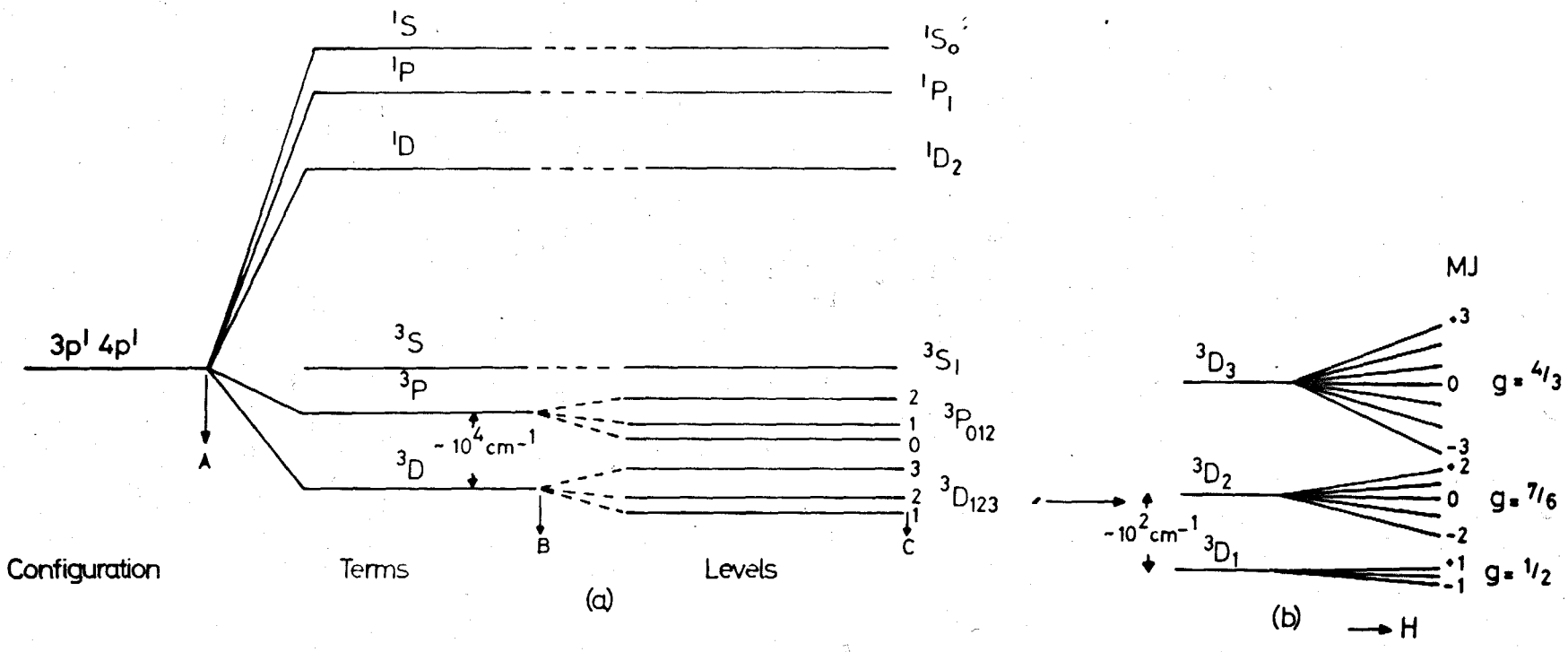

Fig. 2.1. (a) Schematic Illustration of the energy levels of a configuration $3p^1\,4p^1$ when Russell-Saunders coupling holds.
(b) Zeeman splitting of ground state triplet ^3D.

differences between levels of different J. These energy levels are split by spin-orbit coupling which can be represented by a term

$$\mathcal{H}_{so} = \lambda \bar{L}.\bar{S}. \qquad 2.8$$

Therefore if any interaction, including the Zeeman interaction, is larger than or of the same order as the spin-orbit interaction the Lande g factor is no longer applicable. In some rare earth ions in solids, where the unpaired electrons are screened from the lattice, this is still applicable but for 3d ions in a solid, where the unpaired electrons are in the outer shell, the crystalline electric field has a larger interaction energy than the spin-orbit coupling and hence equation 2.7 is no longer valid.

Fig. 2.1. shows, for illustration purposes, the energy levels associated with a free atom with a configuration $3_p{}^1\ 4_p{}^1$. Initially electrostatic interaction between electrons (coulomb and exchange) couples the orbital angular momenta of the individual unpaired electrons and similarly the spin angular momenta of the unpaired electrons according to the Russell-Saunders coupling scheme. The ground term is found by Hund's rules to be ^3D. Spin-orbit interaction further splits the terms into levels according to the total angular momentum quantum number J. The separation between successive levels is given by

$$W_J - W_{J-1} = \lambda J \qquad 2.9$$

which is known as the Landé interval rule. The level with the

smallest value of J lies lowest if the shell is less than half filled but is highest when the shell is more than half filled. Finally the magnetic interaction

$$\beta\ \bar{B}.(\bar{L} + 2\ \bar{S}) \qquad 2.10$$

is treated as a perturbation upon the levels. This splits each level into (2J + 1) Zeeman levels.

Hyperfine Structure -

In a free atom or ion which has a resultant electronic angular momentum $\bar{J}$, and nuclear spin $\bar{I}$, the two are generally coupled together through the magnetic interaction between the electronic and nuclear dipole moments. Within a manifold of given J this usually takes the form

$$\mathcal{H} = a(\bar{J}.\bar{I}) \qquad 2.11$$

this couples $\bar{J}$ and $\bar{I}$ together to form a set of levels with quantum numbers

$$F = (J + I) \ldots . (J - I) \qquad 2.12$$

The separation beteen successive levels is

$$W_F - W_{F-1} = a\ F \qquad 2.13$$

The hyperfine interaction energy is usually very small being $\sim 10^{-1}$ cm^{-1} and is smaller than the Zeeman energy thus $\bar{I}$ and $\bar{J}$ will not couple to form $\bar{F}$. The hyperfine interaction must be considered as a perturbation upon the electronic Zeeman levels. In the strong field limit (the Back-Goudsmit region) the

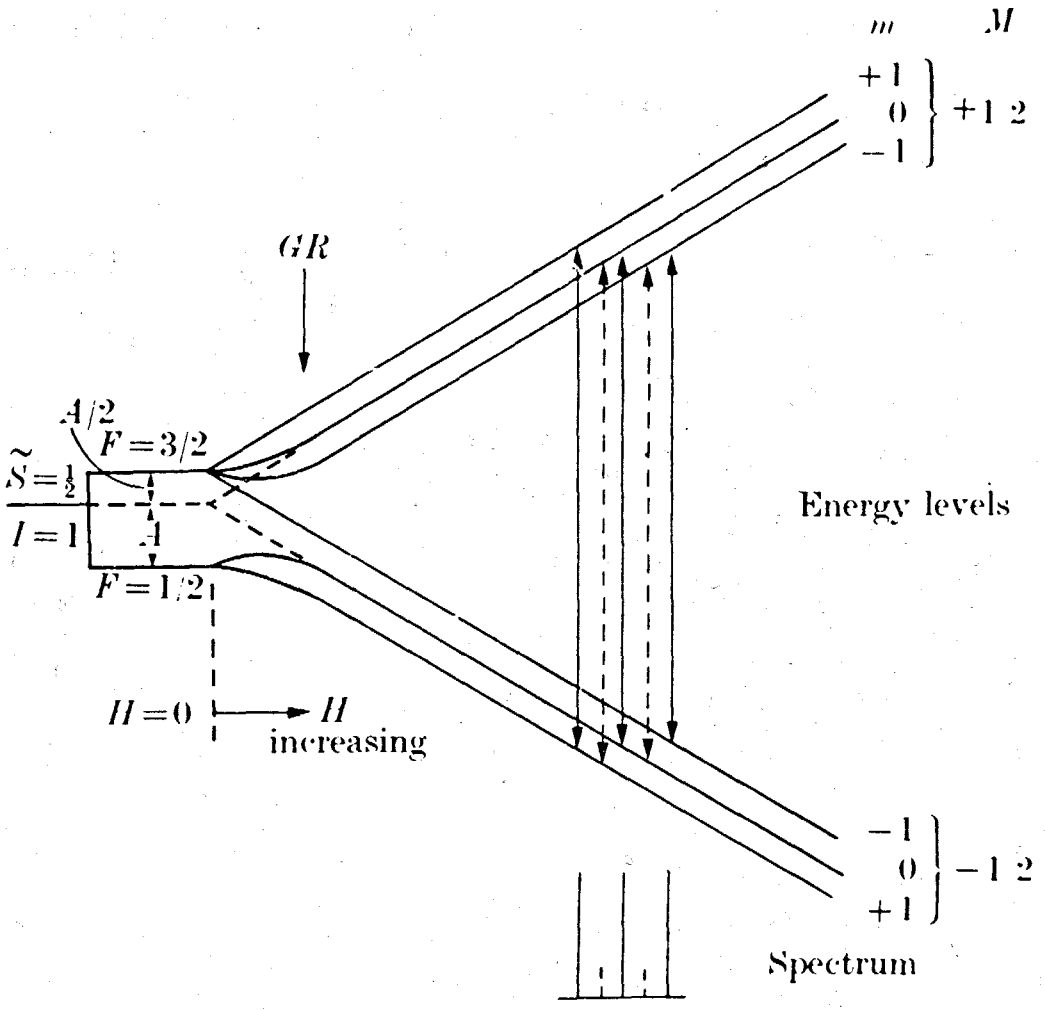

FIG. 2. 2. Energy levels and allowed transitions for $\tilde{S} = \frac{1}{2}$, $I = 1$ for the Hamiltonian (with no anisotropy)

$$\mathscr{H} = g\beta(\mathbf{H} \cdot \tilde{\mathbf{S}}) + A(\tilde{\mathbf{S}} \cdot \mathbf{I}).$$

electronic moment precesses about the external field independantly of the nuclear moment. Therefore the magnetic hyperfine interaction results in a magnetic field of the nucleus whose steady component $\bar{B}e$ is parallel to the external field $\bar{B}$. The nuclear moment then precesses about $(\bar{B} + \bar{B}e)$. Conversely the nuclear moment generates a magnetic field and the electronic moment precesses about the combined field $(\bar{B} + \bar{B}n)$.

Then from the magnetic hyperfine energy $a(\bar{J}.\bar{I})$, if B is along the z axis

$$a\ Jz\ Iz = g_J\ \beta\ Jz\ Bn = -\ g_I\ \beta\ Iz\ Be \qquad 2.14$$

then for the electrons

$$We = g_J\ \beta\ Jz\ (B + Bn) \qquad 2.15$$

where since Bn is proportional to Iz, it has $(2I + 1)$ values, equally spaced.

Similarly for the nucleus

$$Wn = -\ g_I\ \beta\ Iz\ (B + Be) \qquad 2.16$$

where since Be is proportional to Jz, it has $(2J + 1)$ values, equally spaced.

The hyperfine splitting for an ion with $\bar{S} = \frac{1}{2}$ and I = 1 is shown in Fig. 2.2.

2.3. Magnetic Resonance

When a magnetic dipole $\bar{\mu}$ is placed in a magnetic field the interaction between them can be represented by the Hamiltonian

$$\mathcal{H} = -\ \bar{\mu}.\bar{B} \qquad 2.17$$

for a free atom the electronic magnetic dipole moment is from 2.7

$$\bar{\mu}_J = - g_J \beta \bar{J} \qquad 2.18$$

Thus the Hamiltonian for the Zeeman interaction of the dipole moment $\bar{\mu}_J$ with $\bar{B}$ is

$$\mathcal{H} = - (\bar{\mu}_J . \bar{B}) = g_J \beta (\bar{B} . \bar{J}) \qquad 2.19$$

The vector $\bar{J}$ has $(2J + 1)$ values corresponding to the different projections of this vector in the direction of the applied magnetic field $\bar{B}$. Therefore the $(2J + 1)$ degeneracy of level J is lifted in the field and the energy of each component M_J is given by :-

$$W_M = g_J \beta B M_J \qquad 2.20$$

From quantum mechanics it is found that transitions between the component levels designated by M_J are allowed when $\Delta M_J = \pm 1$. Therefore such transitions require an energy quantum

$$h\nu = g_J \beta B \qquad 2.21$$

This applies to free atoms where one is dealing with a group of $(2J + 1)$ levels that are well separated from other levels. In the solid state this is far from the case and the theory has to be modified as will be seen in Chapter 3. Transitions between the Zeeman levels are stimulated by an oscillating magnetic field of frequency ν. It is now necessary to consider the quantum mechanical conditions for stimulation of transitions between the Zeeman levels by an applied oscillatory magnetic field.

Consider an oscillatory magnetic field applied in a plane normal to $\bar{B}$, the static magnetic field, with components Bx, By. This introduces an additional perturbation described by the Hamiltonian

$$\mathcal{H}^1 = - (Bx\ \mu x + By\ \mu y) \qquad 2.22$$

The oscillatory field can be represented by a rotating field with components $Bx = B_1 \cos \omega t$, $By = B_1 \sin \omega t$, this can be written as

$$\mathcal{H}^1 = - \tfrac{1}{2} B_1 [\mu+ \exp(-i\omega t) + \mu- \exp(i\omega t)] \qquad 2.23$$

where $\mu+ = \mu_x + i\mu_y$, $\mu- = \mu_x - i\mu_y$

Time dependent perturbation theory must be applied since $\mathcal{H}^1$ is oscillatory.

The Schroedinger equation is

$$(\mathcal{H} + \mathcal{H}^1)\ \Psi = - \frac{h}{i} \frac{d\Psi}{dt} \qquad 2.24$$

Now the wavefunctions can be expressed as a series involving the complete set of orthogonal wave functions for the unperturbed system Un at time t

$$\Psi(t) = \Sigma_n\ a_n(t)\ Un \exp\left(-i \frac{Wn\ t}{h}\right) \qquad 2.25$$

where Wn is the energy of the nth state and a_n is the amplitude of this base state n in the wavefunction Ψ

Substituting 2.25 into the Schroedinger equation 2.24 yields the relation

$$\frac{da_m(t)}{dt} = (ih)^{-1} \Sigma_n \mathcal{H}mn(t)\ a_n(t) \exp\left[i \frac{(Wm - Wn)}{h} t\right] \qquad 2.26.$$

These are a set of simultaneous differential equations in the function a_m (t) where $\mathcal{H}_{mn}$ is the expectation value (matrix element) of the oscillatory perturbation between the base states m and n.

$$\text{i.e. } \mathcal{H}_{mn} = \langle Um|\mathcal{H}^1|Un\rangle \qquad 2.27$$

Now for the oscillatory perturbation ^{1} (equation 2.23) the only finite matrix elements are those between states M and M $\pm$ 1, which are

$$\langle M+1|\,\mu+\,|M\rangle = \langle M+1|\gamma h J+\,|M\rangle = \gamma h\left[J(J+1) - M(M+1)\right]^{\frac{1}{2}}$$
$$\langle M-1|\,\mu-\,|M\rangle = \langle M-1|\gamma h J-\,|M\rangle = \gamma h\left[J(J+1) - M(M-1)\right]^{\frac{1}{2}} \qquad 2.28$$

giving rise to the selection rule $\Delta M = \pm 1$. M can refer to the projection on the magnetic field $\bar{B}$ of (a) $\bar{J}$, the total angular momentum or (b) $\bar{L}$, the orbital angular momentum, or (c) $\bar{S}$, the spin angular momentum.

If we assume that the system is initially in the state Jz = M, so all the coefficients a_n are initially zero except a_M, which is unity, then since $(W_M \pm 1 - W_M)/\hbar = \mp \gamma B$ for small values of the perturbation we have approximately

$$\frac{da_{M\pm1}}{dt} = \tfrac{1}{2}\, i\,\gamma\, B_1 \langle M\pm1|\, J\pm|\, M\rangle \exp\left[i((W_{M\pm1} - W_M) \mp \hbar\,\omega)\, t/h\right]$$
$$= \tfrac{1}{2}\, i\,\gamma\, B_1 \langle M\pm1|\, J\pm|\, M\rangle \exp\left[\mp i\,(\gamma\, B + \omega)\, t\right] \qquad 2.29$$

This can be integrated and yields for the probability $(a\,a^*)_{M\pm1}$ of finding the system in the state $M\pm1$ after a time t

$$(a\ a^*)_{M\pm1} = (\gamma\ B_1)^2\ \langle M\pm1|\ J\pm|\ M\rangle^2\ \frac{\sin^2 \frac{1}{2}(\gamma B + \omega)t}{(\gamma B + \omega)^2}$$

$$= (\gamma\ B_1)^2\ \langle M\pm1|\ J\pm|\ M\rangle^2\ \frac{\sin^2 \frac{1}{2}(\omega - \omega_L)t}{(\omega - \omega_L)^2} \qquad 2.30$$

If the resonance condition is satisfied exactly then

$$(a\ a^*)_{M\pm1} = (\gamma\ B_1)^2\ \frac{\langle M\pm1|\ J\pm|\ M\rangle^2}{4}\ t^2 \qquad 2.31$$

This refutes Einsteins theory for transitions which says that the transition probability increases linearly with time. In reality there are a large number of more or less identical systems. The levels are homogeneously broadened so that $\omega_m - \omega_n$ has a distribution of values. We define a line shape function $f(\omega)$ which describes the distribution of energy levels between which the transition is occurring. This is normalised by the condition

$$\int_0^\infty f\ (\omega)\ d\omega = 1 \qquad 2.32$$

The transition probability per unit time W is given by the time derivative $d(a\ a^*)/dt$ integrated over a distribution of Larmor frequencies

$$W = (\gamma\ B_1)^2\ \langle M\pm1|\ J\pm|\ M\rangle^2 \int_{-\infty}^{\infty} \frac{\sin(\omega - \omega_L)t}{2(\omega - \omega_L)}\ f\ (\omega_L)\ d\omega_L \qquad 2.33$$

$$W = \frac{\pi}{2}\ (\gamma\ B_1)^2\ \langle M\pm1|\ J\pm|\ M\rangle^2\ \ f\ (\omega) \qquad 2.34$$

Therefore time dependant perturbation predicts that if an oscillating magnetic field B_1 is applied to a paramagnetic sample perpendicular to the applied static field, transitions will occur between states differing in M by ± 1. Also the transition probability increases linearly with time and as the square of the field strength B_1. The frequency of B_1 must be approximately equal to the Larmor frequency ω_L, ω must be within the distribution $f(\omega)$.

The oscillating perturbation $\mathcal{H}^1$ was taken in the above analysis to be in the general form

$$\mathcal{H}^1 = \gamma\, h\, \bar{J}.\, \bar{B}_1 \qquad 2.35$$

A more useful form of this Hamiltonian for determining the transition probability of electrons belonging to ions in crystals is

$$\mathcal{H}^1 = \beta\, \bar{B}_1.g.\bar{S} \qquad 2.36$$

where g is a tensor.

If g and $\bar{S}$ are colinear we get, on expanding, the following

$$\mathcal{H}^1 = \beta\, \bar{B}_1.\, (g_x\, S_x + g_y\, S_y + g_z\, S_z) \qquad 2.37$$

The transition probability per unit time becomes

$$W = \frac{\pi^2\beta^2}{h^2}\ (\bar{B}_1.(\langle\psi_j|g_xS_x|\psi_i\rangle + \langle\psi_j|g_yS_y|\psi_i\rangle + \langle\psi_j|g_zS_z|\psi_i\rangle))^2\ f(\omega)$$

2.38

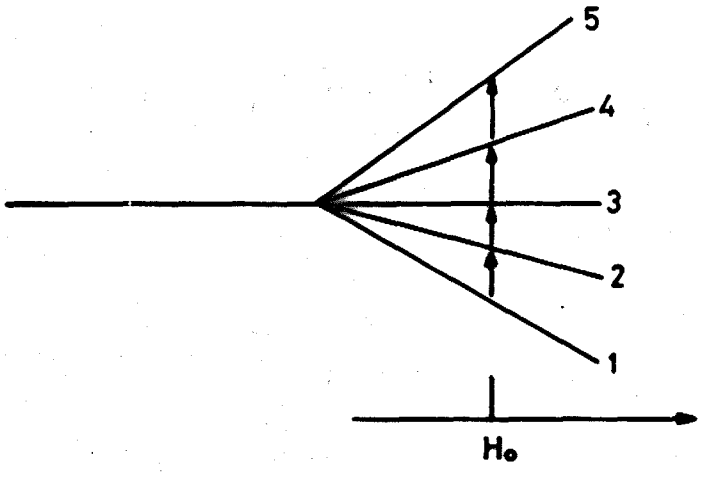

The population of each of the five levels is determined by the Boltzmann distribution function.

$$N_i = \frac{N g_i \exp(-W_i/kT)}{\sum_n g_i \exp(-W_i/kT)}$$

N_i is the population of the ith level.

W_i is the energy of the ith level.

g_i is the degeneracy of the ith level which equals unity in this case.

Fig. 2.3. Population distribution between Zeeman levels.

2.4. Thermal Equilibrium

From equation 2.34 it is seen that the transition probability for upward transitions, corresponding to absorption of energy, and for downward transitions, corresponding to emission of energy, are the same. Consider a two level system situated in a magnetic field B_o such that the resonance condition $h\nu = g\beta B_o$ is satisfied, $h\nu$ being the microwave quantum causing the transition. If the populations of the two levels are equal there will be no absorption of microwave energy as the absorption rate is equal to the emission rate. However the distribution of the atoms between levels 1 and 2 are given according to the Boltzmann equation

$$\frac{N_2}{N_1} = \exp(-h\nu/kT) \qquad 2.39$$

where N_1 and N_2 are the populations of levels 1 and 2. Therefore $N_1 > N_2$ so that there will be a net absorption of energy. We can write the rate equation for the change of population of the lower state in the presence of a microwave field as

$$\frac{dN_1}{dt} = N_2 W_{21} - N_1 W_{12} \qquad 2.40$$

Inspection of 2.34 shows that $W_{12} = W_{21}$ since

$$\langle M\pm1|\ J\pm|\ M\rangle^2 = \langle M|\ J\pm|\ M\pm1\rangle^2$$

and therefore $$\frac{dN_1}{dt} = W(N_2 - N_1) \qquad 2.41$$

where $W = W_{12} = W_{21}$

We can replace N_1 and N_2 by the total population N and the population difference n

$$N = N_1 + N_2$$

$$n = N_1 - N_2$$

The equation 2.41 becomes $\frac{dn}{dt} = -2Wn$ 2.42

The rate of change of population difference between the two levels is proportional to the population difference. If there is initially a population difference, it will eventually disappear due to the transitions induced by the applied radiation. Therefore resonance absorption would cease after a short while if there was not a means for atoms to return to the lower level in a non radiative way. Relaxation processes occur via interactions with lattice phonons providing such a mechanism.

2.5. Spin-Lattice Relaxation

In the absence of any microwave radiation the populations of levels 1 and 2 are given by the Boltzmann function. Now if the resonance transition between the two levels is saturated by the application of a large microwave field the populations N_1, N_2 will tend to equalise. When the radiation is removed the populations will revert back to their original level. Therefore, the relaxation probabilities for upward and downward transitions, by spin lattice effects, are not equal. It can be seen that

$$\frac{N_1}{N_2} = \frac{\omega_{21}}{\omega_{12}} = \exp \frac{h\nu_{12}}{kT} \qquad 2.43$$

where ω_{21} and ω_{12} are the downward and upward relaxation transition probabilities.

Taking into account the relaxation effect the rate equations for the two levels are

$$\frac{dN_1}{dt} = N_2 (W + \omega_{21}) - N_1 (W + \omega_{12})$$

$$\frac{dN_2}{dt} = - \frac{dN_1}{dt} \qquad 2.44$$

Using the same substitutions as in equation 2.42 we obtain

$$\frac{dn}{dt} = N(\omega_{21} - \omega_{12}) - n(2W + \omega_{21} + \omega_{12}) \qquad 2.45$$

Before considering the general solution of equation 2.45, we first use it to define the spin lattice relaxation time τ_1. Suppose the transition 1 →2 is saturated by a pulse of microwave power and we wish to know how n returns to its thermal equilibrium value n_o after the pulse. If at t = o, n = o and W = o it can be shown that the solution of 2.45 is

$$n = n_o\left[1 - \exp (- t/\tau_1)\right] \qquad 2.46$$

where $1/\tau_1 = (\omega_{21} + \omega_{12})$

This defines the spin lattice relaxation time for the two level system under consideration. When there are more than two levels, the effective relaxation time depends on a combination of all the ω_{1j} and it is no longer possible to define a unique time constant.

The steady state population differences between levels 1 and 2 can be found by putting $\frac{dn}{dt} = o$ in 2.45, this yields

$$n = N\left[\frac{\omega_{21} - \omega_{12}}{2W + \omega_{21} + \omega_{12}}\right] \qquad 2.47$$

it can be seen that

$$\frac{n}{n_o} = \frac{n(W)}{n(o)} = \frac{\omega_{21} + \omega_{12}}{2W + \omega_{21} + \omega_{12}} \qquad 2.48$$

$$\frac{n}{n_o} = \frac{1}{1 + 2W\,\tau_1} \qquad 2.49$$

If the term $2W\,\tau_1$ is small then the population difference between levels 1 and 2 will remain close to the thermal equilibrium value n_o. The expression 2.49 is the saturation condition, the full significance of which is appreciated by expanding W according to 2.38.

Taking the lineshape function to be Lorentzian

$$f(\omega) = \frac{2\tau_2}{1 + \tau_2^{\,2}(2\pi)^2\,(\nu-\nu_o)^2}$$

The parameter τ_2 is called the spin-spin or transverse relaxation time. In a paramagnetic system with identical spins there is a resonance interaction between these spins (dipole-dipole) which shortens the lifetime of the individual spin states through mutual spin flips. τ_2 is often defined as the average lifetime of a spin state. The line in such a case is said to be 'homogeneously broadened', the spins emit or absorb wave trains of finite length whose mean duration in time is τ_2 and whose probability distribution is of the form $\exp(-t/\tau_2)$.

For a two level system the transition probability is

$$\langle \tfrac{1}{2} | \; B_1 \, g_1 \, Sx | \; -\tfrac{1}{2} \rangle \;=\; \tfrac{1}{2} \, B_1 \, g_1$$

and

$$\frac{g\beta}{\hbar} = \gamma$$

then

$$W = \frac{1}{4} \gamma^2 \, B_1^{\,2} \, \frac{2 \, \tau_2}{1 + \tau_2^{\,2} (2\pi)^2 (\nu - \nu_o)^2} \qquad 2.50$$

At the centre of the line $\nu = \nu_o$ we obtain

$$\frac{n}{n_o} = \frac{1}{1 + \frac{1}{4} \gamma^2 \, B_1^{\,2} \tau_1 \, \tau_2} \qquad 2.51$$

Saturation is dependent on the intensity of the microwave power incident on the sample and therefore it is necessary to keep the power level low to avoid saturating the transition. The amount of power absorbed by a sample before saturation ensues will depend on the relaxation times τ_1 and τ_2.

2.6. Power Absorbed by Sample.

The rate of absorption of energy by a paramagnetic system is

$$\frac{dE}{dt} = n\ W.\ h\nu \qquad 2.52$$

This is at one specific frequency ν but we have already seen that absorption occurs over a range of frequencies and therefore we have to substitute a line shape function.

$$\frac{dE}{dt} = n.\ W\ h\nu\ f(\omega) = \frac{n\ \pi^2\ \beta^2}{h^2}\ h\nu\ f(\omega)\ \ \langle\psi_2|\ \bar{B}_1.g.\bar{S}|\ \psi_1\rangle^2 \qquad 2.53$$

Assuming that B_1 is sufficiently low so that saturation does not occur we can write the power absorbed by the sample at the centre of the resonance line as

$$\frac{dE}{dt} = \frac{N\ \pi^2\nu_o^2\beta^2\tau_2}{kT}\ \ \langle\psi_2|\ \bar{B}_1.g.\bar{S}|\ \psi_1\rangle^2 \qquad 2.54$$

where we have substituted $n \tilde{\simeq} \frac{1}{2}\ N\ \frac{h\nu_o}{kT}$ from equation 2.39 and used a Lorentzian lineshape function. The above applies to a two level system but it may be generalised for the case when the effective spin is S.

$$\left(\frac{dE}{dt}\right)_{max} = \frac{2N\pi^2\nu_o^2\beta^2\tau_2}{(2S+1)\ kT}\ |\langle\psi_m|\ \bar{B}_1.g.\bar{S}|\ \psi n\rangle|^2 \qquad 2.55$$

The power absorbed by a paramagnetic sample in an oscillating field $\bar{B}_1 \sin \omega t$ can be expressed in terms of a complex susceptibility

$$\chi = \chi^1 - i\ \chi^{11} \qquad 2.56$$

An applied field $B_1 \sin \omega t$ will induce a magnetisation in a paramagnetic sample of magnitude M.

$$M = \chi^{1} H_1 \sin \omega t - \chi^{11} H_1 \cos \omega t \qquad 2.57$$

where $B_1 = \mu\mu_o \bar{H}_1$

The energy of a magnetic moment $\bar{M}$ in a field $\bar{B}$ is $\bar{M}.\bar{B}$ per unit volume so the mean power absorbed by a sample of magnetisation M per cycle is given by

$$P = \int_o^{2\pi/\omega} B \, (dM/dt). \, dt$$

and the average rate of absorption of energy is $P/2\pi/\omega$ which on expanding is seen to be

$$\frac{dE}{dt} = \frac{\omega}{2\pi} \int_o^{\frac{2\pi}{\omega}} B_1 \sin \omega t \left[\omega \frac{B_1}{\mu\mu_o} \chi^{1} \cos \omega t + \omega \frac{B_1}{\mu\mu_o} \chi^{11} \sin \omega t \right] dt \qquad 2.58$$

$$\frac{dE}{dt} = \frac{\frac{1}{2} \omega \chi^{11} B_1^{2}}{\mu\mu_o} \qquad 2.59$$

The complex part of the susceptibility represents the power absorption when a paramagnetic system is passed through resonance whilst the real part corresponds to a change of phase. We can equate 2.59 with 2.55 and relate the absorptive component of χ to the microscopic parameters

$$\chi 11 = \frac{4\pi\nu_o N B^2 \tau_2 \mu\mu}{(2S + 1) \, kT} \, |\psi_m| \bar{b}.g.\bar{S} \mid \psi_n>|^2 \qquad 2.60$$

where b is a unit vector along B_1.

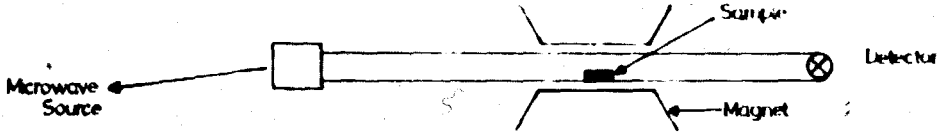

(a) Simple Transmission Spectrometer.

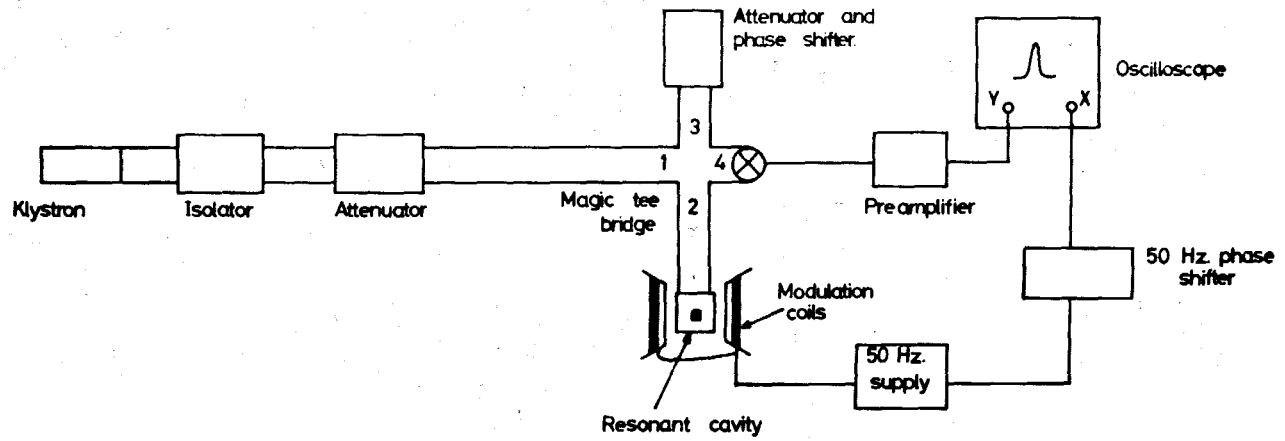

Fig. 2.4. (b) Crystal video detection using a reflection cavity.

The rate of absorption of microwave energy is dependant on the transition probability between levels m and n and the rate increases with frequency ν and with increasing values of τ_2.

2.7. Detection of E.P.R. Signals

From the above theory it can be seen that in order to produce e.p.r. essentially all that is required is a static magnetic field to cause the Zeeman splittings and a radio-frequency magnetic field, perpendicular to the static field, to induce transitions between the Zeeman levels. A means of detecting the absorption of the radiofrequency power will also be required in order to observe the resonance. A paramagnetic system can be tuned to resonance either by sweeping the magnetic field B with the microwave frequency fixed, or by varying the microwave frequency and keeping the magnetic field constant. In practice the former technique is preferable as microwave components have a narrow band width thus making frequency variations complicated whilst it is a relatively simple task to vary the field of an electromagnet.

A simple transmission spectrometer is shown in Fig. 2.4(a) consisting of a microwave source, waveguide, detector and magnet. If a paramagnetic sample is placed on one wall of the waveguide and is situated between the poles of the magnet, then as the magnetic field is increased a signal will be detected at resonance. At resonance the sample will absorb part of the microwave power which can be detected as a reduction in current from the output

of a crystal detector. Such a simple transmission system would not be sensitive enough for normal requirements.

A reflection spectrometer has twice the theoretical maximum efficiency of a transmission spectrometer as the power delivered to the sample can be increased without increasing the power arriving at the detector. Fig. 2.4(b) shows a simple reflection spectrometer incorporating a magic tee microwave bridge. When power is incident at the magic tee along arm 1 with arms 2 and 3 matched, the power will be equally divided between these two arms. Power will only arrive at the detector in the fourth arm of the bridge when there is a mis-match between the resonant cavity (arm 2) and the matching arm (3). To ensure that maximum absorption of microwave energy occurs the sample is placed in a resonant cavity with a circuit magnification factor $Q \sim 10^3 - 10^4$. Microwave power is supplied by a klystron to a magic tee bridge via an isolator and attenuator. The isolator prevents any reflected waves interfering with the frequency stability of the klystron and the attenuator controls the microwave power level.

The magic tee bridge is adjusted by balancing the real and reactive components of the wave in the second arm, containing the cavity, by means of an attenuator and phase shifter in the third arm. A completely balanced bridge will detect both absorption and dispersion, whilst any off balance in amplitude causes the bridge to be sensitive to absorption and similarly off balance in phase only will make the bridge sensitive to dispersion only.

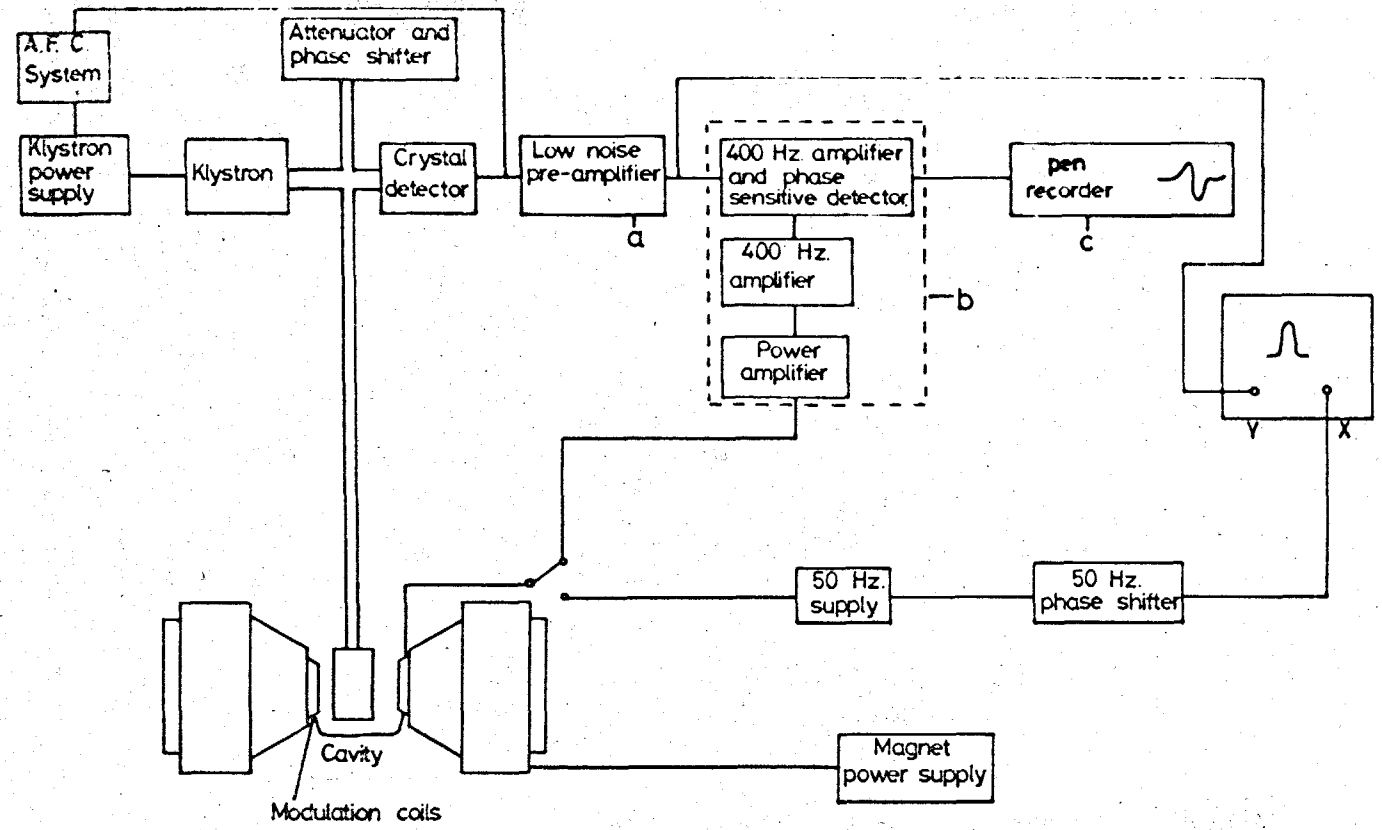

Fig. 2.5. Block diagram of 400 Hz modulation spectrometer using phase sensitive detection.

With crystal video detection the magnetic field is modulated at 50 Hz. The crystal detector output is fed to an oscilloscope, the time base of which is triggered at 50 Hz, so that either an absorption or dispersion signal can be directly displayed on the oscilloscope screen.

A block diagram of a spectrometer using 400 Hz modulation is shown in Fig. 2.5. In this system the sensitivity is much improved by the use of phase sensitive detection. The modulation amplitude used is less than the linewidth of the resonance so the first derivative of the absorption is observed as shown in Fig. 2.6. Absorption by the sample at resonance causes a change in the Q of the resonant cavity and this causes a mis-match between the second and third arms of the magic tee bridge. The crystal detects a signal at the modulation frequency(400 Hz,) and this is amplified by a narrow band pre-amplifier, and a narrow band amplifier, before entering a phase sensitive detector (P.S.D.). The P.S.D. is controlled by a reference signal at the modulation frequency. The phase difference between the output and reference signals is adjusted to be zero.

The components of any signal (noise) out of phase with the reference signal will be rejected. Finally the P.S.D. produces a d.c. output which is fed to a pen recorder. A modulation frequency of 400 Hz was used in the spectrometer employed for these studies, but the flicker noise of the crystal detector is high at such low frequencies, and this represents the limit to the sensitivity of this spectrometer. The noise of a crystal

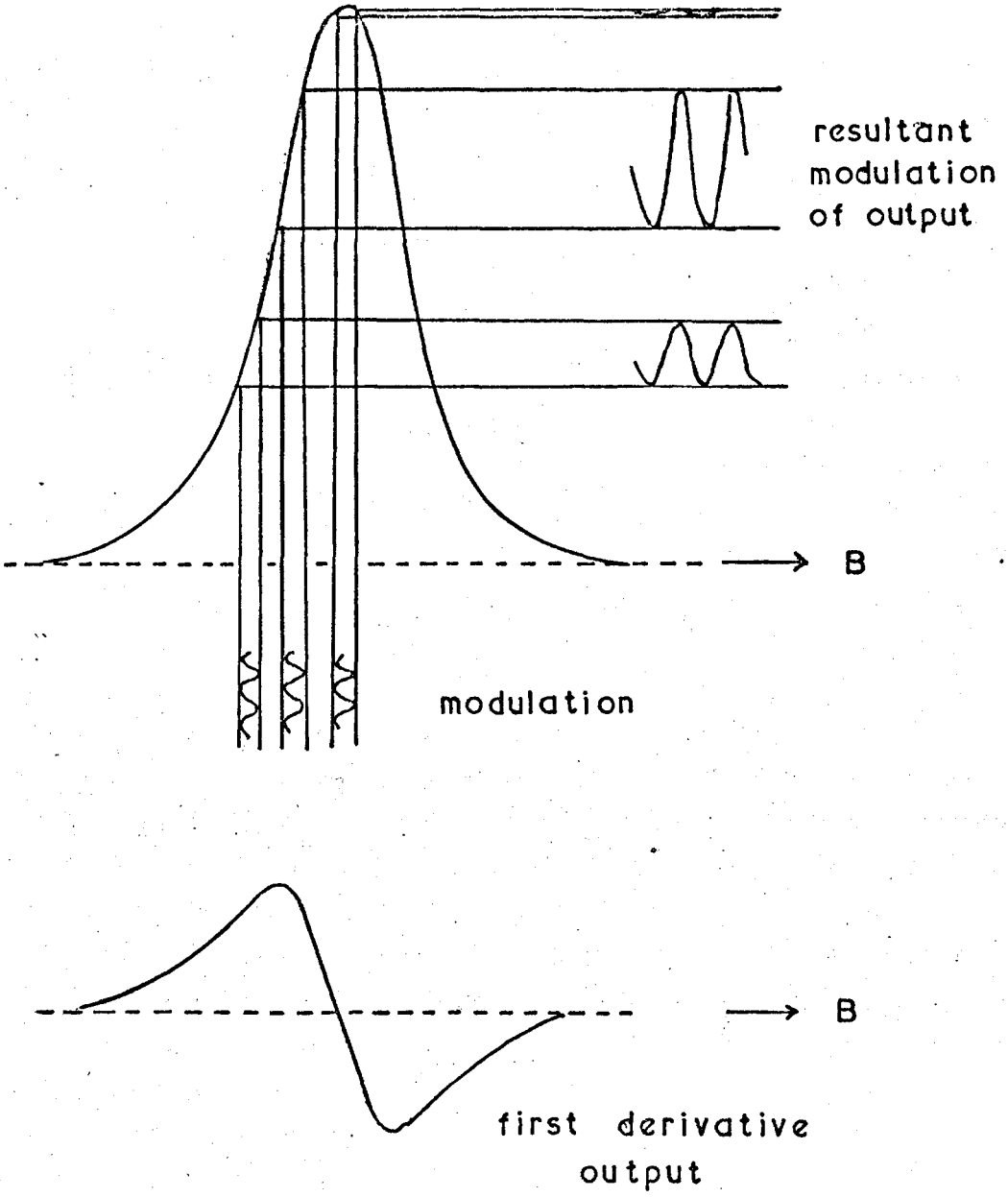

FIG. 2.6 FIRST DERIVATIVE OF ABSORPTION SIGNAL

detector is inversely proportional to the frequency and usually 100 K Hz modulation frequency is adopted.[2] This frequency is chosen to compromise between crystal noise and amplifier gain. A point contact crystal detector needs to be biassed since the conversion loss and noise output from such crystals are dependant on incident microwave power. Again an optimum level is found where these two effects are balanced which is around 1 mW of bias power. Biassing of the crystal imposes a restriction on the bridge system since at low powers there may be insufficient power available to bias the detector. This problem is overcome by using a bucking arm, where power is delivered separately to the crystal for biassing purposes rather than by unbalancing the bridge. A review of microwave circuits suitable for e.p.r. spectrometers has been given by Faulkner[3].

REFERENCES

1. B.I. Bleaney, B. Bleaney, Electricity and Magnetism, p574 O.U.P.
2. H.A. Buckmaster, J.C. Dering, Canadian J. Phys. 43, 1088, 1965.
3. E.A. Faulkner, Laboratory Practice, Nov., 1065, 1964.

CHAPTER 3

PARAMAGNETIC IONS IN CRYSTALS

3.1. Introduction

When atoms come together in the formation of a crystalline lattice there arise large forces between neighbouring atoms. These forces are mainly electrical in origin and their interaction must be added to the free ion Hamiltonian. The inclusion of this extra term will thus generate a new set of energy levels.

Although most free atoms have a permanent magnetic dipole moment it is found in the solid state that most substances consist of ions with closed shells of electrons and are therefore diamagnetic. However the 'transition elements' have a shell in the process of being filled. These elements have more than one chemical valency, and most of their ions of different valency are paramagnetic. In the lanthanide series the unfilled 4f shell is sheltered by outer electrons and hence interaction between the 4f electrons with the surrounding lattice is small. The paramagnetism of such ions is similar to free ions whilst in the iron group the unfilled 3d shell is exposed to the lattice and the interaction with the lattice considerably modifies the paramagnetic properties of these ions.

The effect of the diamagnetic environment upon an ion in a lattice is calculated by including this interaction in the free ion Hamiltonian. The Hamiltonian for this interaction can be calculated by using Crystal Field Theory. This theory

considers the paramagnetic ion to be surrounded by point charges which create a crystalline electric potential. Crystal field theory does not allow for any overlap of wavefunctions between the surrounding ligands and the paramagnetic ion but in many crystals there are covalent bonds between ions and in such cases Crystal Field Theory is inadequate. When covalency occurs the paramagnetic ion and its neighbours are treated as a unit and the eigenvectors are calculated by a linear combination of atomic orbitals. A general theory called 'Ligand Field Theory' allows for all interactions occurring between the ion and its neighbours and this approach includes cystal field theory and molecular orbital theory.

3.2. Crystalline Electric Field

The crystal field is an additional interaction which must be added to the free ion Hamiltonian. The eigenvalues of the general Hamiltonian for a free ion are evaluated by considering each term as a perturbation in order of diminishing interaction energy, and the ligand interaction must be introduced at the appropriate point relative to the sequence of interactions internal to the paramagnetic ion.

Consider first the Hamiltonian representing all the interactions within a free ion including interaction with a magnetic field. In order of diminishing interaction energy the Hamiltonian can be written :-

$$\mathcal{H} = \sum_i \frac{Pi^2}{2m} - \sum_i \frac{Ze^2}{r_i} + \sum_{i>k} \frac{e^2}{r_{ik}} + \sum_i \eta\, \bar{l}_i.\bar{s}_i + \sum_i \beta\, (l_i + 2S_i)\, \bar{B} \qquad 3.1$$

The first three terms account for the coulomb interaction of the electrons with the nucleus and mutual repulsion between electrons. In the Hartree Foch, or other approximation methods, an electron is considered to move in the coulomb field of the nucleus plus a potential due to an averaged electronic field with central symmetry due to the other electrons in the ion. This results in the electronic levels being grouped into configurations. The mutual electrostatic repulsion of the electrons, not represented by a central field, including exchange effects, give rise to LS coupling which splits each configuration into a series of terms of different LS. The separation between different terms is of the order $10^4 cm^{-1}$. This is called Russell-Saunders or LS coupling in which $L = \sum_i l_i$ and $S = \sum_i s_i$ are the quantum numbers defining a given term. The ground term is found by Hund's rule. This states that the term with

(a) maximum S,

(b) within the group of S_{max} the level with the largest value of L,

lies lowest. An example of the application of Hund's rules is given in Fig. 2.1. for the configuration 3p '4p' where the term $^3D(S = 1, L = 2)$ is the ground state.

The fourth term in 3.1 is the spin orbit coupling interaction which in the case of LS coupling may be written $\lambda \bar{L}.\bar{S}$. This splits a given term into a multiplet of levels of different values of J, the total angular momentum. $\bar{L}$ and $\bar{S}$ no

longer commute with the Hamiltonian whereas $\bar{J} = \bar{L} + \bar{S}$ does commute with $\mathcal{H}$. When operators commute there are simultaneous eigenstates, so if the angular momentum operators $\bar{L}$ and $\bar{S}$ commute with the Hamiltonian operator $\mathcal{H}$ the eigenvalues of $\mathcal{H}$ are also eigenvalues of $\bar{L}$ and $\bar{S}$ and therefore such eigenvalues can be designated by L and S. Thus when spin-orbit coupling is included in the Hamiltonian the resultant levels are designated by J. Finally the magnetic field interaction completely lifts the degeneracy of the multiplet levels into a series of Zeeman levels designated by M_J. The above analysis is only valid if LS coupling is applicable for the ion being considered. Sometimes the spin-orbit interaction is larger than residual electrostatic energy where the so called j-j coupling scheme is applicable. Often an intermediate situation between LS and j-j coupling schemes is the case as discussed on page 269 ref. 1.

If we now introduce the crystalline electric field interaction into the Hamiltonian 3.1. We must know at which stage to introduce this perturbation which requires a knowledge of the magnitude of this interaction relative to other terms in the Hamiltonian. If we adopt Crystal Field Theory where the ligands are regarded as charged ions located on given lattice points, giving rise to a crystalline potential Vc, then three cases arise :-

(1) <u>Weak ligand field</u> (Crystal potential Vc < spin orbit coupling)

This applies to rare earth (4f) and actinide (5f) groups in which the unfilled shells are screened by outer filled shells. The free ion calculation of levels is valid but the crystal

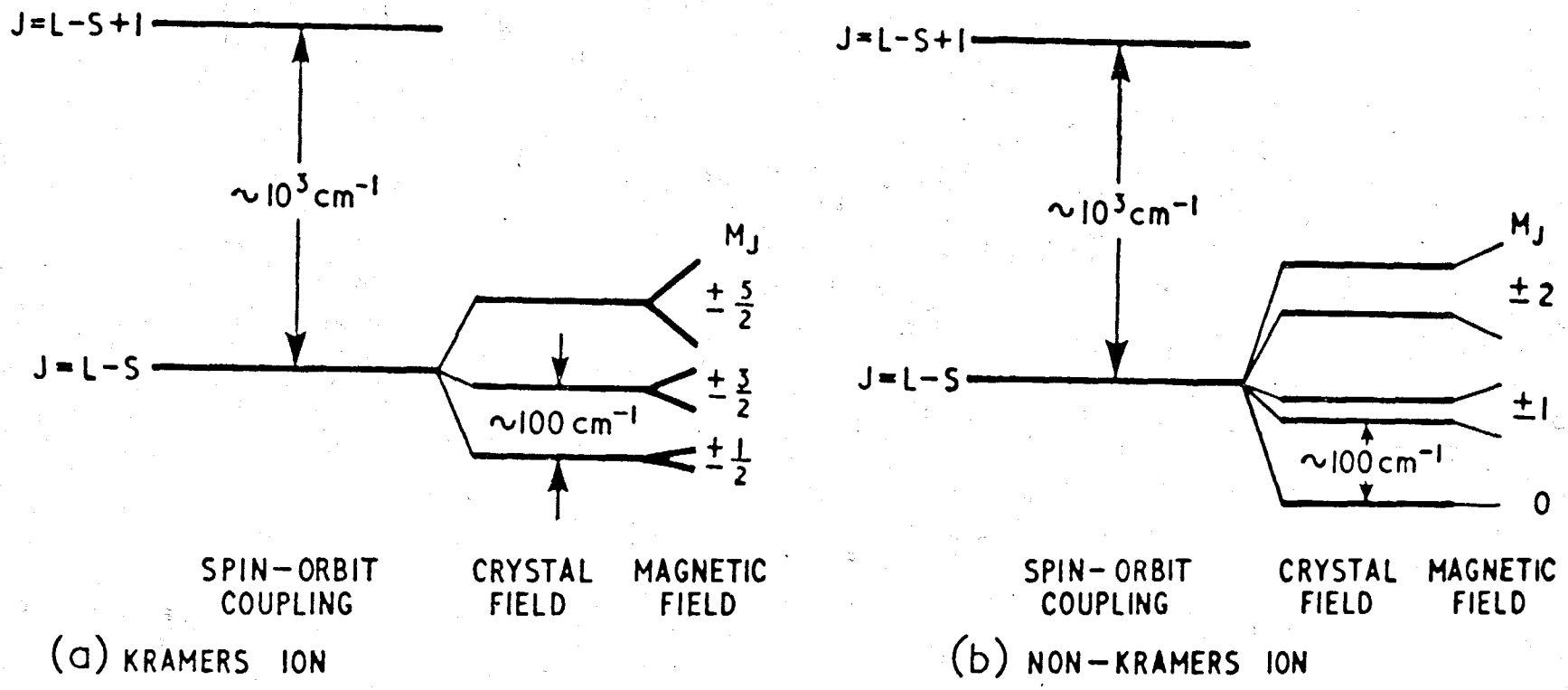

Fig. 3.1. Energy level diagrams to illustrate typical behaviour of (*a*) a Kramers and (*b*) a non-Kramers ion in a 'weak' crystal field (splittings not to scale)

potential Vc must be considered before the magnetic field interaction i.e. at C in Fig. 2.1. The multiplet levels are described by the total angular momentum J but the ligand field lifts the (2J + 1) fold degeneracy by 10 - 100 cm^{-1}. Resonance in the 4f and 5f groups are usually only observed at low temperatures where only the lowest level is populated. This is because the lifetimes of the excited states are generally so short, due to strong relaxation via the lattice phonons, that transitions between them are too broad to be observable.

If an ion has an odd number of unpaired electrons, J is half integral. (2J + 1) is then an even number and the crystal field will split the (2J + 1) levels into degenerate pairs characterised by $M_J = \pm\frac{1}{2}, \pm\frac{3}{2} \ldots\ldots \pm J$. This is the result of an important theorem due to Kramers which states that for any ion with an odd number of unpaired electrons the degeneracy cannot be completely lifted by an electric field. The pairs of states called Kramers' doublets involved are time conjugate, one being obtained from the other by use of a time reversal operator whose square is -1; they can be split by a magnetic perturbation which is a time-odd operator, but not an electrostatic perturbation, which is even under time reversal.

An ion with an even number of electrons may have the degeneracy completely lifted leaving a singlet ground state. The next level may then be separated by an energy too large for e.p.r. transitions to occur. The two cases of Kramers and non Kramers ions are illustrated in Fig. 3.1.

We can still use the quantum number J with corrections for coupling to states of different J, if necessary. The Zeeman interaction is then of the form

$$\mathcal{H} = g_J \beta (\bar{B}.\bar{J}) \qquad 3.2.$$

(2) Medium ligand field (spin orbit coupling < crystal potential Vc < electrostatic interaction)

In this situation, which arises mainly in 3d ions, we can use L and S. Within a given state L, S the diagonal Zeeman interaction is

$$\mathcal{H} = \beta \bar{B}.(\bar{L} + 2\bar{S}) \qquad 3.3.$$

The crystal field lifts the orbital degeneracy of the ground term into (2L + 1) levels with splittings of the order $10^4 cm^{-1}$ and therefore only the lowest level is populated at normal temperatures. If the resultant ground level is an orbital singlet ($M_L = 0$) then the only contribution to the paramagnetism is from spin and the orbital motion is said to be quenched. This occurs in 3d ions and originally quenching of the orbital motion was postulated in order to explain magnetic susceptibility results.

(3) Strong ligand field (electrostatic interaction > crystal potential Vc)

In this case the ligand field interaction is of greater magnitude than the electrostatic interaction. The crystal potential Vc is applied as a perturbation upon the configuration

and is considered before the coulomb and exchange interactions. $\bar{L}$ and $\bar{S}$ will no longer commute with the Hamiltonian and therefore single electron operators must be used.

The Zeeman interaction becomes

$$\mathcal{H} = \beta \bar{B} . \sum_i (\bar{l}_i + g_s \bar{s}_i) \qquad 3.4$$

where the sum is over all electrons in unfilled shells.

The strong field case arises usually in strongly covalent systems. The ions of platinum (4d) and palladium (5d) groups form covalent bonds with neighbouring ions resulting in a strong ligand field. Also certain ions of the 3d group form covalent bonds with adjacent ions as will be seen in the case of ferric myoglobin. Conversion to the low spin form ($S = \frac{1}{2}$) of the ferric state occurs in the iron in myoglobin when complexing with certain ligands due to a strong crystal electric field.

3.3. Crystal Field Theory

This approach ignores the finite extent of charges on the ions, the overlap of the magnetic ions wave functions with those of the neighbouring ions, and the complex effect of screening. The electric field potential is calculated on the basis of a simple point-charge ionic model of the crystal lattice.

The electrostatic potential $V(r, \theta, \phi)$ due to the surrounding point charges (negatively charged ligand ions) at a point (r, θ, ϕ) near the origin of the magnetic ion in question is

$$V(r, \theta, \phi) = \sum_j \frac{qi}{[\bar{R}_j - \bar{r}]} \qquad 3.5.$$

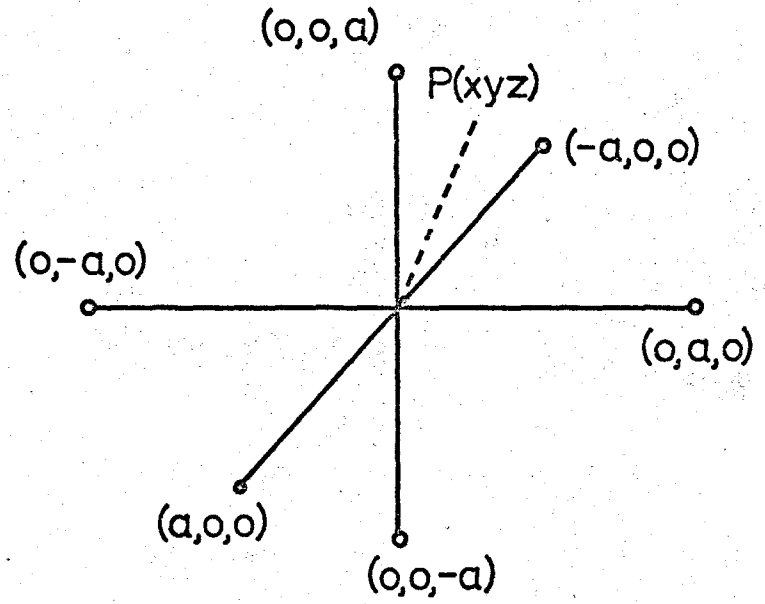

Fig. 3.2. Co-ordinates of atoms in an octahedral complex.

where q is the charge at the jth neighbouring ion, a distance Rj from the origin. If the magnetic ion has charge q_i at (r_i, θ_i, ϕ_i), then the perturbing crystalline potential will be

$$Vc = \sum_i q_i V_i = \sum_i \sum_j \frac{q_i q_j}{[R_j - r_i]} \qquad 3.6.$$

It is only necessary to sum $\sum_i$ over electrons in unfilled shells, as the crystal field merely raises the energy of orbitals in closed shells, but it does not affect their splittings.

Consider a paramagnetic ion in an octahedral environment. Then the potential V(xyz) at a point P(xyz), as shown in Fig. 3.2., due to charges q at the corners of an octahedron is

$$V(xyz) = Vx + Vy + Vz$$

where

$$Vx = q\left[\frac{1}{(r^2 + a^2 - 2ax)^{\frac{1}{2}}} + \frac{1}{(r^2 + a^2 + 2ax)^{\frac{1}{2}}}\right] \qquad 3.7$$

This can be shown to be equal to[2]

$$V(xyz) = \frac{6q}{a} + \frac{35q}{4a^5}\left[(x^4 + y^4 + z^4) - {}^3/_5\, r^4\right] - \frac{21q}{2a^7}\left[\ldots\ldots\right] \qquad 3.8$$

The perturbing Hamiltonian operator will be

$$\mathcal{H}_L = - |e| \sum_i V(x_i\, y_i\, z_i) \qquad 3.9$$

where the sum is over the magnetic electrons.

If the crystal field potential is expressed in spherical harmonics the splittings of the orbital levels, of a given term, can be determined by evaluating the expectation value of the Hamiltonian between the free ion wavefunctions. Raising of the orbital degeneracy of the ground term by means of a crystal electric field is illustrated in Appendix 1, where the energy levels are calculated for a $3d^1$ ion in a ligand field with octahedral symmetry. In general, we require evaluation of matrix elements for multi-electron states, and these can be calculated by writing these compound states as determinental products of single electron wavefunctions, as described by Bleaney and Stevens[3]. A much simpler method has been devised by Stevens[4] based on operator equivalents. In this method the individual electrons are considered as coupled together to give a total angular momentum represented by the quantum number L. The crystal field is then taken to interact with this coupled system so as to raise the (2L + 1) fold orbital degeneracy. Operators are formed from each term in the crystal field potential by replacing coordinates x, y, z by the operators Lx, Ly, Lz and r^2 by L(L + 1). The operator equivalents of various crystal field potentials have been listed by Stevens[4] and Low[5].

3.4. Symmetry Considerations in 3d ions

Group theory has been successfully applied to the study of crystal field effects. From a knowledge of the symmetry of an ion's environment, group theory gives a detailed qualitative

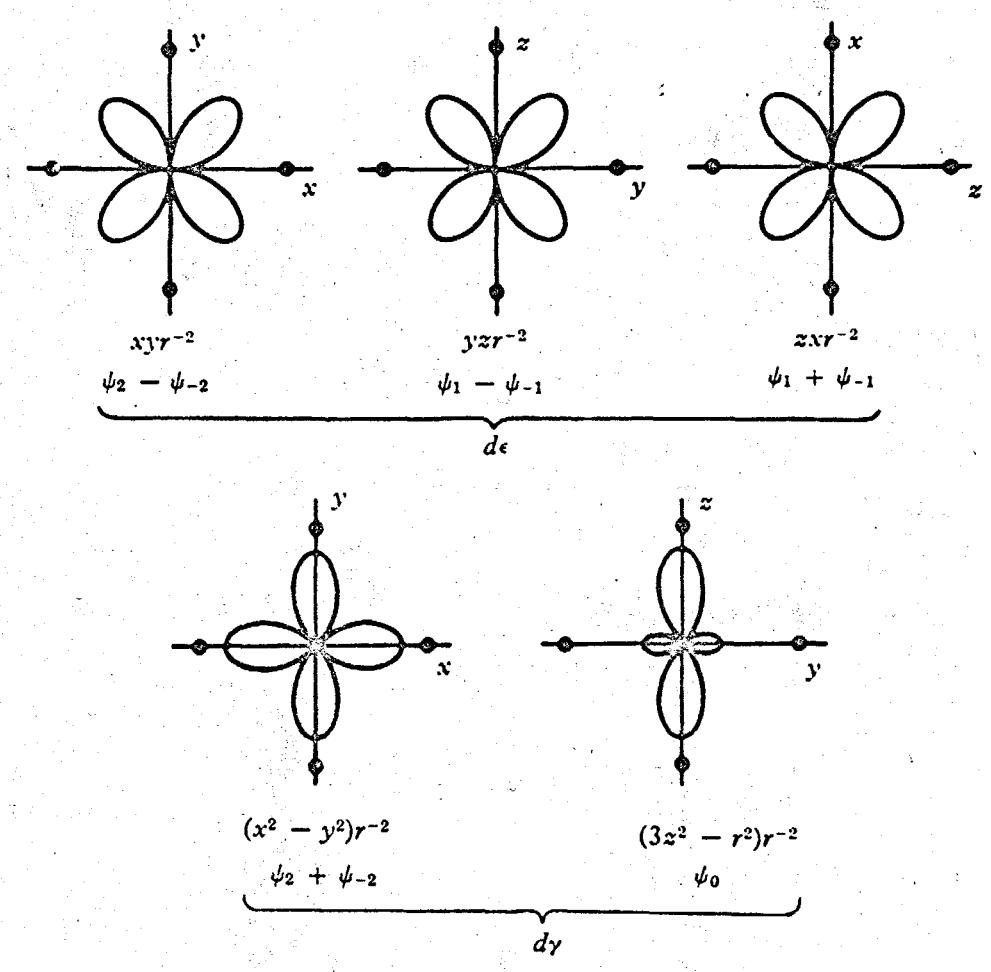

Fig. 3.3. Orbitals of the d electrons.

account of the way in which the orbital degeneracy of a magnetic ion is lifted by a crystal field. It is necessary only to assume a knowledge of the angular properties of the electron wavefunctions which are to be considered. Consider the case of iron group ions (3d electrons), and a crystal field of medium strength, so that the electronic wavefunctions may be described in terms of L and S.

The wavefunctions for d orbitals are, assuming a central field approximation, the one electron orbitals.

$$\psi = \sqrt{\frac{15}{8\pi}}\ f(r) \begin{cases} \frac{1}{4}\sin^2\theta \exp(2i\phi) & m = +2 \\ -\sin\theta\cos\theta\exp(i\phi) & m = +1 \\ \frac{1}{\sqrt{6}}(3\cos^2\theta - 1) & m = 0 \\ +\sin\theta\cos\theta\exp(-i\phi) & m = -1 \\ \frac{1}{4}\sin^2\theta\ \exp(-2i\phi) & m = -2 \end{cases} \qquad 3.10.$$

It is convenient to use linear combinations of these functions to obtain five real functions. The electron densities for the five orbitals are shown in Fig. 3.3. In the free ion these orbitals have the same energy, but if a 3d ion is introduced into a lattice there will be electrostatic repulsion between the negatively charged ligands and the 3d orbitals. The interaction between the ligands and orbitals is not the same for each orbital and it will also depend on the symmetry of the lattice. Consider the case of an ion with a single 3d electron in an octahedral crystal field. An examination of Fig. 3.3. shows that orbitals dxy, dyz, dzx, have the same energy in an octahedral field,

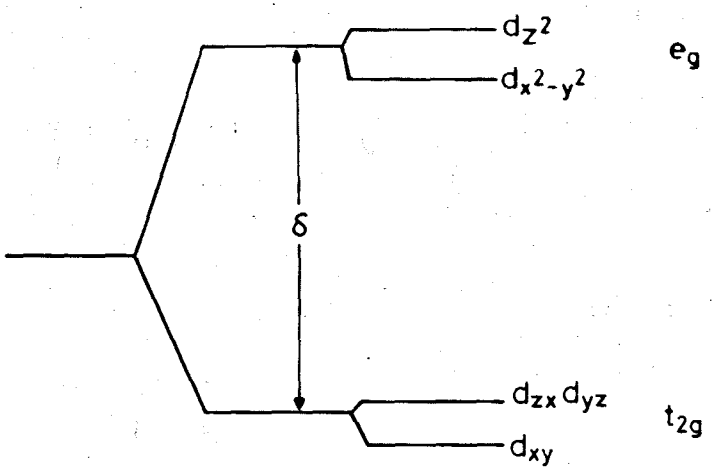

(a)

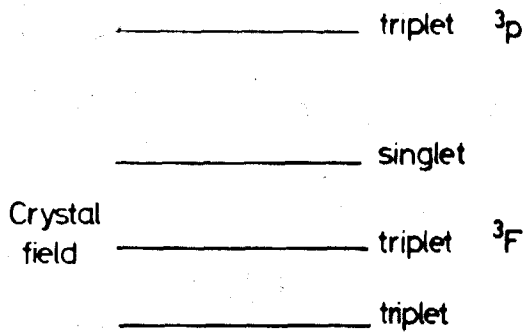

(b)

Fig. 34. (a) Splittings of 3d orbital levels in an octahedral and tetragonal crystal field.

(b) Energy levels of $3d^2$ configuration in an octahedral crystal field.

whilst the energy of the d_{z^2} and $d_{x^2 - y^2}$ orbitals are raised by electrostatic repulsion. The first three functions are called the d_ε or t_{2g}, and the second pair are the d_γ or e_g functions. The t,e nomenclature derives from group theory. Fig. 3.4(a) shows qualitatively the splittings of the 3d orbital levels in tetrahedral and rhombic crystal fields.

Knowing the splittings of the orbitals it is now possible to determine qualitatively how the orbital degeneracy of the ions is lifted, i.e. how the terms are split. This is done by considering the way in which the orbitals are filled. Consider an ion with a configuration $3d^2$ in a crystalline electric field of octahedral symmetry. The orbital levels are split as shown in Fig. 3.4(a) into t_{2g} and e_g levels. The two electrons can be placed in the five levels in ${}^5C_2 = 10$ different ways. The lowest total energy corresponds to both electrons being in the t_{2g} triplet, there being ${}^3C_2 = 3$ ways of distributing them, so this lowest level will be tripley degenerate. The maximum total energy occurs when both electrons are in the e_g levels and this is a singlet state as there is only one way of doing this. Also one electron can be in a t_{2g} level and the other in an e_g level, and this can be achieved in 6 ways. These arrangements have not all got the same energy if the repulsive interaction between the orbitals is considered. This is obvious from consideration of the spatial distribution of the 3d orbitals in Fig. 3.3. The net result for the d^2 configuration is three triplet levels and one singlet level, as shown in

Fig. 3.4(b). The upper triplet state will occur when the crystal field interaction is greater than the exchange effect between the electrons, and thus is the strong ligand field case.

3.5. Covalent Bonding

Although the crystal field theory can be made to account quite well for paramagnetic resonance results, there are many reasons for believing this theory to be insufficient. In haem proteins, for example, the electron configuration is $3d^5$, which means from Hund's rules the ground state is $^6S_{\frac{5}{2}}$. Therefore the ground state has spin $\frac{5}{2}$, but if a cyanide or azide ion is complexed with the iron ion, the ground state has an effective spin of $\frac{1}{2}$. This means a strong ligand field interaction which is not expected from an ionic model. Several ions of the 3d, 4d and 5d groups suffer 'strong field' interaction because the unpaired electrons are the outer electrons which suggests covalent bonding with a neighbouring ion or ions.

When including the effects of covalency a different approach to the calculation of orbital energy levels is adopted called Molecular Orbital Theory. The magnetic ion and its neighbours are considered as a molecule and the electrons of the metal and ligand ions are taken to belong to the molecule as a whole. The unpaired electrons of the metal and surrounding atoms are considered not to be involved in the bonding and are correctly described by the Hartree-Foch functions of the corresponding atoms. The valence orbitals of the metal and

ligands are considered to be linear combinations of the atomic Hartree-Foch orbitals of these atoms. The way in which these atomic orbitals are combined is determined mainly by symmetry considerations.

3.6. The Spin Hamiltonian

Resonance spectra of paramagnetic ions in crystals are usually very complex, and analysis would be extremely difficult unless some mathematical expression could be found to describe the spectra. This is the purpose of the Spin Hamiltonian, devised by Abragam and Pryce[6], which describes the paramagntic state of an ion by a series of terms, the coefficients of which are determined from the resonance spectra. Having obtained these coefficients experimentally, one can then attempt a theoretical interpretation of electronic field interactions with the ion, spin-orbit coupling, etc., by studying the resultant spin Hamiltonian. The form of the Spin Hamiltonian can often be guessed from consideration of crystal symmetry.

A paramagnetic ion in a crystal can exist in many electronic energy levels, each being an eigenvalue of the Hamiltonian, which represents the total energy of the ion. As a result of the crystal field the ground state of a paramagnetic ion consists of a group of electronic levels, with a separation of a few wavenumbers, which are well separated from the next group of levels (see Fig. 3.4). It is these ground levels which are involved in e.p.r., and they are ascribed an effective spin S where (2S + 1) is the number of levels in the group. In most

cases S is the true spin value of the ion. The base states are taken to be $|M\rangle$ where M takes the values S, S - 1, ... -S. Then the energies of the various ground state levels may be obtained as the eigenvalues En of the spin Hamiltonian $\mathcal{H}_s$, which operates only on the spin states $|M\rangle$.

$$\mathcal{H}_s \, |\psi n\rangle = En|\psi n\rangle$$

$$\text{where} \qquad |\psi n\rangle = \sum_i a_{n_i} \, |M_i\rangle \qquad 3.11$$

The effect of the orbital angular momentum is equivalent to an anisotropic coupling between the electron spin and the external magnetic field.

The general form of the spin Hamiltonian contains a large number of terms, representing the Zeeman interaction of electrons with an external magnetic field, splittings due to indirect effects of the crystal field (fine structure), hyperfine structure due to the presence of nuclear magnetic dipole and electric quadrupole moments in the central or surrounding ions, and the Zeeman interaction of the nuclear moment with the external field.

(a) Electronic Zeeman Interaction.

This may be written as

$$\begin{aligned}\beta \, \bar{B}.g.\bar{s} = \beta \, (&gxx \, Bx \, Sx + gyy \, By \, Sy + gzz \, Bz \, Sz + gxy \, Bx \, Sy + \\ &gyx \, By \, Sx + gyz \, By \, Sz + gzy \, Bz \, Sy + gzx \, Bz \, Sx + \\ &gxz \, Bx \, Sz).\end{aligned} \qquad 3.12.$$

If (xyz) axes are the principal axes this reduces to

$$\mathcal{H} = \beta(g_x B_x S_x + g_y B_y S_y + g_z B_z S_z)$$

This is the general case where the symmetry is rhombic and therefore three g values are necessary to define the system. This Hamiltonian may be solved by expanding it as

$$\mathcal{H} = \beta B (g_{\cdot} \, lS_x + g_y \, m \, S_y + g_z \, n \, S_z) \qquad 3.13.$$

where the magnetic field is in a general direction having direction cosines l, m, n, with respect to the magnetic axes (principal) xyz. We can solve this Hamiltonian by expanding $S_x = \frac{1}{2}(S+ + S-)$ and $S_y = -\frac{1}{2} i(S+ - S-)$ and using the properties

$$\begin{aligned} S_z \, |M\rangle &= M \, |M\rangle \\ S+ \, |M\rangle &= (S(S+1) - M(M+1))^{\frac{1}{2}} \, |M+1\rangle \\ S- \, |M\rangle &= (S(S+1) - M(M-1))^{\frac{1}{2}} \, |M-1\rangle \end{aligned} \qquad 3.14$$

The secular determinant is then

$$\begin{bmatrix} \frac{1}{2} g_z \beta B_n - E\pm & \frac{1}{2} g_x \beta B_l - \frac{1}{2} i g_y \beta B_m \\ \frac{1}{2} g_x \beta B_l + \frac{1}{2} i g_y \beta B_m & -\frac{1}{2} g_z \beta B_n - E\pm \end{bmatrix}$$

Expanding we get $E = \pm \frac{1}{2} \beta B (g_x^2 l^2 + g_y^2 m^2 + g_z^2 n^2)^{\frac{1}{2}}$

We can define an effective g value g(lmn) by putting

$$E+ - E- = g(lmn) \beta B$$

then $$g(lmn) = (g_x^2 l^2 + g_y^2 m^2 + g_z^2 n^2)^{\frac{1}{2}} \qquad 3.15$$

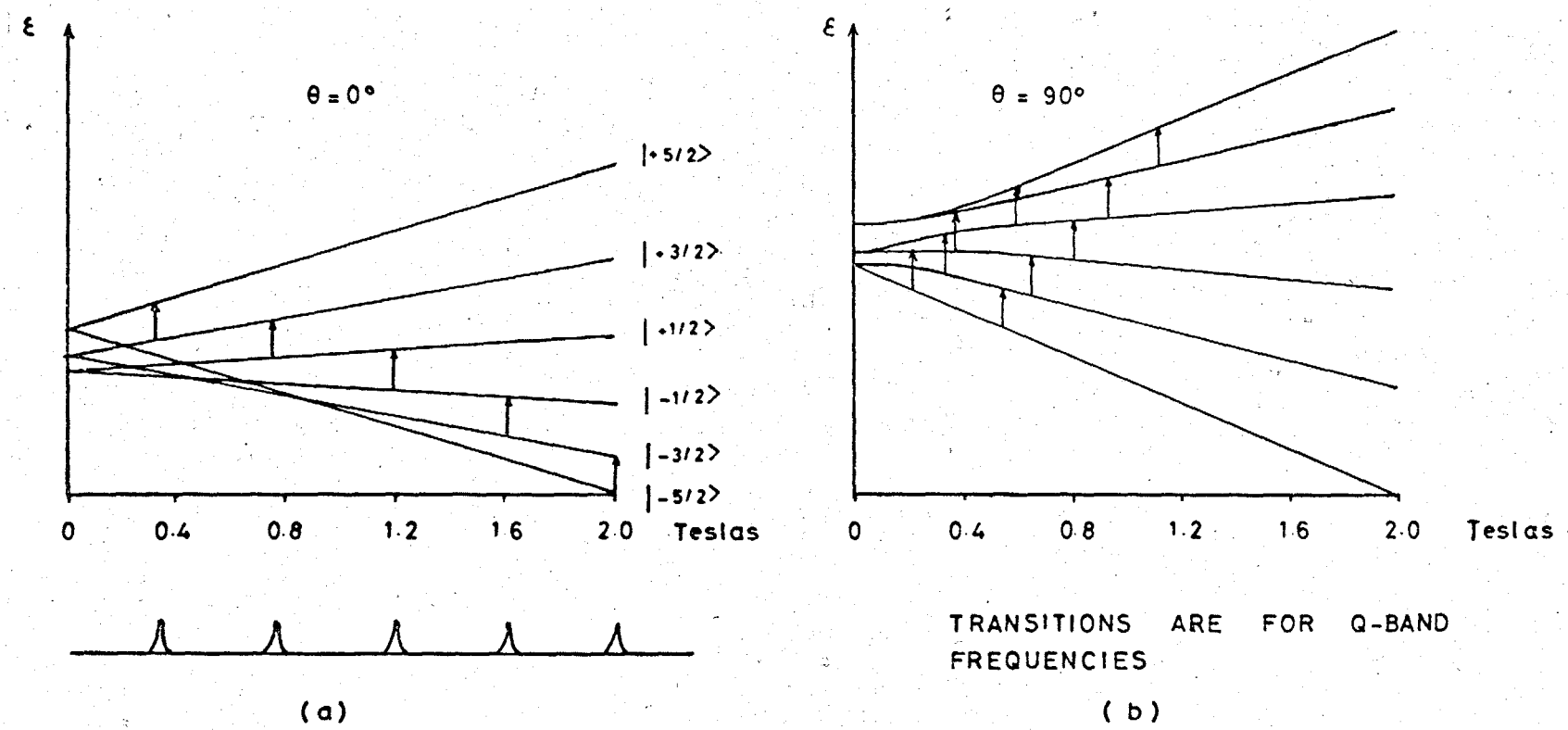

FIG 3.5 (a) FINE STRUCTURE SPLITTING OF RESONANCE LINE IN AN AXIAL $S = 5/2$ SYSTEM. ($g_x = g_y = g_z = 2.0$, $D = 0.2$)

(b) POSSIBLE TRANSITIONS WHEN THE BASE STATES ARE ADMIXED.

(b) Fine Structure.

When $S \geq 1$ the general state Zeeman levels may be split even in zero field if the site of the ion is no longer cubic. This results in the resonance line splitting into 2S components as illustrated in Fig. 3.5. If the zero field splitting is very large ($>> h\nu$) then not all the transitions will be seen. This situation occurs in the high spin form of Fe^{3+} in ferric myoglobin where the splitting is so large that only one transition between the lowest Kramers doublet is seen.

Consider for illustration purposes an ion with two unpaired 3p electrons in a ligand field of medium strength. Exchange and dipole-dipole effects cause the ground state term to be ^3P. The crystalline electric field can be treated as a perturbation upon the ^3P term. It will raise the orbital degeneracy leaving an $M_L = 0$ ground state with an $M_L = \pm 1$ level raised in energy by Δ. The Zeeman and spin orbit interactions being smaller than the crystal field interaction act as perturbations upon the orbital ground state $M_L = 0$. The two interactions may be treated simultaneously since the spin-orbit interaction only affects the level by second order perturbation and this effect is of comparable magnitude to the first order Zeeman perturbation. The appropriate Hamiltonian is then

$$\mathcal{H} = \beta \bar{B}.(\bar{L} + 2\bar{S}) + \lambda \bar{L}.\bar{S} \qquad 3.16$$

First order perturbation produces a change

$$\mathcal{H}^1 = \sum \beta Bi\ 2\ (Sij)\ S_j \qquad 3.17$$

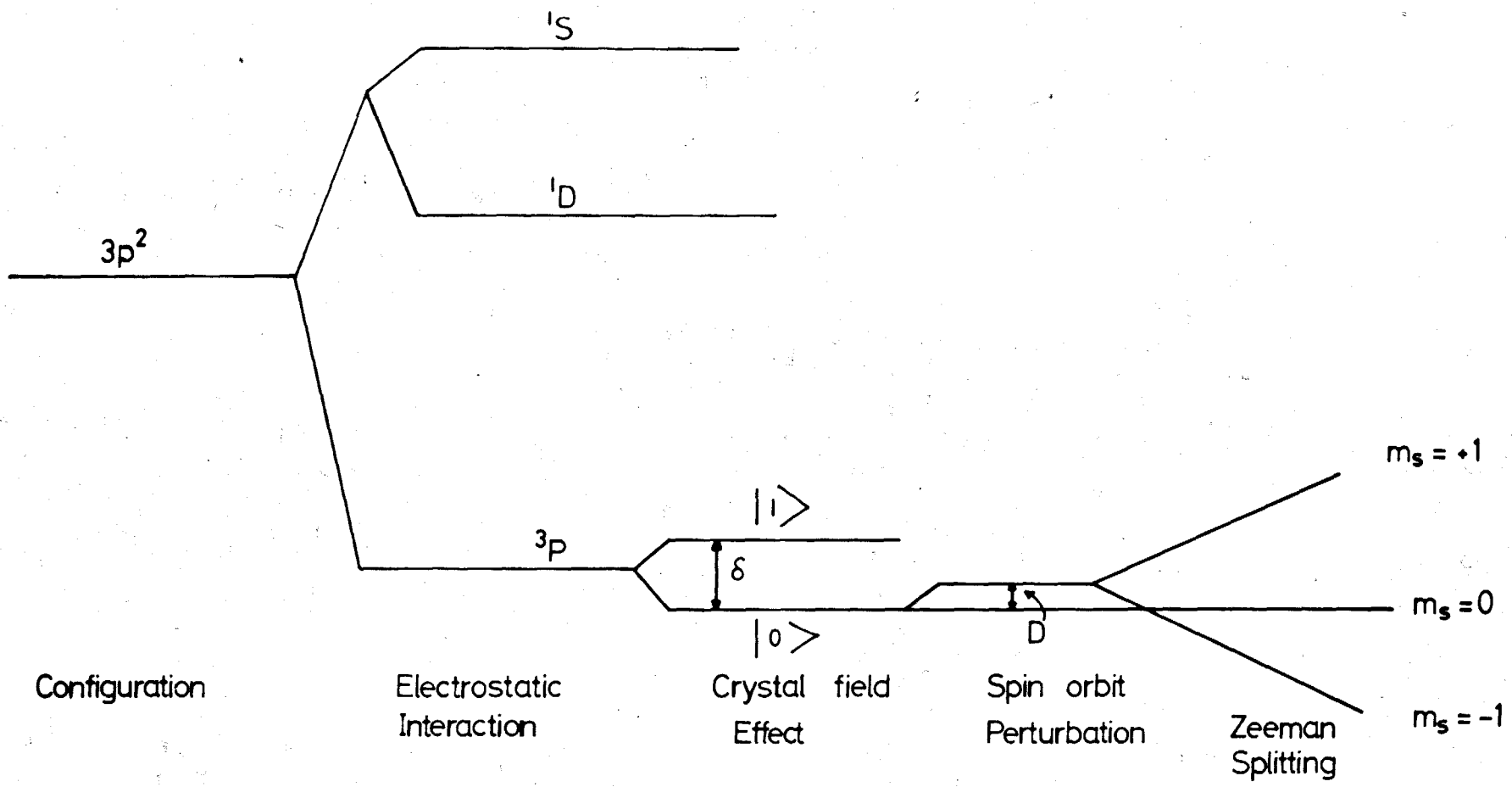

Fig. 3.6. Energy levels of an ion with configuration $3p^2$ in a lattice such that the crystal field is of medium strength.

where Sij is the Kronecker delta

and second order perturbation yields

$$\mathcal{H}^{11} = \sum ij \Lambda ij \, (\beta^2 \, Bi \, Bj + 2\beta\lambda \, Bi \, Sj + \lambda^2 \, Si \, Sj) \qquad 3.18$$

where $$\Lambda ij = \sum n=o \; \frac{\langle o|\, Li\,|\, n\rangle \langle n|\, Lj\,|\, o\rangle}{\Delta}$$

the first term in ref. 3.18 affects all levels equally and therefore can be ignored. The total Hamiltonian for the spin-orbit and Zeeman perturbation is

$$\mathcal{H}S = \sum ij \; \beta \, Bi \, (2 \, Sij + 2\lambda\Lambda ij) \, Sj + \lambda^2 \, Si \, \Lambda ij \, Sj) \qquad 3.19$$

by putting $g = 2 \, Sij + 2\lambda\Lambda ij$ and $D = \lambda^2 \, Si \, \Lambda ij \, Sj$

the spin Hamiltonian can be written as

$$\mathcal{H}S = \beta \, \bar{B}.\bar{\bar{g}}.\bar{S} + \bar{S}.\bar{\bar{D}}.\bar{S} \qquad 3.20$$

where g and D are both tensors

It can be shown that for a field of axial symmetry the splittings of the spin levels may be formally represented by the operator $D(S_z^{\,2} - \frac{1}{3} \, S \, (S + 1))$ so for the above case of two 3p electrons, where the ground state is 3p (S = 1) the levels characterised by $M_S = \pm 1$ are separated from the level $M_S = 0$ by $D(1^2 - 0) = D$. The zero field splitting is therefore D for this case, which is equal to $\lambda^2 \, Si \, \Lambda ij \, Sj$ and hence is proportional to (a) the square of the spin orbit coupling constant and (b) inversely proportional to the separation of the orbital

levels Δ, which is dependant on the crystalline electric field.

If the crystalline electric field has a symmetry lower than axial then an additional term $E(Sx^2 - Sy^2)$ has to be included in the Hamiltonian.

(c) Nuclear interactions

Allowing for quadrupole and nuclear dipole interactions the spin Hamiltonian can be shown to take the form :-

$$\mathcal{H}S = \beta(g_z B_z S_z + g_x B_x S_x + g_y B_y S_y) + D\,(S_z^2 - \tfrac{1}{3} S(S+1)) + E(S_x^2 - S_y^2) + A\, I_z S_z + A_x S_x I_x + A_y S_y I_y + Q(I_z^2 - \tfrac{1}{3} I(I+1)) + Q^1(I_x^2 - I_y^2) + g_n \beta_n \bar{B}.\bar{I} \qquad 3.21$$

where the terms with coefficients A account for nuclear dipole interactions, the Q terms are the quadrupole interactions and the final term is the quantisation of the nuclear moment in the applied external field.

3.7. $3d^5$ ions

Consider now the case of an ion with configuration $3d^5$. This is of particular importance in this study as this is the configuration of Fe^{3+}, the paramagnetic ion in ferric haem-proteins. When the ion is situated in a ligand field of medium or weak strength, the ground state is an orbital singlet ($^6S_{\frac{5}{2}}$) and therefore the crystal field has no degeneracy to lift. The spin sextet should have no splitting other than that due to the Zeeman interaction and therefore one would expect a single resonance line at g = 2.0023. However this is not the case and

fine structure is observed. The reasons for this are discussed in detail in section 4.2.

The fine structure for such an ion can be represented by a series of spin operators O_k^q. Such operators are related to the symmetry of the crystal field and the crystal field interaction can be expanded in spin operation form

$$\mathcal{H}_{\text{ligand}} = \sum_{k=2,4} \sum_{q=-k}^{k} B_k^q \; O_k^q$$

In the case of predominantly cubic symmetry with a small axial distortion about the tetragonal or trigonal axis, the appropriate forms of the spin Hamiltonian are

Tetragonal $\mathcal{H} = \beta (\bar{B}.\bar{g}.\bar{S}) + B_4(O_4^0 + 5\, O_4^4) + B_2^0\, O_2^0 + B_4^0\, O_4^0$

Trigonal $\mathcal{H} = \beta (\bar{B}.\bar{g}.\bar{S}) + \frac{2}{3} B_4(O_4^0 + 2\sqrt{2}\, O_4^3) + B_2^0\, O_2^0 + B_4^0\, O_4^0$

3.22

Which can be expressed in the more usual form as

$$\mathcal{H} = \beta(\bar{B}.\bar{g}.\bar{S}) + D\,(S_z^2 - S(S+1)/3) + E(S_x^2 - S_y^2) + \frac{1}{6}\left[S_\xi^4 + S_\eta^4 + S_\zeta^4 + \frac{1}{5} S(S+1)(3S^2 + 3S - 1)\right] + \frac{1}{180} F\left[35\, S_z^4 - 30\, S(S+1)\, S_z^2 + 25\, S_z^2 - 6S(S+1) + 3S^2(S+1)^2\right]$$

3.23

Terms of the fourth degree are included when $S \geq 2$ and these terms with coefficients a and F represent the effect of the cubic and axial components of the crystal field respectively. The coordinate system ξ,η,ζ refers to the principal axes of the crystal electric field. If the principal axes of the g tensor

$$S_x = \begin{bmatrix} 0 & \frac{\sqrt{5}}{2} & 0 & 0 & 0 & 0 \\ \frac{\sqrt{5}}{2} & 0 & \sqrt{2} & 0 & 0 & 0 \\ 0 & \sqrt{2} & 0 & \frac{3}{2} & 0 & 0 \\ 0 & 0 & \frac{3}{2} & 0 & \sqrt{2} & 0 \\ 0 & 0 & 0 & \sqrt{2} & 0 & \frac{\sqrt{5}}{2} \\ 0 & 0 & 0 & 0 & \frac{\sqrt{5}}{2} & 0 \end{bmatrix} \qquad S_x^2 = \begin{bmatrix} \frac{5}{4} & 0 & \sqrt{\frac{5}{2}} & 0 & 0 & 0 \\ 0 & \frac{13}{4} & 0 & \frac{3}{\sqrt{2}} & 0 & 0 \\ \sqrt{\frac{5}{2}} & 0 & \frac{17}{4} & 0 & \frac{3}{\sqrt{2}} & 0 \\ 0 & \frac{3}{\sqrt{2}} & 0 & \frac{17}{4} & 0 & \sqrt{\frac{5}{2}} \\ 0 & 0 & \frac{3}{\sqrt{2}} & 0 & \frac{13}{4} & 0 \\ 0 & 0 & 0 & \sqrt{\frac{5}{2}} & 0 & \frac{5}{4} \end{bmatrix}$$

$$S_y = i \begin{bmatrix} 0 & -\frac{\sqrt{5}}{2} & 0 & 0 & 0 & 0 \\ \frac{\sqrt{5}}{2} & 0 & -\sqrt{2} & 0 & 0 & 0 \\ 0 & \sqrt{2} & 0 & -\frac{3}{2} & 0 & 0 \\ 0 & 0 & \frac{3}{2} & 0 & -\sqrt{2} & 0 \\ 0 & 0 & 0 & \sqrt{2} & 0 & -\frac{\sqrt{5}}{2} \\ 0 & 0 & 0 & 0 & \frac{\sqrt{5}}{2} & 0 \end{bmatrix} \qquad S_y^2 = \begin{bmatrix} \frac{5}{4} & 0 & -\sqrt{\frac{5}{2}} & 0 & 0 & 0 \\ 0 & \frac{13}{4} & 0 & -\frac{3}{\sqrt{2}} & 0 & 0 \\ -\sqrt{\frac{5}{2}} & 0 & \frac{17}{4} & 0 & -\frac{3}{\sqrt{2}} & 0 \\ 0 & -\frac{3}{\sqrt{2}} & 0 & \frac{17}{4} & 0 & -\sqrt{\frac{5}{2}} \\ 0 & 0 & -\frac{3}{\sqrt{2}} & 0 & \frac{13}{4} & 0 \\ 0 & 0 & 0 & -\sqrt{\frac{5}{2}} & 0 & \frac{5}{4} \end{bmatrix}$$

$$S_z = \begin{bmatrix} \frac{5}{2} & 0 & 0 & 0 & 0 & 0 \\ 0 & \frac{3}{2} & 0 & 0 & 0 & 0 \\ 0 & 0 & \frac{1}{2} & 0 & 0 & 0 \\ 0 & 0 & 0 & -\frac{1}{2} & 0 & 0 \\ 0 & 0 & 0 & 0 & -\frac{3}{2} & 0 \\ 0 & 0 & 0 & 0 & 0 & -\frac{5}{2} \end{bmatrix} \qquad S_z^2 = \begin{bmatrix} \frac{25}{4} & 0 & 0 & 0 & 0 & 0 \\ 0 & \frac{9}{4} & 0 & 0 & 0 & 0 \\ 0 & 0 & \frac{1}{4} & 0 & 0 & 0 \\ 0 & 0 & 0 & \frac{1}{4} & 0 & 0 \\ 0 & 0 & 0 & 0 & \frac{9}{4} & 0 \\ 0 & 0 & 0 & 0 & 0 & \frac{25}{4} \end{bmatrix}$$

TABLE 3.1 SPIN MATRICES FOR $S = 5/2$

and fine structure (x,y,z) are coincident with the axes ξ,η,ζ then the Hamiltonian can be written

$$\mathcal{H} = \beta(\bar{B}.\bar{g}.\bar{S}) + D(S_z^2 - S(S+1)/3) + E(S_x^2 - S_y^2) + \frac{F}{180}$$
$$\left[35\, S_z^4 - 30\, S(S+1)\, S_z^2 + 25\, S_z^2 - 6\, S(S+1) + 3\, S^2 (S+1)^2\right] + \frac{a}{48}\left[S_+^4 + S_-^4\right] \qquad 3.24$$

The relations between the parameters in the two types of Hamiltonian 3.22 and 3.24 are

$$a = 120\, B_4, \qquad D = 3\, B_2^o, \qquad F = 180\, B_4^o.$$

When determining the eigenvalues of the spin Hamiltonian two convenient directions of quantisation are normally used: one is the principal axis system of the g tensor, and the other is closely related to the magnetic field direction. Both formulations are based on the standard properties of angular momentum as given in equation 3.14. The spin matrices up to the second power are given in table 3.1. The matrix elements of the spin Hamiltonian (eqn 3.24) in the g - tensor axis system can readily be written since all the elements follow directly from table 1, except those involving the magnetic field. The Hamiltonian for these terms is

$$\mathcal{H} = \beta\, g_{zz}\, S_z\, B \cos\theta + \beta g_{xx}\, S_x\, B \sin\theta \cos\phi + \beta g_{yy}\, S_y\, B \sin\theta \sin\phi$$

where θ and ϕ are the conventional polar angles between the g tensor and the magnetic field direction. The secular matrix for a Hamiltonian including the first three terms only is given

SECULAR MATRIX $|A_{lk} - \epsilon_n \delta_{lk}|$

$A_{lk} = \int \phi_l^* \mathcal{H} \phi_k d\tau$ where ϕ_k are the 'base states $|+\frac{5}{2}\rangle$ etc. and $\mathcal{H}$ is the Hamiltonian

$$P S_z + Q S_x + R S_y + D\left[S_z^2 - \frac{35}{12}\right] + E\left[S_x^2 - S_y^2\right]$$

	$\|+\frac{5}{2}\rangle$	$\|+\frac{3}{2}\rangle$	$\|+\frac{1}{2}\rangle$	$\|-\frac{1}{2}\rangle$	$\|-\frac{3}{2}\rangle$	$\|-\frac{5}{2}\rangle$
$\|+\frac{5}{2}\rangle$	$\frac{5}{2}P + \frac{10}{3}D - \epsilon_n$	$\sqrt{\frac{5}{2}}[Q - iR]$	$\sqrt{10}\,E$	0	0	0
$\|+\frac{3}{2}\rangle$	$\sqrt{\frac{5}{2}}[Q + iR]$	$\frac{3}{2}P - \frac{2}{3}D - \epsilon_n$	$\sqrt{2}[Q - iR]$	$3\sqrt{2}\,E$	0	0
$\|+\frac{1}{2}\rangle$	$\sqrt{10}\,E$	$\sqrt{2}[Q + iR]$	$\frac{1}{2}P - \frac{8}{3}D - \epsilon_n$	$\frac{3}{2}[Q - iR]$	$3\sqrt{2}\,E$	0
$\|-\frac{1}{2}\rangle$	0	$3\sqrt{2}\,E$	$\frac{3}{2}[Q + iR]$	$-\frac{1}{2}P - \frac{8}{3}D - \epsilon_n$	$\sqrt{2}[Q - iR]$	$\sqrt{10}\,E$
$\|-\frac{3}{2}\rangle$	0	0	$3\sqrt{2}\,E$	$\sqrt{2}[Q + iR]$	$-\frac{3}{2}P - \frac{2}{3}D - \epsilon_n$	$\sqrt{\frac{5}{2}}[Q - iR]$
$\|-\frac{5}{2}\rangle$	0	0	0	$\sqrt{10}\,E$	$\sqrt{\frac{5}{2}}[Q + iR]$	$-\frac{5}{2}P + \frac{10}{3}D - \epsilon_n$

$P = \beta B \cos\theta$, $Q = \beta B \sin\theta \cos\phi$, $R = \beta B \sin\theta \sin\phi$

TABLE 3.2

in table 3.2. If the corresponding values for each parameter are substituted in this matrix then it can be diagonalised numerically on a computer by the Jacobi[8] or other methods. The resultant diagonal elements are the eigenvalues of the spin Hamiltonian, and the diagonalising matrix contains the coefficients of the eigenvectors, a_{in}, as defined in equation 3.11. Fig.3.7 shows the eigenvalues as a function of magnetic field β for the case of acid met myoglobin.

The magnetic properties of a paramagnetic sample can be described by a spin Hamiltonian and the various parameters (g, D, E, etc.) in this Hamiltonian can be determined from the e.p.r. spectra. The value in e.p.r. as a research tool lies in interpretation of the magnetic properties, in the form of a spin Hamiltonian, in some useful way towards an understanding of the physical and chemical properties of the sample under investigation. In the study of haem-proteins important information can be derived from the e,p.r. spectra concerning the functioning of such molecules as enzymes. The magnetic properties of haem-proteins, and the interpretation drawn from them so far, is discussed in the following chapter.

ZEEMAN ENERGY LEVELS FOR A HIGH SPIN MYOGLOBIN DERIVATIVE

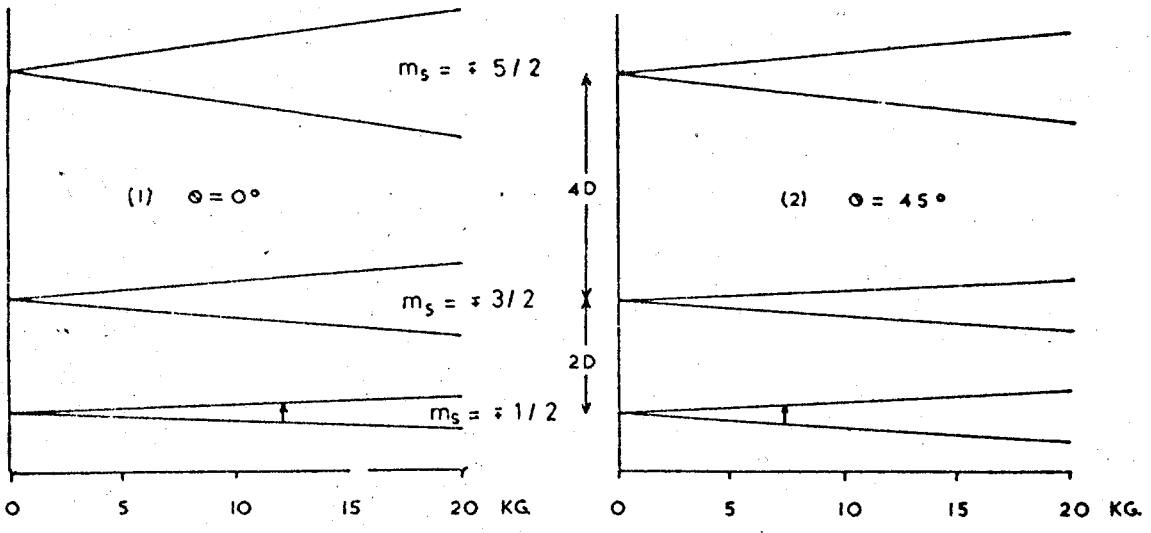

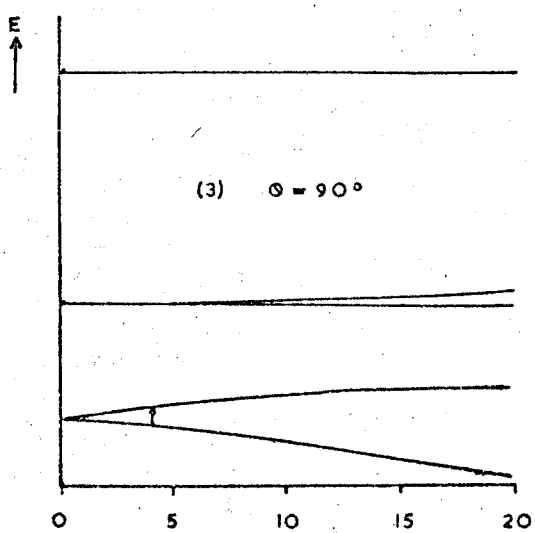

THESE ENERGY LEVELS CAN BE DESCRIBED BY A SPIN HAMILTONIAN —

$$\mathcal{H} = \beta \bar{g} . \bar{H} . \bar{S} + D\left[S_z^2 - 1/3\, S(S+1)\right] + E(S_x^2 - S_y^2)$$

FOR ACID-MET DERIVATIVE
$D = 5\ CM^{-1}$, $E = 0{\cdot}001\ CM^{-1}$

TRANSITIONS SHOWN ARE FOR Q-BAND MICROWAVE FREQUENCY RANGE

FIG 3.7

REFERENCES.

1. R.B. Leighton, Principles of Modern Physics, p268, McGraw-Hill, 1959.

2. M.T. Hutchings, Solid State Physics, 16, 227, 1964.

3. B. Bleaney, K.W.H. Stevens, Rept. Progress Phys. 16, 108, 1953.

4. K.W.H. Stevens, Proc. Phys. Soc. A65, 209, 1952.

5. W. Low, Paramagnetic Resonance in Solids, Solid State Physics - Supplement 2, 16, 1960.

6. H.M.L. Pryce, Proc. Phys. Soc. A63, 25, 1950.

7. A. Abragam, H.M.L. Pryce, Proc. Roy. Soc. A205, 135, 1951.

8. Mathematical Methods for Digital Computers, A.Ralston, H.S. Wilf, John Wiley & Sons, 1962.

CHAPTER 4.

MAGNETIC PROPERTIES OF HAEM-PROTEINS

4.1. Haem-Proteins

Iron occurs in numerous biological systems and particularly in proteins. Iron-proteins fall into two main groups, which are, haem proteins, and iron-sulphur proteins, (ferrodoxin, rubredoxin). Haem-proteins are biochemical systems whose active centre is the iron-porphyrin complex, shown in Fig. 2.1. As already mentioned, the iron atom is complexed octahedrally with five nitrogen atoms plus an oxygen or water molecule or another ion at the sixth coordination point. From X-ray data the iron atom is found to protrude out of the plane, formed by the four nitrogens,[1] by 0.5 - 0.6 Å. Essentially haem-proteins may be divided into four groups which are :-

(a) Oxygen Carriers

This group includes haemoglobin and myoglobin, the proteins responsible for transport of oxygen in the blood, and storage of oxygen in the tissues respectively. It is not known how O_2 is attached to the iron ion, nor is the charge on the oxygen molecule known when it is attached. It is obviously important to determine these factors. An important clue to this problem is the observation of an absorption[2] peak at 1000 nm (I.R.) which only occurs when O_2 is attached. In the blood haemoglobin (Hb) is in the ferrous form (Fe^{2+}) but the spin state of Fe^{2+} changes from high spin (S = 2) when deoxygen-

ated to low spin (S = 0) on oxygenation. It is possible to convert the iron ion to the ferric state (Fe^{3+}) by attaching water or other molecules at the sixth coordination point. Again high spin (S = $\frac{5}{2}$) or low spin (S = $\frac{1}{2}$) states are possible, and often the two exist in thermal equilibrium with each other. This situation of the iron ion existing at the cross-over point between two spin states would seem to be an important factor for the function of the molecule as an enzyme.

Haemoglobin consists of four units, two α chains and two β chains, which are intertwined to form the quarternary structure of the molecule. Each chain is similar in structure to a myoglobin molecule and contains one haem centre. It is found that when one haem accepts an oxygen molecule then the affinity for oxygen of the remaining three haems greatly increases, and they similarly attach an oxygen molecule. This phenomena, called cooperative ligand binding, is thought to be due to some form of haem-haem interaction.

One mechanism, proposed by R.J.W. Williams[3], involves a series of conformational changes induced in the chains by a change of spin state of the iron in the first haem site. These conformational effects cause a change in the environment of the iron atom in the next chain such that the energy of the high spin state is reduced and therefore oxygen affinity is increased.

In 1965 Bucci and Fronticelli[4] discovered a way of separating the four chains in a haemoglobin molecule, and since then much research has been concentrated on the optical[5-8] and

magnetic properties of the separated chains.[9-11] Another active area of research is investigations of abnormal haemoglobins.[12-22] In these molecules the unique amino acid sequence is destroyed. This usually causes two of the chains to be in the ferric state which renders them available for investigation by e.p.r.

(b) Oxygenases, Peroxidases, Catalases.

In this group the haem is the same as in Hb and Mb with the iron atom complexed in a six coordination system, and the fifth being imidazole (except in catalase). Catalase is involved in the decomposition of hydrogen peroxide, whilst peroxidase, in conjunction with hydrogen peroxide, oxidises certain organic compounds.

(c) Oxidases.

The most important enzymes here are the cytochromes a_3, a_2, O. In each case the protein is connected to an electron transfer chain. The haem is thought to be open sided as for the above cases. One of these proteins P-450, in the ferric form, has an interesting e.p.r. spectra showing that the Fe iron has a strong rhombic distortion.

(d) Electron-transfer proteins

The crystal structure of one of these proteins, cytochrome C, is known. The haem lies in a crevice and is bound to two proteins through the iron-methionine and histidine.

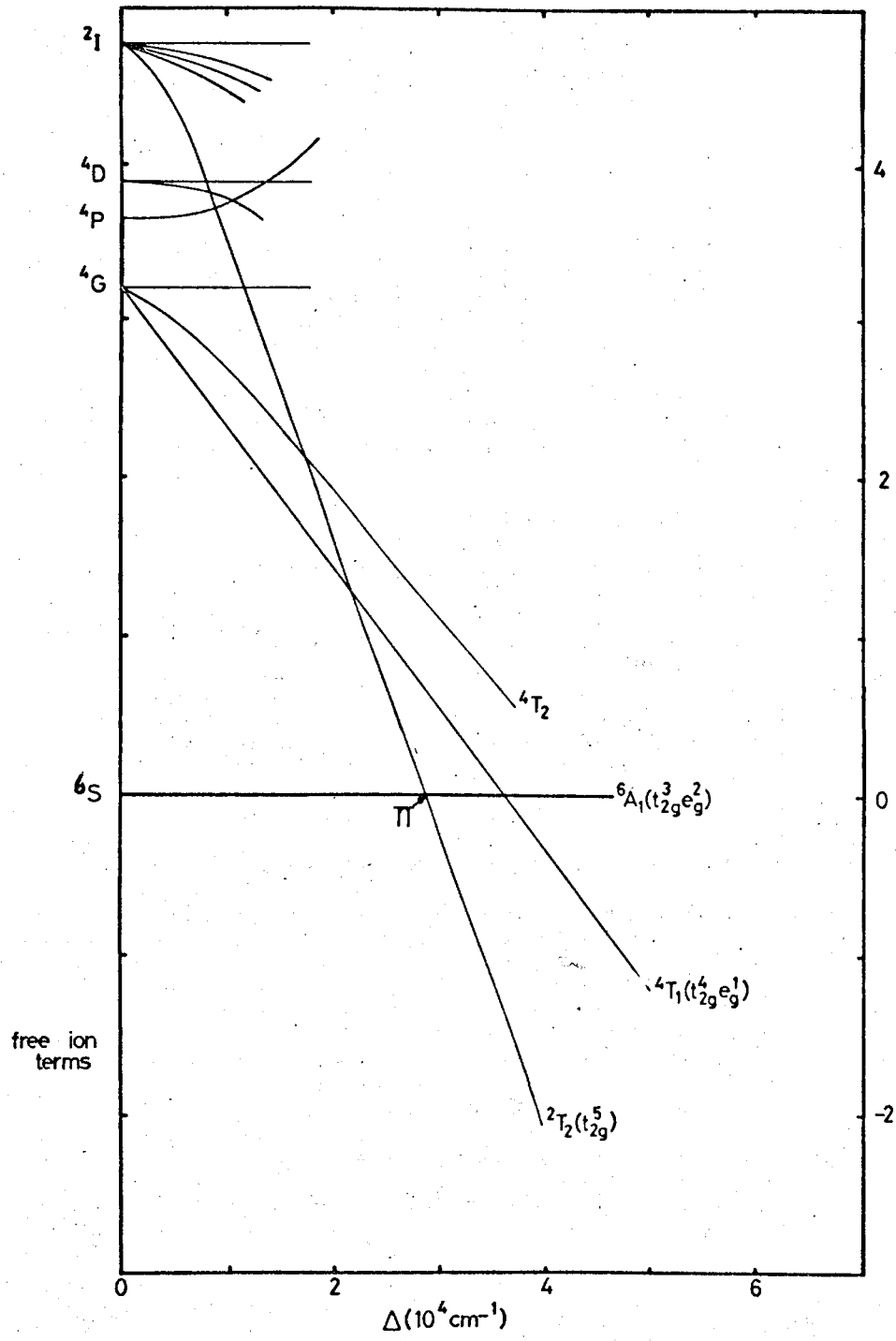

Fig. 4.1. Term diagram for configuration d^5 as a function of crystal field strength.

4.2. High and Low Spin States

The met, ferric form of haem-proteins has a configuration $(3d)^5$. If the crystal field surrounding the ion is of medium strength then Russell-Saunders coupling applies, and the ground term is $^6S_{\frac{5}{2}}$ Therefore there is no orbital degeneracy so crystal field and spin orbit interactions leave the ground state with spin $\frac{5}{2}$. This is the high spin state of the ferric ion. If, however, the crystal field perturbation is sufficiently large as to destroy Russell-Saunders coupling, the $^6S_{\frac{5}{2}}$ term will no longer be the ground state. Fig. 4.1. shows how the energy levels of a typical d^5 ion are shifted with increasing magnitude of a ligand field.[23] It is seen that when $\Delta = \pi$ the spin state changes to $\frac{1}{2}$ as the $^2T_2$ level crosses the $^6A_1$ level. This change of spin state can be understood by considering the d orbitals shown in Fig. 3.3. The energy of these orbitals when they are situated in a crystal field of octahedral symmetry are split into two groups, as illustrated in Fig. 3.4. When the crystal field is of 'medium' strength all five orbitals are occupied and the $^6A_1(t_{2g}^{\ 3}\ e_g^{\ 2})$ level lies lowest. If, however, the crystal field strength increases, the splitting (δ) between the energy of the orbitals t_{2g} and e_g will increase until the 'strong' crystal field limit is reached where δ is greater than the exchange energy between electrons. The five electrons will then pair up in the t_{2g} levels leaving a single unpaired electron and hence $S = \frac{1}{2}$. The $^2T_2\ (t_{2g}^{\ 5})$ level is now the ground state.

The high spin form of the ferric iron in haem-proteins occurs when the sixth ligand is ionically bound to the iron ion

whilst in low spin derivatives the binding of the sixth ligand is more covalent. In myoglobin the following ligands are found to produce high spin derivatives

F^-, H_2O, HCO_2^-, $CH_3CO_2^-$, NO_2^- namely fluoride, acid met, formate, acetate, nitroxide

OCN^- cyanate.

whilst the following ligands produce low spin derivatives

CN^-, N_3^-, OH^-, NO namely cyanide, azide, hydroxide, nitrosyl.

In order for a ligand to force a change of spin state it must either considerably reduce internal electron-electron repulsion, or produce a large crystalline electric field.[24] The common ligands can be arranged in an order of increasing ligand-field strength. This order is nearly independent of the particular metal ion studied so the magnitude of a crystal field is characteristic of the complexing ligands. This order is given by the Spectrochemical Series[25] which is found empirically to be

I^-, Br^-, F^-, C_2H_3OH, H_2O, NH_3, NO_2^-, CN^-

The members on the extreme left are π donors to the t_{2g} orbitals, while the members on the right are either π acceptors, or strong donors, or both. This series must be considered together with the Nephelauxetic series,[24] which grades ligands according to their effect upon the spin pairing of the metal ion, in determination of the ability of a ligand to change the spin state of a metal ion. The six ligands surrounding the iron atom in myoglobin produce an

electric field of strength Δ (see Fig. 4.1.) It is possible that Δ is such that the energy levels $^6A_1$ and $^2T_2$ are within kT of one another at temperature T. The two spin states of the ferric ion would then exist in thermal equilibrium with each other. This situation actually arises for most derivatives of myoglobin. Originally such a theory was postulated[26] to explain the early susceptibility results for myoglobin and now it has been proved by observation of changes in e.p.r., optical absorption and magnetic susceptibility with variation of temperature.

4.3. E.P.R. Spectra of High and Low Spin Derivatives.

E.P.R. of haem proteins was first observed by Bennett, Gibson and Ingram,[27] in 1957. They found that in a single crystal there is only one resonance line and this has a very large g-value anisotropy. The g-value varied from 2.0 when the magnetic field was parallel to the haem normal ($g_{\parallel}$) to approximately 6.0 when the magnetic field is in the haem plane ($g_{\perp}$). From measurements of this anisotropy they determined the orientation of the haem planes relative to the crystal axes in type A Sperm Whale myoglobin. They later extended these measurements to other crystal types[28] (1961). The observed spectra was ascribed to an $S = \frac{5}{2}$ system with a large zero field splitting, so that only a transition between the lowest Kramer's doublet is excited. This situation was originally considered by Griffith[29] (1956), and he estimated that the zero field splitting between the lowest pair of Kramer's doublets was around 10 cm^{-1} for acid met myoglobin. The system

was considered to be axial in these calculations.

Gibson and Ingram[30] (1957) also investigated the low spin azide derivative of myoglobin. They found there was a large reduction in the axial symmetry inherent in the high spin derivatives, and found the g-values were spread around 2.0. The principal axes were found to be rotated away from the directions of the principal axes of the acid met derivative. These results have subsequently been checked and compared with the detailed X-ray information now available (Helcke , Ingram, Slade, 1968). The principal g-values were found to be 1.71, 2.19 and 2.82, and the z axis was found to be rotated 9^{o} away from the haem normal.

The initial experimental results of acid met myoglobin suggested that the crystal field was axial, but very careful measurements of the g-value in the haem plane have shown that there is not complete axial symmetry (Helcke, Ingram, Slade, 1968).[31] The g-value was found to vary in this plane between 5.98 and 5.86. Similar investigations were undertaken by Kotani and Morimoto[32] on the acid met and fluoride derivatives of myoglobin. They found the rhombicity defined by $\lambda = {}^{E}/_{D}$ to be 0.0025 and 0.0038 for these compounds respectively. Since the magnitude of splitting is less than the linewidth, no splitting has been observed in the first derivative e.p.r. signal at g = 6 of a paste spectrum. In the fluoride derivative, though, a splitting of the resonance line near g = 6 has been observed in single crystals.[33,34] This has been ascribed to superhyperfine structure from the ^{19}F ligand. Also such a splitting has been detected from the $g_{\parallel}$ = 2 signal

from paste spectra.

In other haem proteins larger rhombic distortions have been reported.[35,36] In horseradish peroxidase, catalases[37] and their fluoride derivatives λ has been estimated to be >0.01. A more complex spectrum is found for cytochrome p450, where a signal is observed at g = 4.3, in addition to the g = 6 signal. This situation has been studied by various authors who have shown that when D and E are large compared with $g\beta B$, a signal at g = 4.3 can arise if the rhombicity λ is equal to $\frac{1}{3}$. The significance of this value of λ was pointed out by Blumberg.[38] He noted that if λ = 0 represents axial symmetry, then an increase in λ represents a departure towards rhombic symmetry. $\lambda = \frac{1}{3}$ represents maximum possible rhombic symmetry with equally spaced Kramers doublets and values of λ greater than a $\frac{1}{3}$ represent a convergence towards axial symmetry again, with λ = 1 representing entirely axial symmetry. An interesting consequence of this rhombic situation ($\lambda = \frac{1}{3}$) is that although the minimum effective g-values of the g =4.3 signal lie along the x and y axes, the maximum does not necessarily lie along the z axis.

Consider the general case of $S = \frac{5}{2}$ with a small zero field splitting, as shown in Fig. 3.5. The possible transitions are five $\Delta m_s = \pm 1$ as shown, four $\Delta m_s = \pm 2$, three $\Delta m_s = \pm 3$, two $\Delta m_s = \pm 4$ and one $\Delta m_s = \pm 5$. Under normal circumstances only $\Delta m_s = \pm 1$ transitions are observed, but D and E may cause sufficient mixing of the base states when the magnetic field B is away from the z axis to cause other transitions to have a finite probability.

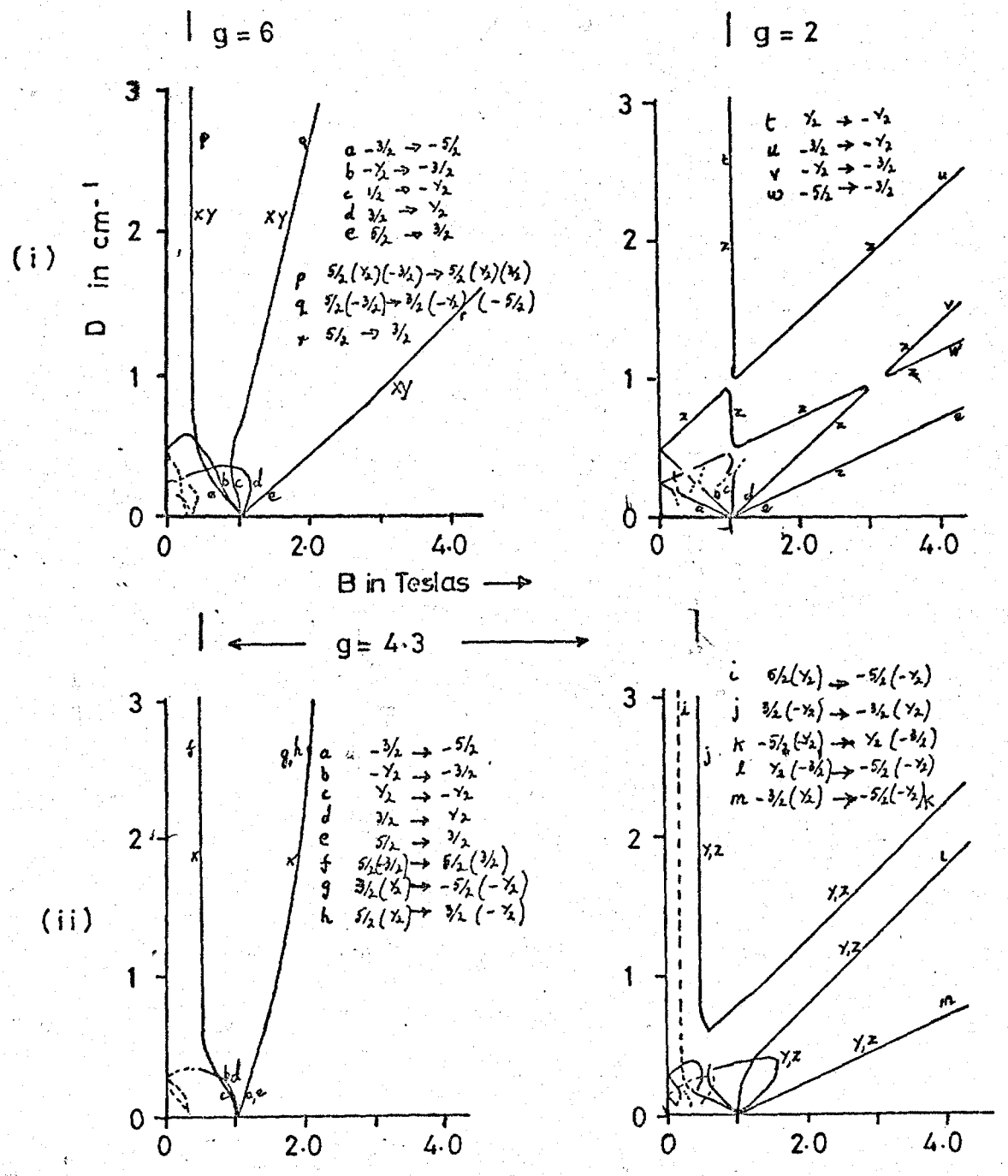

FIG. 4.2 PREDICTED E.S.R. TRANSITIONS FOR S = 5/2 AS A FUNCTION OF THE ZERO-FIELD SPLITTING PARAMETER D. (i) AXIAL CASE $\lambda = 0$ (ii) MAX. RHOMBIC CASE $\lambda = 1/3$

When D becomes large, of course, the separation may be too great for a transition to be induced at the microwave frequency being used, even though the transition probability is finite. A general solution for high spin d^5 systems has been given graphically by Dowsing and Gibson.[39] They solved the spin Hamiltonian

$$\mathcal{H} = \beta \bar{B}.\bar{\bar{g}}.\bar{S} + D\left[S_2^2 - \tfrac{1}{3} S(S+1)\right] + E(Sx^2 - Sy^2) \qquad 4.1.$$

for a range of values of D and λ and plotted the allowed transitions, when the magnetic field points along the principal axes of the fine structure tensor, on a graph of D versus magnetic field B. Two of the graphs are shown in Fig. 4.2. for the axial case ($\lambda = 0$), and the completely rhombic case ($\lambda = 0.333$). From the first graph it can be seen at Q-band frequencies if $D \simeq 5\ cm^{-1}$ there are just two transitions at g = 6 and g = 2 for axial symmetry. Whilst for the completely rhombic situation there is a signal at g = 4.3, and another signal with g < 1. Aassa[40] (1970) has extended these calculations to include possible extra lines that may occur when the field is orientated along directions other than the fine structure axes.

For the low spin d^5 systems the only term in the spin Hamiltonian is the Zeeman term, and therefore little use can be made of the Hamiltonian in this form for analysis of low spin derivative spectra. Griffith[41] has made a theoretical study of such systems. He supposed that the t2g orbitals d_{zx}, d_{yz}, d_{xy} had energies $-\frac{1}{2}V$, $\frac{1}{2}V$, Δ, respectively in the crystal electric field. He extended the Hamiltonian to include terms accounting

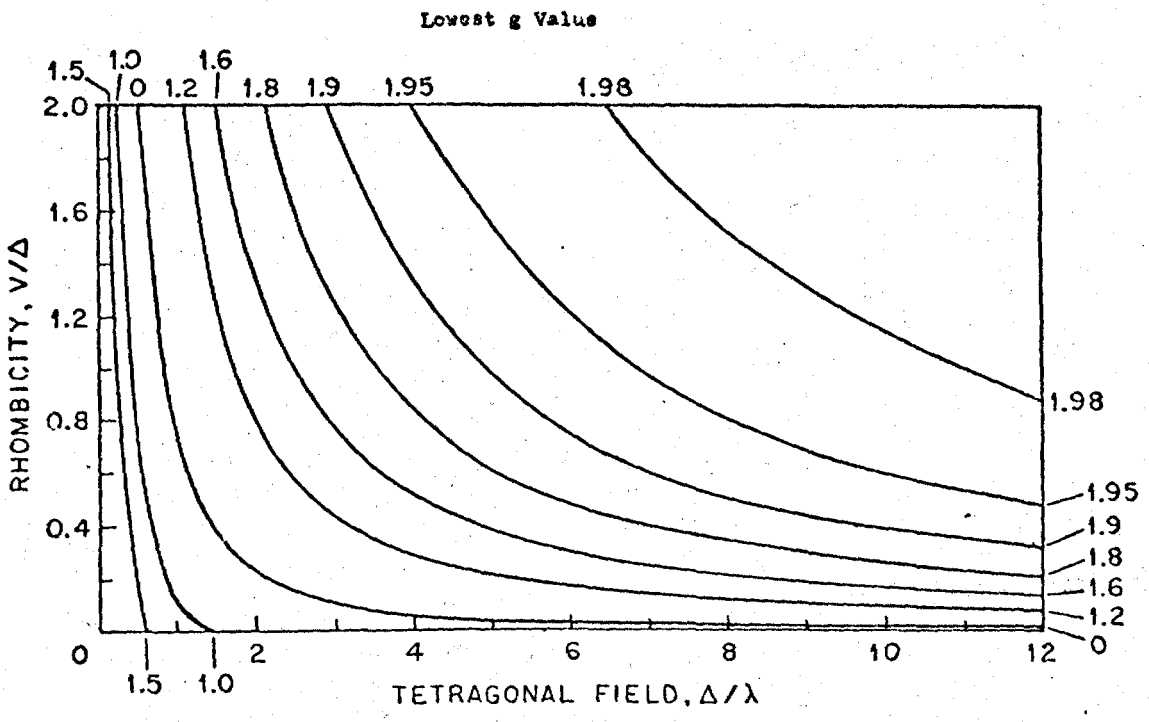
Lowest g Value
1.5
1.0
1.6
0
1.2
1.8
1.9
1.95
1.98
2.0
1.6
1.2
0.8
0.4
RHOMBICITY, V/Δ
1.98
1.95
1.9
1.8
1.6
1.2
0
0
1.5
1.0
2
4
6
8
10
12
TETRAGONAL FIELD, Δ/λ

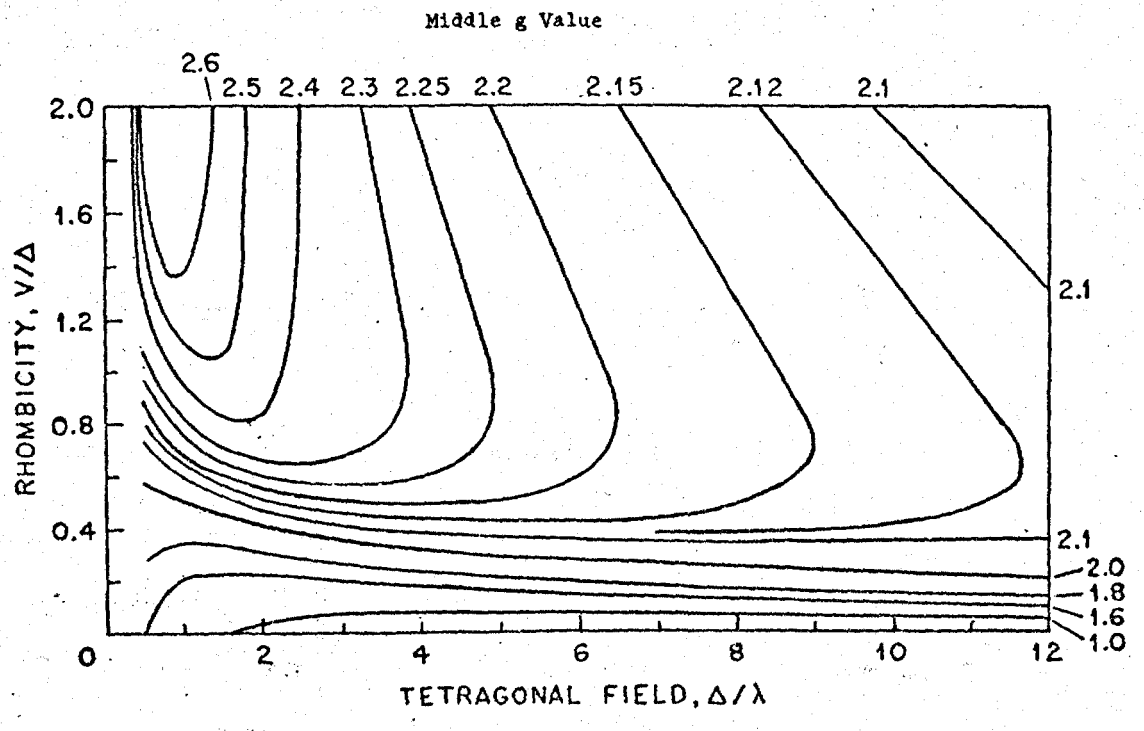
Middle g Value
2.6
2.5
2.4
2.3
2.25
2.2
2.15
2.12
2.1
2.0
1.6
1.2
0.8
0.4
RHOMBICITY, V/Δ
2.1
2.1
2.0
1.8
1.6
1.0
0
2
4
6
8
10
12
TETRAGONAL FIELD, Δ/λ

FIG. 4-3

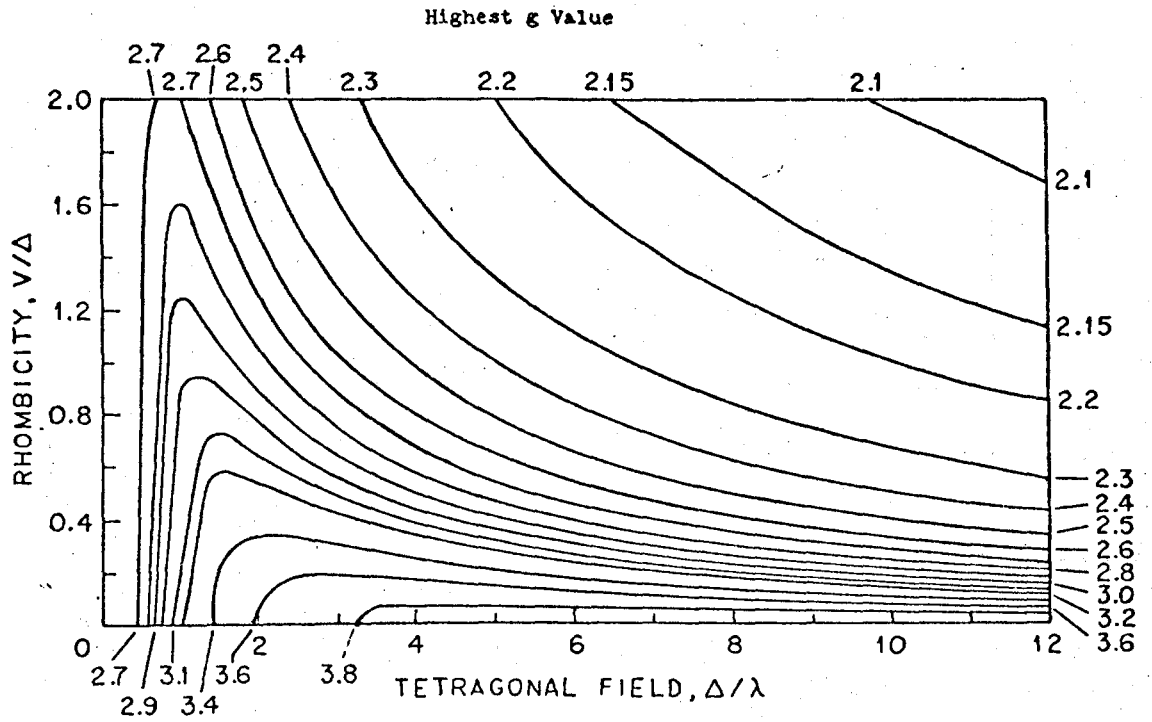
Highest g Value
2.7 2.6 2.4
2.7 2.5 2.3 2.2 2.15 2.1
2.0
1.6
1.2
0.8
0.4
RHOMBICITY, V/Δ
2.1
2.15
2.2
2.3
2.4
2.5
2.6
2.8
3.0
3.2
3.6
0 2 4 6 8 10 12
2.7 3.1 3.6 3.8
2.9 3.4
TETRAGONAL FIELD, Δ/λ

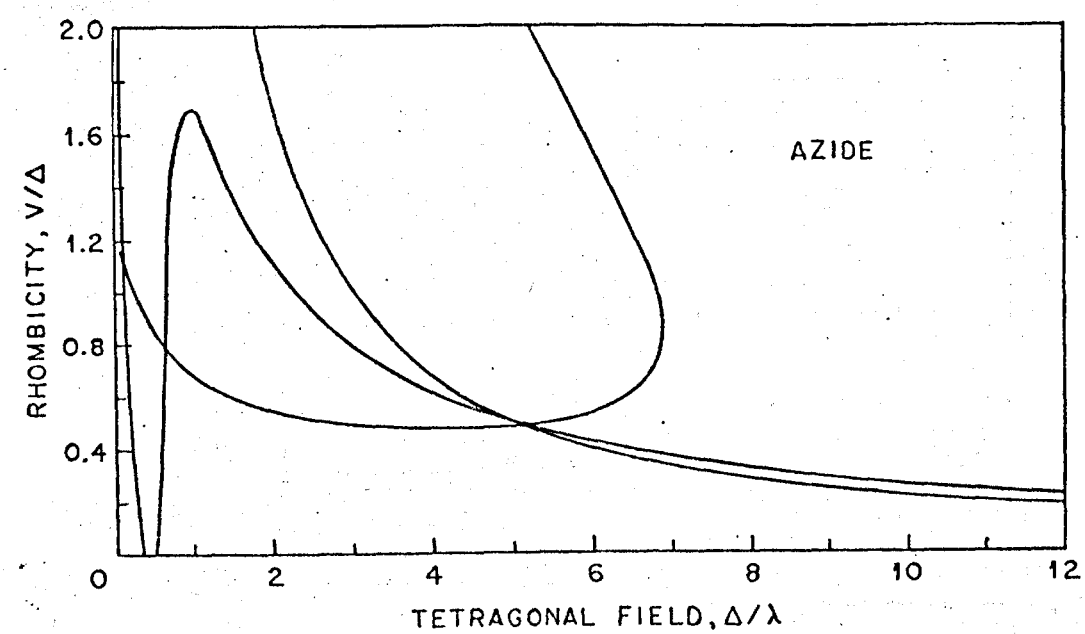
2.0
1.6
1.2
0.8
0.4
RHOMBICITY, V/Δ
AZIDE
0 2 4 6 8 10 12
TETRAGONAL FIELD, Δ/λ

FIG. 4.3

for the splitting of the t2g orbitals and spin-orbit coupling. Solving the Hamiltonian enables one to relate the measured g-values to the terms V, Δ and spin-orbit coupling parameter λ.

Blumberg has produced a graphical solution of this low spin Hamiltonian which is shown in fig. 4.3. By taking the line corresponding to each measured g-value and superimposing the three lines there is an intersection point. This intersection gives the orbital level splittings V and Δ in terms of the spin-orbit coupling parameter λ.

4.4. Origin of Zero Field Splittings in $3d^5$ Systems.

The origin of zero field splittings in $3d^5$ systems has been sought theoretically for many years. Such ions have no orbital degeneracy to be lifted by the crystal electric field. Therefore the usual mechanism of spin orbit coupling admixing with the ground orbital level certain higher orbital levels, that have been lifted in energy by the crystal field potential, is not applicable in these cases.

The first attempt to explain small Z.F.S. in $3d^5$ systems was made by Van Vleck and Penney.[43] They were considering splittings of the order 0.001 cm^{-1} in nearly cubic systems, and their theory was based on high (5th) order perturbations due to the cubic field and spin-orbit coupling. Meijer[44] found that the discrepancy between

the Z.F.S. values for ferric alum from specific heat and e.p.r. measurements, could be accounted for by introducing a trigonal field perturbation and simultaneous spin-orbit coupling. Pryce[45] adopted a different approach involving spin-spin coupling combined with the action of a tetragonal field component. The tetragonal field produces a slight ellipsoidal deformation of the spherically symmetric electron density. Then the mutual energy of the spin magnetic moments will depend on their orientation relative to the symmetry axis. Watanabe[46] made calculations involving the crystal field (cubic with a small axial component), spin-orbit coupling and spin-spin coupling, with the ground and excited spin quartets of the $3d^5$ configuration. Powell et al[47] repeated Watanabe's calculations with the inclusion of the spin doublets of the $3d^5$ configuration. However, none of these calculations produce a value of the Z.F.S. parameter D of the order of several wave-numbers, and therefore are unsuitable for the case of haem-proteins.

Griffith[48] has considered this special case, and he ascribes the large splittings to second order spin-orbit coupling between the ground orbital level $^6A_1$ and the excited $^4T_1$ level, which is grossly split by an axial crystal field. The $^6A_{1g}(t_{2g}^3\ e_g^2)$ ground state has a non zero matrix element of spin-orbit coupling with the $^4T_1\ (t_{2g}^4\ e_g)$ excited state, all other matrix elements with quartet states being zero. Under this perturbation there is a second order correction to the energy of the ground state, but provided that T_{1g} retains its threefold orbital degeneracy, the six spin states of $^6A_1$ are each shifted by the same amount. Thus

in a cubic crystal field, this process will not give a zero field splitting. If the symmetry of the crystal field is reduced the $^4T_1$ state will split into either two or three components. Griffith assumed a large axial splitting, and so considered the $^4A_2$ component of the split $^4T_1$ state only, this lying at a lower energy than the ^2E component. Kotani[49] assumed that the $^4T_{1g}$ state was split into three components by a rhombic crystal field, and considered the interaction of all three with the ground state. In both cases, the second order correction to the energy of the ground state, by the spin-orbit coupling perturbation, results in a splitting of $^6A_{1g}$ into three doublets. If the energies of the three components of the $^4T_1$ level, which is split by the rhombic crystal field, are E_1, E_2, and E_3 above the $^6A_1$ state, then the zero field splitting parameter can be found to be

$$D_2 = \frac{c^2\lambda^2}{3}\left[\frac{1}{E_3} - \frac{1}{2E_1} - \frac{1}{2E_2}\right] \qquad 4.3.$$

where λ is the spin-orbit coupling constant
and c is the percentage of the free ion ^4P level in the lowest $^4T_1$ component, as spin-orbit coupling will only admix this state with ^6S.

Similarly considering an axial field with the $^4T_1$ level split into two components with energies $E(^4A_2)$ and $E(^4E)$.

Then
$$D_2 = \frac{c^2\lambda^2}{3}\left[E(^4E) - E(^4A_2)\right] \qquad 4.4$$

For positive values of D the wavefunction ($\pm\frac{1}{2}$) lies lowest, corresponding to the $^4A_2$ level lying lower than the ^4E

level. This occurs in haemoproteins in which the iron symmetry is tetragonally elongated, while trigonally compressed situations give negative D values. In the tetragonal geometry, a crystal field point charge approach would predict that elongation would stabilize the d_{z^2} orbital relative to the $d_{x^2-y^2}$ and the d_{xz}, d_{yz} pair with respect to d_{xy}. The spin quartet state, corresponding to the first excited state of the molecule, should then correlate with $(xz, yz)^3 (xy)^1 (z^2)^1$, arising from $^4T_1 (t_{2g}^4 e_g^1)$. This level correlates with the ^4E term arising from the octahedral $^4T_1$ (^4G), and the predicted Z.F.S. is with D negative. A reversed ordering of the orbitals d_{xz}, d_{yz}, d_{xy}, leading to the configuration $(xy)^2 (xz, yz)^2 (z^2)^1$ is required to explain the positive spin of D in haemoproteins. Griffith suggested that π - bonding involving donation from the filled ligand π orbital could cause this reversal.

It can be seen that there have been numerous attempts to explain splittings from $3d^5$ ions. Although Grifith's theory provides a suitable explanation for the large Z.F.S. in ferric haem proteins, it is essential to gain accurate values for the Z.F.S. of various haem-protein derivatives to check the validity of this theory.

REFERENCES

1. M.F. Perutz, Nature, 228, pp 726-739, November 21st, 1970.
2. R.J.P. Williams, Fourth International Conference on Magnetic Resonance in Biological Systems (unpublished), September, 1970.
3. R. Banerjee, Y. Alpert, F. Leterrier, R.J.P. Williams, Biochemistry, 8, No.7, July 1969.
4. E. Antonini, E. Bucci, C. Fronticelli, J. Wyman, A. Rossi-Fanelli, J. Mol. Biol., 12, pp 375-384, 1965.
5. R.W. Briehl, H.M. Ranney, J. Biol. Chem., 245, pp 555-8, 1970.
6. Y. Henry, R. Banerjee, J. Mol. Biol., 50, pp 99-110, 1970.
7. R. Banerjee, R. Cassoly, J. Mol. Biol., 42, p 337, 1969.
8. M. Brunori, E. Antonini, J. Wyman, S.R. Anderson, J. Mol. Biol., 34, p 357, 1968.
9. T. Shiga, K.J. Hwang, I. Tyuma, Biochemistry, 8, No.1., January 1969.
10. J. Peisach, W.E. Blumberg, B.A. Wittenberg, J.B. Wittenberg, L. Kampa, Proc. Nat. Acad. Sci. U.S., 63, pp 934-939, 1969.
11. D.G. Davis, S. Charache, C.Ho, Proc. Nat. Acad. Sci. U.S., 63, pp 1403-1409, 1969.
12. E. Loewenthal, W. Low., Biochemica et Biophysica Acta, 194, pp 348-9, 1969.
13. D.G. Davis, N.H. Mock, T.R. Lindstrom, S. Charache, C. Ho, Biochim. Biophys. Res. Commun., 40, No.2, pp 343-349. 1970.
14. C. Ho, D.G. Davis, N.H. Mock, T.R. Lindstrom, S. Charache, Biochim. Biophys. Res. Commun., 38, pp 779-86, 1970.
15. S. Ogawa, R.G. Shulman, R. Kynoch, H. Lehmann, Nature, 225, pp 1042-3, 1970.

16. A. Hayashi, A. Shimizu, Y. Yamamura, R. Watari, Biochim. Biophys. Act., 102, p 626, 1965.

17. A. Hayashi, A. Shimizu, Y. Yamamura, R. Watari, Science, 152, p.207, 1966.

18. D.G. Davis, N.L. Mock, V.R. Lanan, C. Ho, J. Mol. Biol., 40, 311, 1969.

19. A. Hayashi, T. Suzuki, K. Imai, H. Morimoto, H. Watari, Biochim. Biophys. Act., 194, pp 6-15, 1969.

20. K. Imai, H. Morimoto, M. Kotani, S. Shilata, T. Miyaja, K. Matsutomo, Biochim. Biophys. Acta, 200, pp 197-202, 1970.

21. R.Q. Blackwell, H.J. Yang, C.C. Wang, Biochim. Biophys. Acta, 194, pp 1-5, 1969.

22. G. Bemski, R.L. Nagel, Biochim. Biophys. Acta, 154, pp 592-595, 1968.

23. A.H. Ewald, R.L. Martin, I.G. Ross, A.H. White, Proc. Roy. Soc. A280, pp 235-257, 1964.

24. P.S. Braterman, R.C. Davies, R.J.P. Williams, Advances in Chemical Physics, 7, pp 359-407, 1964.

25. L.E. Orgel, "An Introduction to Transition-Metal Chemistry" Methuen.

26. L. Pauling, "The Nature of The Chemical Bond", pp 117-18, 1940, Oxford University Press.

27. J.E. Bennett, J.F. Gibson, D.J.E. Ingram, Proc. Roy. Soc. A240, p 67, 1957.

28. J.E. Bennett, J.F. Gibson, D.J.E. Ingram, T.M. Haughton, G.A. Kerkut, K.A. Munday. Proc. Roy. Soc. A262, pp 395-408, 1961.

29. J.S. Griffith, Proc. Roy. Soc. A235, 23, 1956.

30. J.F. Gibson, D.J.E. Ingram, Nature, 180, pp 29-30, 1957.

31. G.A. Helcke, D.J.E. Ingram, E.F.Slade, Proc. Roy. Soc. B169, pp 275-288, 1968.

32. M. Kotani, H. Morimoto, "Magnetic Resonance in Biological Systems", 9, p 205, 1967.

33. H. Morimoto, M. Kotani, Biochim. Biophys. Acta, 126, pp 176-178, 1966.

34. T. Yonetani, H.R. Drott, J.S. Leigh, G.H. Reed, M.R. Waterman, T. Asakura, J. Biol. Chem. 245, pp 2998-3003, 1970.

35. Y. Morita, H.S. Mason, J. Biol. Chem. 240, p 2654, 1965.

36. W.E. Blumberg, J. Peisach, B.A. Wittenberg, J.B. Wittenberg, J. Biol. Chem. 243, p 1854, 1968.

37. K. Torii, Y. Ogura, J. Biochem. (Tokyo) 64, p 171, 1968.

38. W.E. Blumberg, "Magnetic Resonance in Biological Systems" p 119, 1967.

39. R.D. Dowsing, J.F. Gibson, J. Chem. Phys. 50, No.1, pp 294-303, January 1969.

40. R. Aassa, J. Chem. Phys. 52, pp 3919-30, 1970.

41. J.S. Griffith, Nature, 180, pp 30-31, 1957.

42. W.E. Blumberg, Fourth International Conference on Magnetic Resonance in Biological Systems. (unpublished), September 1970.

43. J.H. Van Vleck, W.G. Penney, Phil. Mag. 7, p 961, 1934.

44. P.H.E. Meijer, Physica, 17, p 899, 1951.

45. M.H.L. Pryce, Phys. Rev., 80, p 1107, 1950.

46. H. Watanabe, Prog. Theor. Phys. 18, p 405, 1957.

47 M.J.D. Powell, J.R. Gabriel, D.F. Johnston, Phys. Rev. Letters, 5, p 145, 1960.

48. J.S. Griffith, "Quantum Aspects of Polypeptides and Polynucleatides", Interscience, New York, 1964.

49. M. Kotani, Advances in Chemical Physics, VII, pp 159-181.

CHAPTER 5

RESULTS FROM SINGLE CRYSTALS OF MYOGLOBIN.

5.1. Introduction

This chapter contains details of the preparation of single crystals of myoglobin, together with experimental techniques used for measurement of angular variation of g-values in a crystal plane, and analysis of such results. A method for measuring the large zero field splitting of myoglobin derivatives is summarized, and the experimental difficulties of such measurements are discussed. The specification of a resonant cavity designed for angular variation studies is given. This cavity was also used for the intensity variation measurements, as well as for studies of myoglobin solutions, which is discussed in Chapter 6. The principal g-values, and directions of principal axes of the fluoride derivative, are determined by measurement of the angular variation of g-values in three crystal planes, and using perturbation theory, the parameter $\lambda = \frac{E}{D}$ is determined. The axial splitting parameter D is determined by measurement of the variation of intensity of the $g_{\perp} = 6$ signal with temperature and hence E is evaluated.

The formate derivative is found to exist in two forms, and the angular variation of these two types was measured in the ab plane. A peculiar spectrum was observed in crystals of both the cyanide and cyanate derivatives. These spectra are shown, and some discussion is given concerning these results.

5.2. Preparation of Single Crystals

Myoglobin will crystallise in several forms depending on the species and the method used to prepare the crystals. The different crystal types have been listed by Kendrew et al[1]. Sperm whale myoglobin was used in these studies, and the crystal form is type A, which is monoclinic with space group $P2_1$. Sperm whale myoglobin is available commercially in a freeze dried form, but unfortunately this has been found to be unsuitable when large crystals are required. The protein was obtained from the manufacturers prior to the freeze drying process in an ammonium sulphate cake. The ammonium sulphate is used in the final stage of fractionation[2].

The following method used to prepare single crystals is that of Kendrew and Parrish[2]. First the ammonium sulphate was removed by dissolving the protein in water and dialysing the solution against distilled, de-ionized water. Approximately 2 gms of myoglobin were prepared at a time, and dialysis of this quantity took about ten days, during which time the solution was kept at $4^{\circ}C$ to prevent denaturation of the protein. When all the salt had been removed the myoglobin solution was diluted until it contained about 5%, by weight, of the protein. About 2 ml of this solution was poured into a vial and to this was added a saturated solution of ammonium sulphate. The ammonium sulphate was previously recrystallised twice in order to remove any impurities. The ammonium sulphate solution was added until the myoglobin solution became turbid. This occurred when

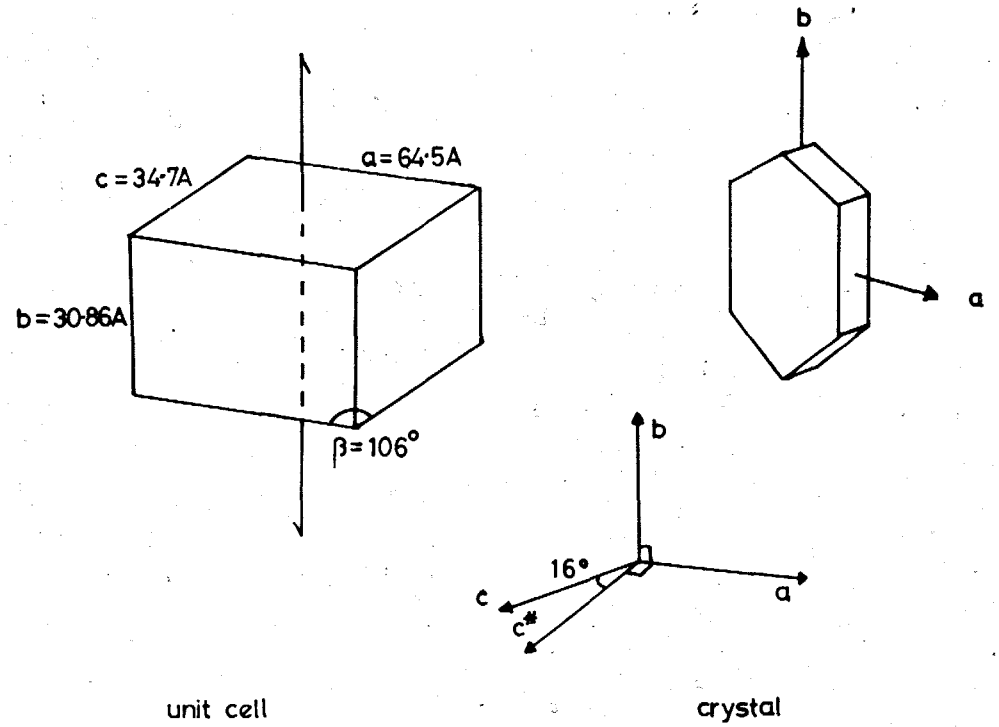

Fig 5·1 TYPE A SPERM WHALE MYOGLOBIN

approximately equal amounts of 5% myoglobin solution and saturated ammonium sulphate solution were mixed. This represented an ammonium sulphate concentration in the final solution of between 2.6 and 3 M. A series of such vials were prepared and buffered to different pH values in the range 5.5 - 7.0. A mixed buffer of sodium di-hydrogen orthophosphate ($Na\ H_2\ PO_4$) and di-potassium hydrogen orthophosphate ($K_2\ HPO_4$) dissolved in distilled and de-ionized water was used. The best results were obtained at pH 6.5, but it was necessary to use a range of pH values as apparent replication of one solution rarely produced the same results. The buffered solutions were then left undisturbed, with the temperature maintained at 20°C, for about ten days. Although Kendrew[2] found that crystallisation was complete within twelve hours, this was not found to be the case for most solutions prepared, and in some solutions myoglobin continued crystallising after three weeks.

The shape of type A crystals is shown in Fig. 5.1. They grow with the (001) face well developed being elongated in the [010] direction at lower pH values. As the pH of the solution approaches 6.5 all faces become equally developed and hence the crystals are more compact. Large crystals were produced by the above procedure with approximate dimensions 2.5 mm x 1.0 mm x 0.75 mm. Sperm whale myoglobin will also form orthorhombic crystals, called type B, when crystallised from a phosphate buffer solution. It is easier to study type A crystals, since they have two molecules per unit cell, compared with four in the orthorhombic

form, and hence the e.p.r. spectrum is more simple.

The crystals grown in this manner are in the acid-met form since a water molecule becomes attached to the sixth co-ordination point of iron during the extraction of the protein from the sperm whale skeletal muscle. It is possible[3] to convert these crystals to other derivatives by adding to the mother liquid (ammonium sulphate solution), the sodium, or potassium salt, of the required ion to a concentration of several milli-molar. By this means the myoglobin derivatives cyanate, formate, acetate, nitrite and fluoride, were prepared in single crystal form.

When sodium cyanide was added to the mother solution the myoglobin molecules were changed to the cyanide form. This could easily be detected by noting a change in colour of the crystals to a deep red. However, it was found that the crystals showed a tendency to crack when converted to the cyanide derivative. This was initially thought to be due to an increase in pH of the solution when sodium cyanide was added. This was found not to be so, so it now seems likely that the explanation is linked with a large conformational change occurring within the molecule when the cyanide ion complexes with the haem group. An alternative method for preparing Mb CN crystals was therefore tried using an ion exchange resin. The ammonium sulphate was removed initially by dialysis, as before, then the myoglobin solution was diluted and allowed to pass through a column of anion-exchange resin (Amberlite IRA - 400 (cl)). This resin had been flushed through

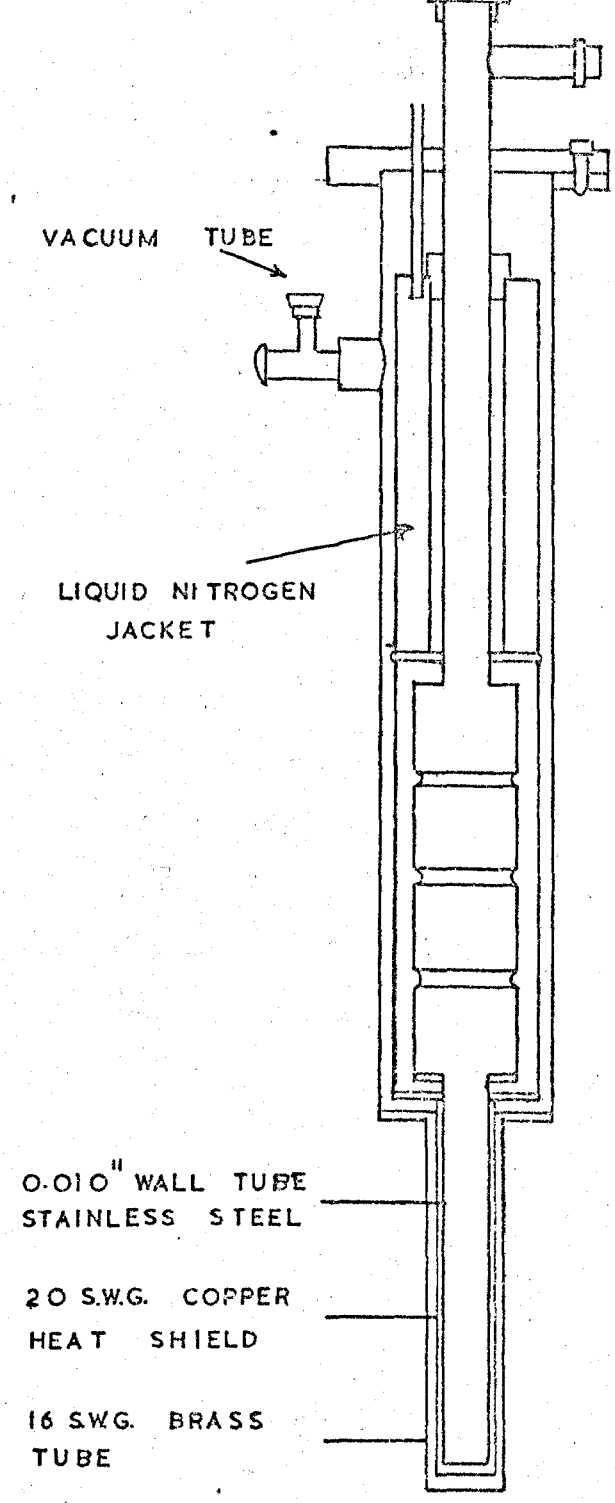

FIG. 5.2 CRYOSTAT USED FOR LIQUID HELIUM STUDIES

with a Na OH solution, followed by a Na CN solution, and finally washed with distilled water. This left CN^- ions attached to the resin which were easily removed by the myoglobin as it travelled down the column.

A cyanide ion was then complexed to the haem sites in each molecule, and crystallisation was achieved as before. Using this technique small crystals of the cyanide derivative were produced, but they were not large enough for e.p.r. studies. Another technique tried was to mount a crystal in position and then place a drop of dilute sodium cyanide solution on the crystal. Again the myoglobin changed to the cyanide derivative, but the crystals tended to crack. A technique called cross-linking[4,5] has been successfully used for strengthening weak protein crystals, and perhaps this could be applied to this problem.

5.3. Experimental Techniques.

Experiments were performed at Q-band microwave frequencies (33.5 G Hz) at both liquid helium and liquid nitrogen temperatures. Studies at 4.2°K were made with the acid of the stainless steel cryostat, shown in Fig. 5.2., whilst at 77°K a simple glass dewar was used. The e.p.r. spectrometer was a simple reflection type using 400 Hz modulation frequency and was essentially the same as shown in Fig. 1.6. A resonant cavity, shown in Fig. 5.3., was designed to operate in the H_{011} mode at 34.5 GHz, when unloaded at room temperature. This frequency was chosen so that the resonant frequency of the loaded cavity between 4.2°K and room temperature

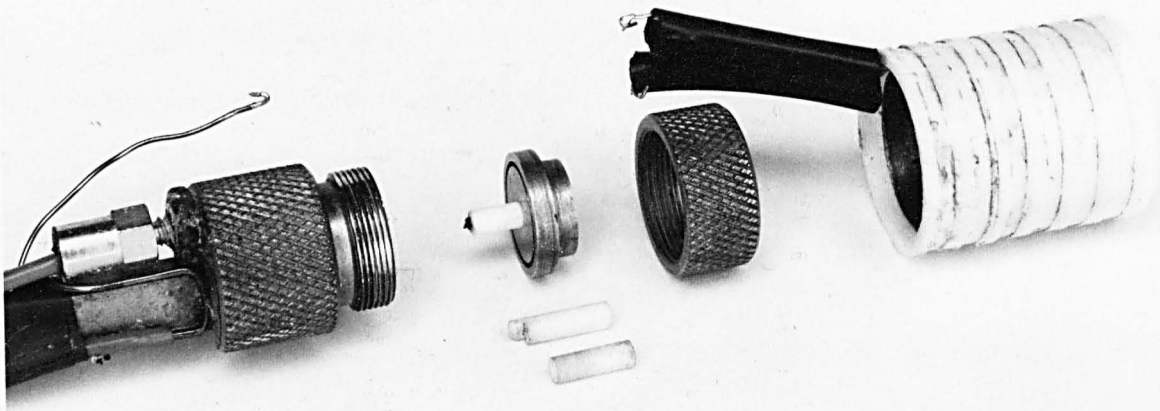

Figure 5.3. O-Band Microwave Resonant Cavity.

would be centred around the maximum power output of the klystron. The cavity was made from high purity brass, with dimensions D = L = 1.14 cms. With the length and diameter of a cylindrical cavity equal, the maximum Q is obtained, and for this cavity a Q factor of 8000 was found initially, although this figure fell with age. In an unloaded cylindrical cavity the H_{011} mode is degenerate with the E_{111} mode, and hence power would be lost to the undesirable E_{111} mode unless it could somehow be quenched. In the E_{111} mode currents flow around the inside wall of the cavity and across the base, thus, by introducing a circular groove around the base of the cylinder, these currents are reduced. Hence the Q of this mode will be reduced allowing power to build up in the H_{011} mode at the expense of the E_{111} mode.

Myoglobin crystals were mounted in the centre of the resonant cavity on a small peg, made of a low dielectric, low loss material (Stycast). The peg fitted into a hole in the base of the cavity, as shown in Fig. 5.3. Crystals were aligned with the aid of a stereoscopic microscope, and were affixed to the mount by means of a smear of silicon grease. For angular variation of g values measurements in the a b plane, a crystal was mounted with the a b plane, flat on the surface of peg 1. A 90° wedge was used for measurements in the b c^* plane and c^*a plane. An a b (001) face of the crystal was mounted flat on the face of the wedge with the b axis horizontal for b c^* plane studies, and vertical for measurements in the c^*a plane.

Alignment could be achieved to an accuracy of about ±2°, although for studies in the a b plane any large misalignment

could be detected from assymetry of the g-value variations for the two sites in the crystal. Similarly in the c^*a plane, the angular variation of g values is identical for the two sites in a unit cell, so the spectra overlap, and any misalignment causes the spectra of the two sites to separate.

A very small amount of dpph was introduced beside the crystal, and g-values were measured by comparing the magnetic field values of the resonance of dpph (g = 2.0035) and myoglobin. The magnetic field value was measured by two means;

(i) Hall probe (Hp2C3 50 mv/mA T)

(ii) Proton resonance.

The former method was used in experiments performed at $4.2^{\circ}K$, since the liquid helium cryostat necessitated a magnet pole gap greater than 4.45 cm. To achieve the necessary magnetic field strength the magnet pole faces had to be small (6.5 cm diameter), and this prevented the insertion of a proton resonance probe between the faces. in a position where the field inhomogeneities were small enough to be able to detect the proton resonance signal. The diameter of the glass dewar used for liquid nitrogen was 3 cms, and hence larger pole tips (11.8 cms diameter) were used allowing space for a proton resonance probe. The proton resonance unit incorporated the transistor limiter oscillator circuit devised by Robinson.[6] Fine adjustment of the frequency was achieved by altering the potential across a varicap (SGS Fairchild BBY - 15), which was placed parallel with the LC tank circuit. The frequency of the r.f. circuit was displayed directly

by feeding the signal from an arial to a counter (Hewlett Packard 5246 L). A field profile was plotted across the pole faces to allow for any field inhomogeneities, so that corrections could be made for the magnetic field at the crystal, compared with the magnetic field at the measuring point.

5.4. Angular Variation Studies in Three Planes.

The magnetic axes of high spin myoglobin derivatives bear no immediate relationship to the crystal axes, and therefore to determine the principal g-values, and directions of the principal axes, it is necessary to measure the angular variation in three mutually perpendicular planes. Now it is known that high spin myoglobin derivatives can be described by a spin Hamiltonian of the form

$$\mathcal{H} = \beta\, \bar{S}.\bar{\bar{g}}.\bar{B} + D(S_z^2 - \tfrac{1}{3} S(S+1)) + E(S_x^2 - S_y^2)$$

In order to determine the parameters g, D, E it would be necessary to perform a transformation from the principal axes to the axis system of the crystal. Since this transformation is not known it would be extremely difficult to determine the true spin Hamiltonian and directions of the principal axes from angular variation measurements. However, we can simplify the task by assuming D is very large, so that we may describe the spectra from the lowest Kramers doublets by a spin Hamiltonian containing the Zeeman term only.

$$\mathcal{H} = \beta\, \bar{S}.\bar{\bar{g}}.\bar{B} \qquad 5.1$$

then if we define an effective g value as $g_{eff} = \frac{h\nu}{\beta B}$

it can be shown that (see p.44)

$$g_{eff}^2 = g_x^2 l^2 + g_y^2 m^2 + g_z^2 n^2 \qquad 5.2$$

When we are not working in the principal axis system of the spin S equation 5.2 is no longer valid, and we must expand 5.2 in the form[7]

$$g_{eff}^2 = \sum_{ij=1}^{3} G_{ij} l_i l_j \qquad 5.3$$

where G_{ij} is a symmetric tensor whose value depends on the choice of reference axes and l_i l_j are the direction cosines of the magnetic field with respect to the reference axes. In component form this can be written as

$$g_{eff}^2 = G_{aa} l_a^2 + G_{bb} l_b^2 + G_{cc} l_c^2 + G_{ab} l_a l_b + 2 G_{bc} l_b l_c + 2 G_{ca} l_c l_a \qquad 5.4.$$

where l_a, l_b, l_c are the direction cosines of the applied magnetic field with respect to the crystallographic axes a b c and G_{aa} etc. are elements of the symmetric tensor $\bar{G} = \bar{g}.\bar{g}$.

For the monoclinic crystal of myoglobin the orthogonal axes chosen were a [100], b [010] and c^*, where c^* is mutually perpendicular to a and b. The angular variation of g-values was determined in three planes, and for each plane equation 5.4. can be simplified so that g_{eff} is a function of one angle θ only.

For the a b plane we have

$$g^2 = G_{aa} \cos^2 \theta + G_{bb} \sin^2 \theta + 2 G_{ab} \cos \theta \sin \theta \qquad 5.5.$$

the tensor components were determined by performing a least squares fit upon the measured angular variation of $g_{eff}(\theta)$. This calculation is given in Appendix 2. Measurement of the g-value variation in three planes determined the six independent coefficients G_{ij} relative to the axes a b c^*. The principal g-values and principal axes are formed by diagonalising the matrix G. The three roots λ_1 λ_2 λ_3 of the secular equation

$$\det (A - \lambda I) = 0 \qquad 5.6.$$

are the squares of the principal g-values; the direction cosines of the principal axes satisfy

$$\sum_{j=1}^{3} G_{ij} l_{kj} = \lambda_k l_{ki} \qquad i = 1, 2, 3 \qquad 5.7.$$

where the l_{kj} (j = 1, 2, 3) are the direction cosines corresponding to the root λk.

The crystal axes directions were determined from the cross-over point of the resonance lines from the two sites in the crystal. Since the crystal structure is P_{21} there is a screw diad axis parallel to the b axis. Therefore if one haem plane is rotated through 180^o and translated through a distance $b/2$ it will be coincident with the other haem plane in that unit cell. So the e.p.r. spectra will be symmetrical about the b axis, and will be identical in the c^*a plane. Hence the g-values of the two sites

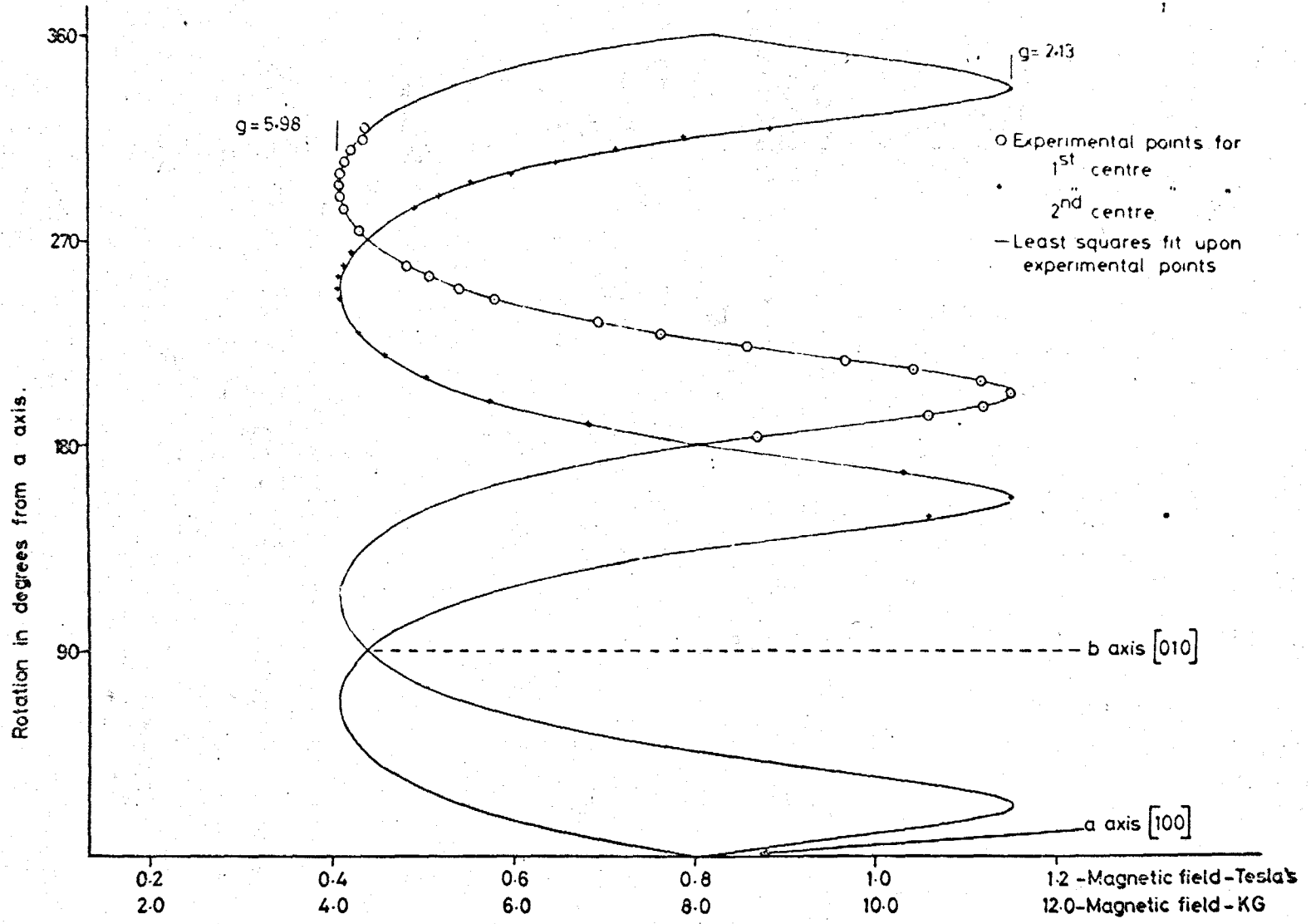

FIG 5·4 Angular Variation of the Fe^{3+} Spectrum of Myoglobin Fluoride in the ab plane at Q-band.

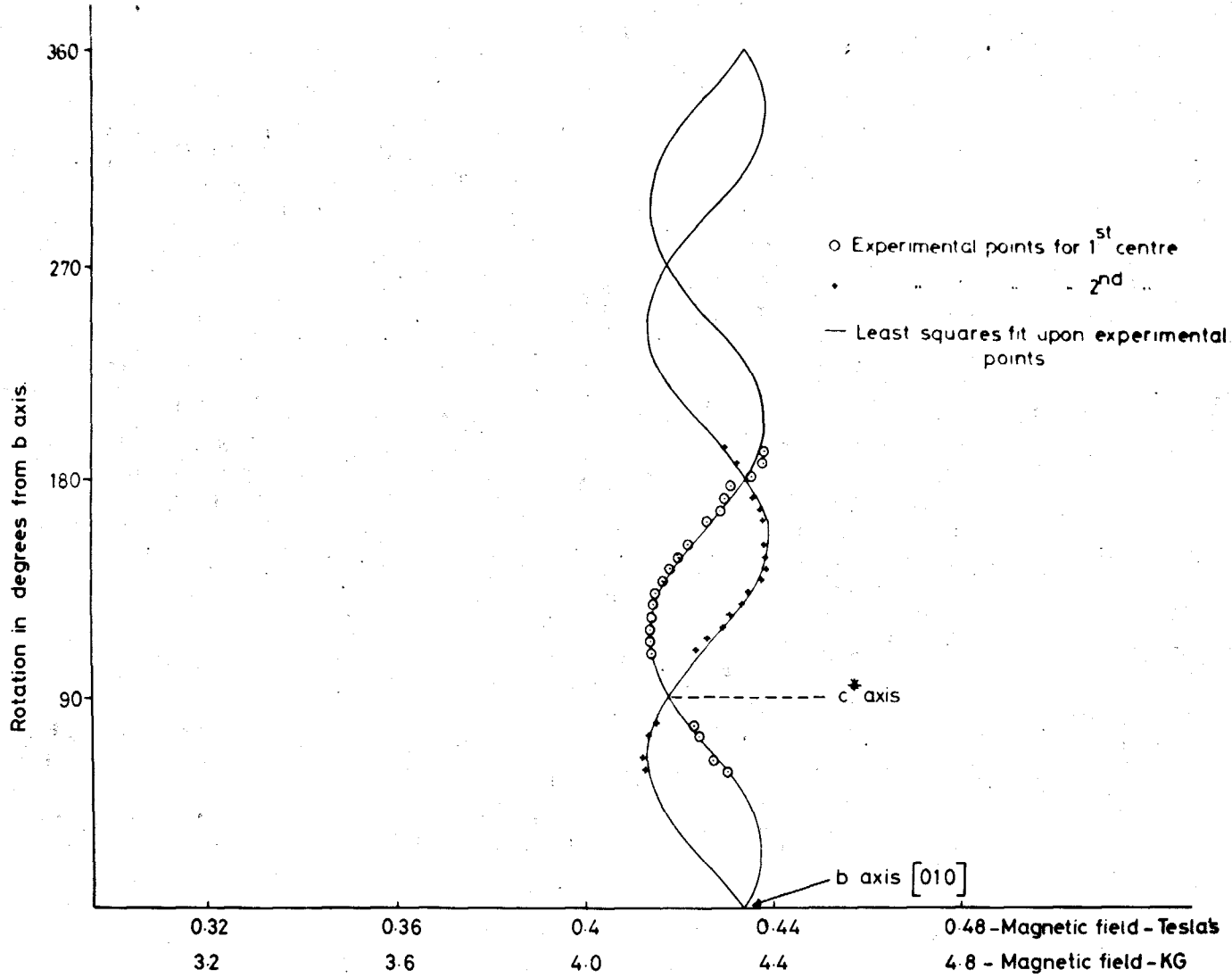

FIG 5·5 Angular Variation of the Fe^{3+} Spectrum of Myoglobin Fluoride in the bc* plane at Q - band.

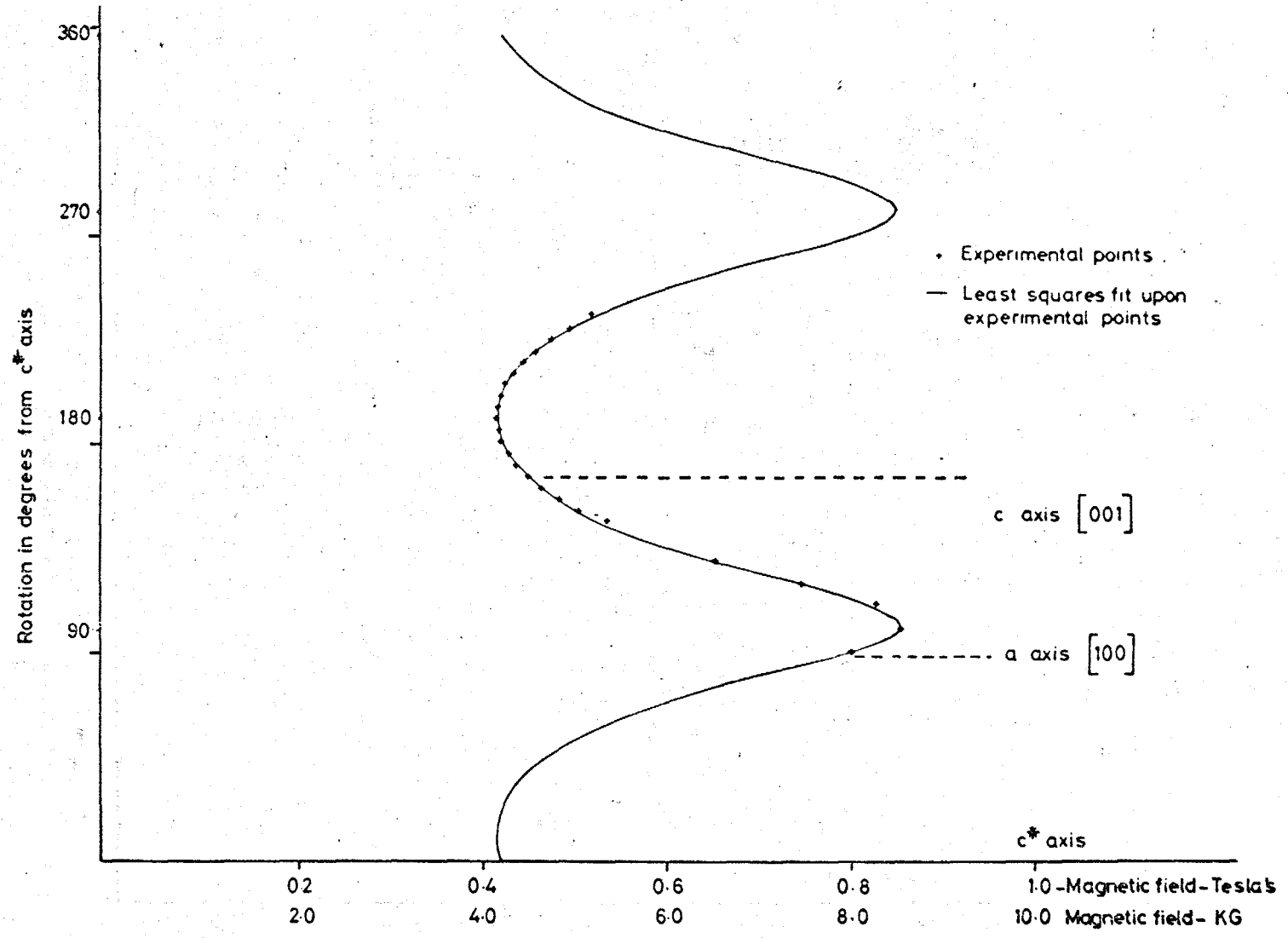

FIG 5·6 Angular Variation of the Fe^{3+} Spectrum of Myoglobin Fluoride in the c^*a plane at Q-band.

are coincident along the a and c^* axes, and therefore they must be the same along the b axis. Therefore in the a b plane the plot of angular variation of g-values for the two sites will cross when the magnetic field is along the a and b axes, and hence $\theta = 0$ and 90° are determined. Also in the b c^* plane the lines cross along the b and c^* axes, but for the c^* plane where the angular variation of g values is the same for the two sites, the zero angle was determined from the corresponding g-values along the a and c^* axis as determined from the other two planes.

5.5. Experimental Results for Fluoride Derivative.

The angular variation of g-values in three planes for the fluoride derivative are given in Figs. 5.4 - 5.6. The components of the tensor G, determined by a least squares fit to the experimental data, are given in table 5.1. Also in table 5.1 are the corresponding principal g-values and direction cosines of the principal axes with respect to the crystal axes a, b, c^*. It can be seen that the two e.p.r. lines are nearly coincident in the b c^* plane, and because of their broad linewidths, the two lines merge into one, so that there is an error of about ±20 gauss incurred in determination of the crossover point of the first derivative of the resonance line. The situation is further complicated by the linewidth of the two resonance lines varying with orientation. In the a b plane the main error will arise from any misorientation of the crystal, but the large linewidths found also prevent accurate measurement of g-values. The variation of linewidth with orientation is shown in Fig. 5.8.

TABLE 5.1.

G-VALUES AND DIRECTIONS OF PRINCIPAL AXES FOR THE TWO MOLECULES PER UNIT CELL IN THE FLUORIDE DERIVATIVE OF SPERM-WHALE MYOGLOBIN.

(a) G tensor components from measurements in 3 crystal planes for first site.

$G_{XX} = 9.28$ $G_{XZ} = G_{ZX} = 5.25$

$G_{XY} = G_{YX} = 10.50$ $G_{ZY} = G_{YZ} = -1.41$

$G_{YY} = 31.13$ $G_{ZZ} = 33.53$

Principal g-values

$g_x = 5.85$, $g_y = 5.98$, $g_z = 2.00$, ± 0.005

Directions of Principal Axes

	a	b	c*
PX	92°	120°	30°
PY	66°	38°	62°
PZ	24°	111°	100°

(b) G tensor components from measurements in 3 crystal planes for second site

$G_{XX} = 9.28$ $G_{XZ} = G_{ZX} = 5.25$

$G_{XY} = G_{YX} = -10.64$ $G_{YZ} = G_{ZY} = 1.55$

$G_{YY} = 31.13$ $G_{ZZ} = 33.53$

Principal g-values

$g_x = 5.85$, $g_y = 5.98$, $g_z = 2.00$, ± 0.005

Directions of Principal Axes

	a	b	c*
PX	90°	63°	26°
PY	114°	35°	114°
PZ	24°	68°	100°

which is similar to that found in the case of acid met myoglobin. This has been discussed by Helke, Ingram and Slade[8], who showed that the linewidth ΔH is proportional to the rate of change of g with θ, due to scatter in the orientations of the haem groups within a crystal.

In the xy plane the angular variation of effective g-values can be described by

$$g_{eff} = 3g_o \left(1 - \frac{4E}{D} \cos 2\phi\right) \qquad 5.8.$$

Where ϕ is the angle in this plane, measured from gx, E is the rhombic component of the electric field and D is the tetragonal component, g_o is the true g-value in the Hamiltonian and is ~ 2.00. Therefore in the xy plane the effective g-values will vary between the values

$$g_x = 3g_o \left(1 - \frac{4E}{D}\right)$$

and

$$g_y = 3g_o \left(1 + \frac{4E}{D}\right) \qquad 5.9.$$

From the measurements of g_x and g_y for the fluoride derivative we can obtain the value of $\lambda = \frac{E}{D}$ with the aid of equations 5.9.

$$\lambda = \frac{(g_x - g_y)}{4(g_x + g_y)} = 0.0027 \text{ cm}^{-1} \qquad 5.10.$$

Therefore the rhombic component in this derivative is very small as is obvious from the small difference between g_x and g_y.

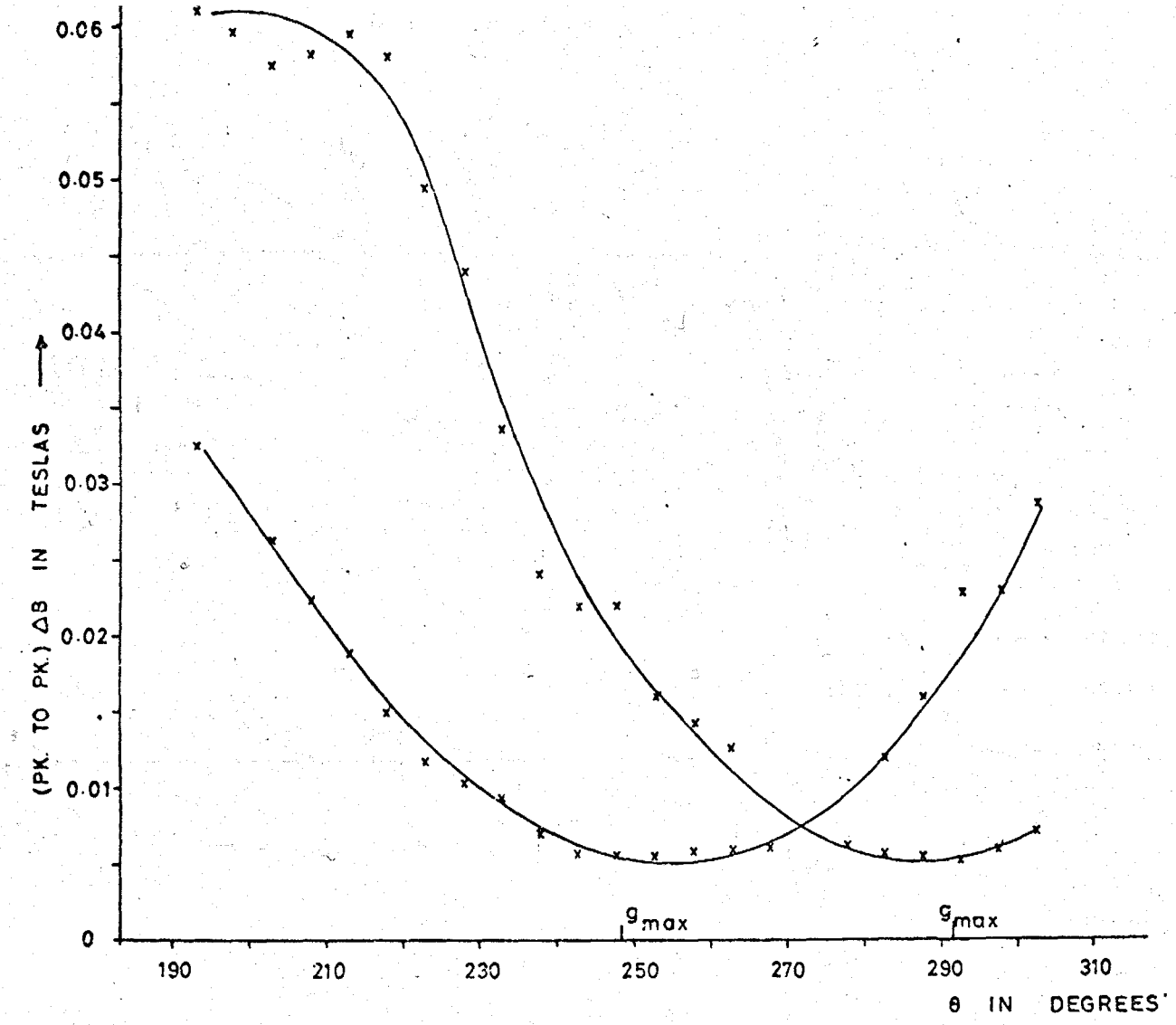

FIG. 5.8 VARIATION OF LINEWIDTH WITH ORIENTATION IN THE ab PLANE

which is similar to that found in the case of acid met myoglobin. This has been discussed by Helke, Ingram and Slade[8], who showed that the linewidth ΔH is proportional to the rate of change of g with θ, due to scatter in the orientations of the haem groups within a crystal.

In the xy plane the angular variation of effective g-values can be described by

$$g_{eff} = 3g_o \left(1 - \frac{4E}{D} \cos 2\phi\right) \qquad 5.8.$$

Where ϕ is the angle in this plane, measured from gx, E is the rhombic component of the electric field and D is the tetragonal component, g_o is the true g-value in the Hamiltonian and is ~ 2.00. Therefore in the xy plane the effective g-values will vary between the values

$$g_x = 3g_o \left(1 - \frac{4E}{D}\right)$$

and

$$g_y = 3g_o \left(1 + \frac{4E}{D}\right) \qquad 5.9.$$

From the measurements of g_x and g_y for the fluoride derivative we can obtain the value of $\lambda = \frac{E}{D}$ with the aid of equations 5.9.

$$\lambda = \frac{(g_x - g_y)}{4(g_x + g_y)} = 0.0027 \text{ cm}^{-1} \qquad 5.10.$$

Therefore the rhombic component in this derivative is very small as is obvious from the small difference between g_x and g_y.

In table 5.2. the coordinates of the atoms in the haem group, as obtained by X-ray studies, are given. The direction of the normal to the haem plane, formed by the four nitrogen atoms N_1, N_2, N_3, N_4 is also listed. The z axis of the g-tensor is found to be almost along the direction of the haem normal, the angle between the two being 5°. Therefore the x and y axes of the g-tensor virtually lie in the haem plane. Figure 5.9. shows the directions of g_x and g_y with respect to the four nitrogen atoms. Also the directions of the principal axes are shown relative to the orthogonal crystal axes a, b, c*. A comparison can be made between the directions of g_x and g_y for the fluoride and acid-met derivatives and it is found, as shown in figure 5.9, that a rotation of 18° occurs between the axes of one derivative and the other.

5.6. Formate Derivative.

E.P.R. studies of single crystals of the formate derivative (axial ligand HCO_2) were undertaken in the ab and bc* planes at 4.2°k. The spectrum was found to consist of four lines, the angular variation of these lines in the ab plane is shown in figure 5.10. These results suggest the presence of two high spin forms of myoglobin present in the same crystal. Unfortunately angular variation measurements in the ab plane were limited to orientations of approximately 90° about g = 6, because at lower g-values broadening of the absorption line ensued and this broadening combined with the low signal intensity made g-value

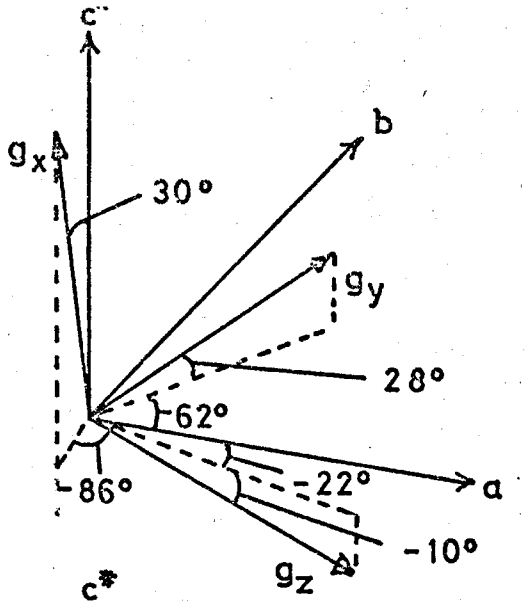

1st. Centre

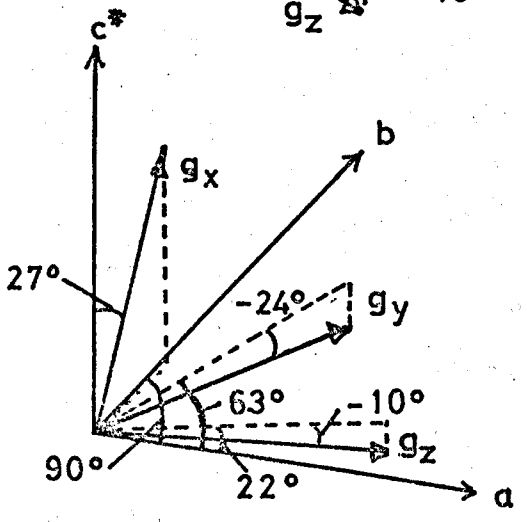

2nd. Centre

(a) DIRECTIONS OF MAGNETIC AXES W.R.T. CRYSTAL AXES FOR FLUORIDE DERIVATIVE

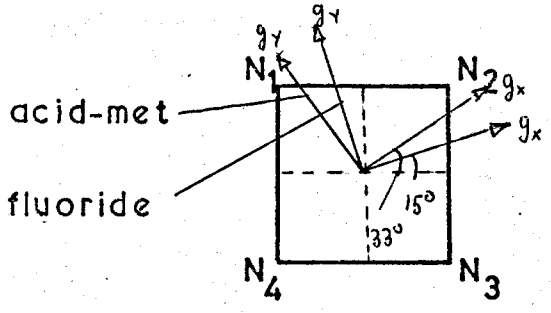

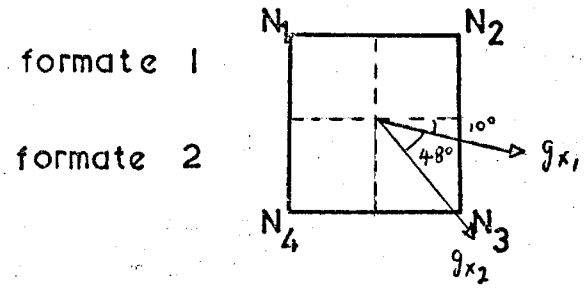

(b). DIRECTIONS OF g_x AND g_y IN HAEM PLANE

FIG. 5·9

TABLE 5.2

CO-ORDINATES OF ATOMS (Å) IN HAEM GROUP OF SPERM-WHALE MYOGLOBIN FROM X-RAY DATA

	a	b	c*
N_1	14.08	26.77	6.15
N_2	14.92	26.65	3.44
N_3	15.96	29.30	3.62
N_4	15.09	29.43	6.33
Fe	14.77	28.13	4.81
HYSTIDINE			
N	10.96	29.63	4.83
C_1	12.10	29.32	5.42
N_2	12.90	28.75	4.48
C	12.22	28.72	3.30
C	11.00	29.27	3.50
O_{XY}	16.74	26.84	4.86

The direction of the normal to the haem plane is

$$\alpha = 27.82^\circ$$

$$\beta = 111.95^\circ$$

$$\gamma = 73.75^\circ$$

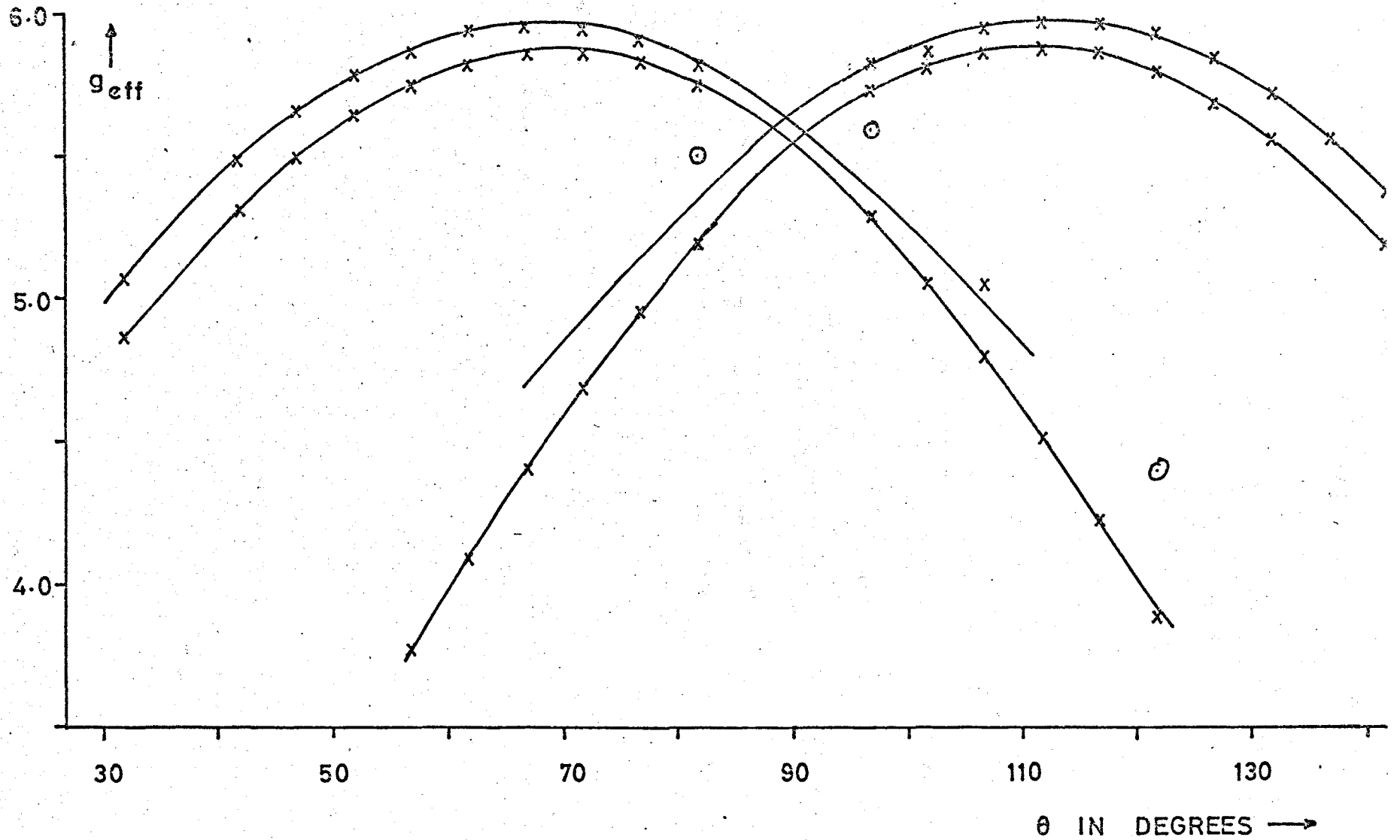

FIG. 5.10 ANGULAR VARIATION OF G VALUES OF MYOGLOBIN FORMATE IN THE ab PLANE

measurements impossible. At all orientations overlapping occurred between the two pairs of lines causing difficulty in one analysis of the spectra. Orientation of the magnetic field in the bc* plane produced a broad line, which was the envelope of the four resonance lines. Small variation in position and height of this broad line prevented any analysis being made in this plane.

The method of analysis used for the fluoride derivative, involving measurements in three planes, could not be applied in this case. Therefore the data obtained from measurements of the g-value variation in the ab plane was used to determine the principal g-values and orientations of principal axes.

Now at any orientation of the magnetic field the effective g-value is given by

$$g^2_{eff} = g_x^2 l^2 + g_y^2 m^2 + g_z^2 n^2 \qquad 5.11$$

where l m n are the direction cosines of the magnetic field with respect to the principal magnetic axes. Putting this into polar coordinates we have

$$g^2_{eff} = \sin^2 \eta(g_x^2 \cos^2 \phi + g_y^2 \sin^2 \phi) + g_z^2 \cos^2 \eta \qquad 5.12$$

where η, ϕ are the polar angles of B with respect to the principal axes. Assuming the magnetic z axis lies along the direction of the haem normal we can calculate for any orientation (θ) in the ab plane the corresponding value of η. Assuming that for the formate derivative $g_z = 2$ we can calculate the g-value (g_h) in the xy

plane, which in this case we have assumed to be the haem plane. Then in the haem plane

$$g_h^2 = g_x^2 \cos^2 \phi + g_y^2 \sin^2 \phi \qquad 5.13$$

Unfortunately we do not know the directions of gx and gy in the plane, but we can take as a reference point the projection of the crystal a axis onto the haem plane and then 5.13 can be expressed as

$$g_h^2 = g_x^2 \cos^2 (\phi + \varepsilon) + g_y^2 \sin^2 (\phi + \varepsilon) \qquad 5.14$$

This can be expanded into the form

$$\begin{aligned} g_h^2 = {} & (g_x^2 \cos^2 \varepsilon + g_y^2 \sin^2 \varepsilon) \cos^2 \phi \\ & + (g_x^2 \sin^2 \varepsilon + g_y^2 \cos^2 \varepsilon) \sin^2 \phi \\ & + 2(g_x^2 - g_y^2) \sin \varepsilon \cos \varepsilon \sin \phi \cos \phi \end{aligned} \qquad 5.15$$

This is of the same form as equation 5.5. and hence the same least squares procedure was used to fit the values of g_h^2 to an equation

$$g_h^2 = G_1 \cos^2 \phi + G_2 \sin^2 \phi + G_3 \sin \phi \cos \phi \qquad 5.15$$

By equating coefficients it is found that

$$\begin{aligned} \tan 2\varepsilon &= \frac{G_3}{G_1 - G_2} \\ g_x^2 + g_y^2 &= G_1 + G_2 \\ \tan^2 \varepsilon &= \frac{G_2 - g_y^2}{G_1 - g_y^2} \end{aligned} \qquad 5.16$$

MYOGLOBIN FORMATE RESULTS

Line 1.

G_1	= 30.915	g_x	= 5.52
G_2	= 34.752	g_x	= 5.94
G_3	= -1.236	ε	= 18°

Line 2.

G_1	= 36.413	g_x	= 5.87
G_2	= 35.300	g_y	= 6.06
G_3	= -1.238	ε	= 66°

TABLE 5.3.

Hence g_x and g_y and ε can be determined where ε is the angle between g_x and the projection of the a axis onto the haem plane.

The results for the two sets of lines are given in table 5.3, and the directions of the principal axes are shown with respect to the four nitrogen atoms in the haem plane in figure 5.9. It is interesting to note that there is a rotation of 48° between the axes in the two derivatives.

5.7 Cyanide and Cyanate Derivatives

The e.p.r. spectrum of myoglobin cyanide (axial ligand CN^-) as shown in figure 5.11. This strange signal was not a first derivative of the absorption as it should have been. The signal moved with orientation of the magnetic field, but such signals were not necessarily reproducible with different crystals. It was thought that these signals were the result of some saturation phenomena, and therefore the temperature of the myoglobin crystal was raised in order to shorten τ_1, the spin-lattice relaxation time. However, the signal disappeared at a temperature in the range $10\text{-}20^{\circ}K$. Difficulties in g-value measurements of the myoglobin cyanide have been encountered by other workers. Peisach[10] resorted to a pulse technique in order to obtain approximate g-values from a paste.

The spectra of the cyanate derivative (axial ligand OCN^-) shown in figure 5.12, is similar to that of myoglobin cyanide, but in addition there is a signal varying about g = 6.

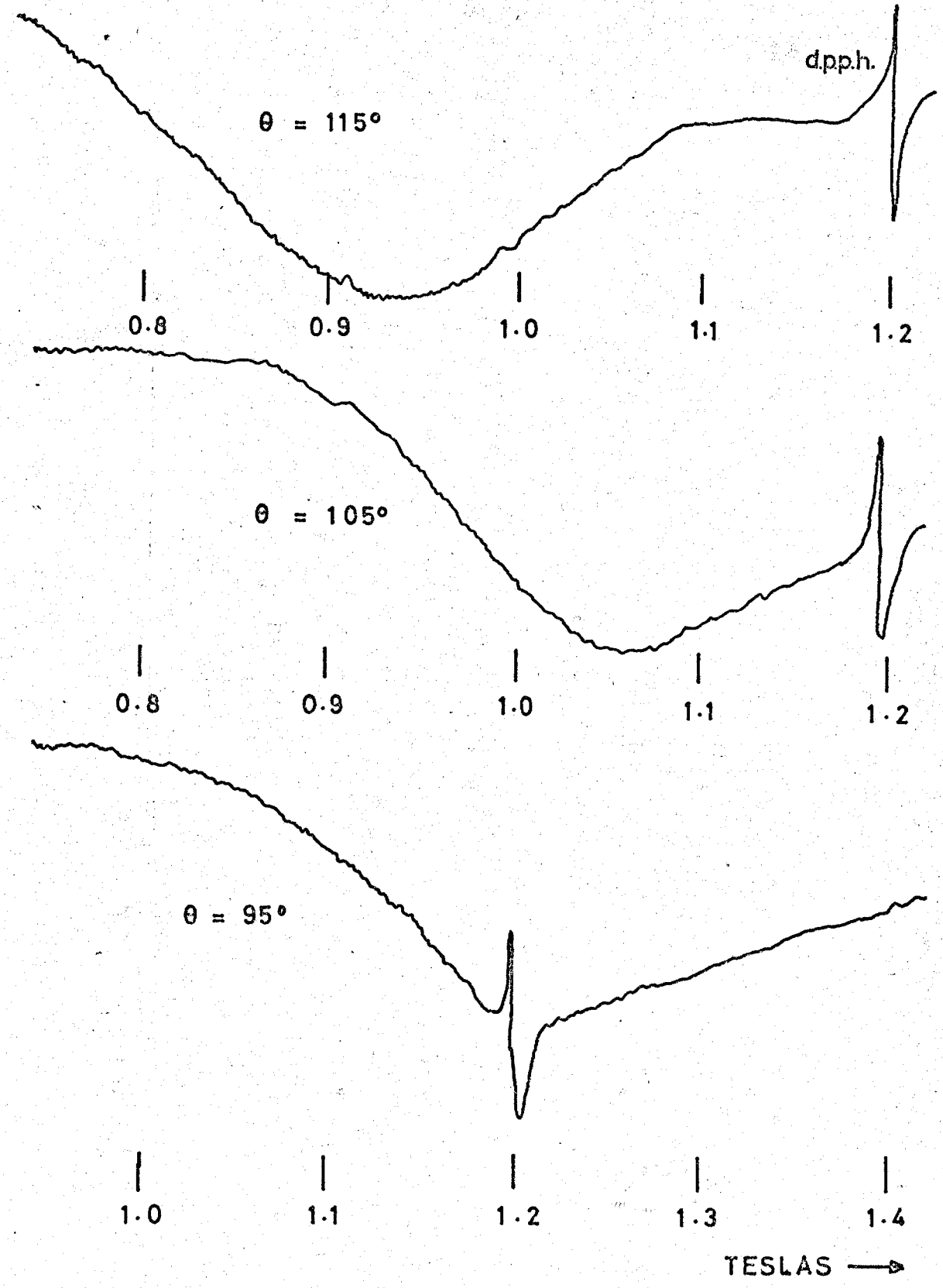

FIG. 5·11 SIGNALS OBSERVED FROM CYANIDE DERIVATIVE

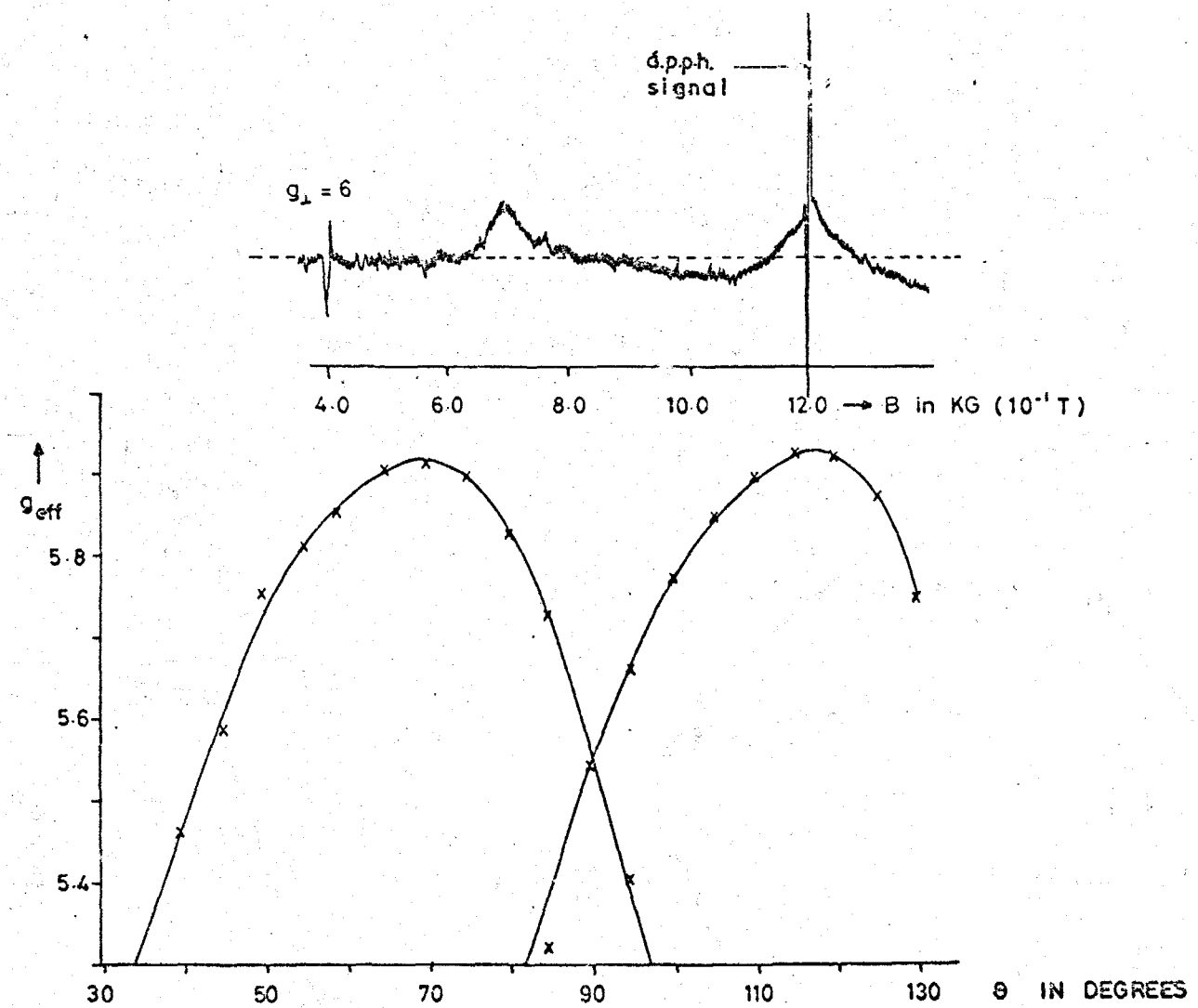

FIG. 5.12 (a) SPECTRUM FROM A SINGLE CRYSTAL OF MYOGLOBIN CYANATE AT 4.2°K.

(b) ANGULAR VARIATION OF HIGH SPIN SIGNAL

This suggests that, as found in the formate crystals, there are two ferric centres present. One of these is a low spin state, and the other a high spin state. The angular variation of the high spin form around g = 6 is also shown in figure 5.12. These measurements were made at 4.2°K. This compound has been found to be anomalous by Scheler[11]. He found that he could correlate optical absorption measurements with magnetic susceptibility results for all derivatives of myoglobin other than cyanate.

5.8. Temperature Variation Studies.

Accurate measurement of the zero field splitting in high spin haem-proteins is difficult, since only one transition is observed using normal microwave frequencies. This transition is between the lowest Kramer's doublets and the effective g-values for this transition are relatively insensitive to variations in the zero field splitting (for values of D in excess of 2 cm^{-1}). In Chapter 6 estimations are made for the zero field splitting parameter D. in certain myoglobin derivatives, from a change in effective g-values with change of microwave frequency. Third-order perturbation theory predicts a reduction in effective $g_\perp$ with increasing microwave frequency in a manner dependant on D.[12] Another technique applied by Feher[13] involved a high resolution Fourier transform spectrometer. He determined the Z.F.S. for chlorahemin (2D = 13.9 cm^{-1}) by detecting a sub-millimeter absorption line corresponding to a direct transition between the ground and first excited Kramer's doublets.

In these studies the zero field splitting of the acid-met and fluoride derivatives were estimated from the temperature dependance of the intensity of the g = 6 signal. A single crystal was rotated in the ab plane until the maximum g-value position was found. The energy levels for this situation will be approximately as shown in figure A2. Now the intensity of the transition between the lowest doublet will vary with temperature in a manner dependant on the splittings between the Kramers doublets. The variation of the intensity of this signal was compared with that of a carbon standard which is a simple two level system, and from these measurements the zero field splitting parameter D can be calculated. The calculations are given in Appendix 3.

A myoglobin crystal was mounted on a hollow support with the ab plane horizontal. The centre of the support was filled with a powdered carbon standard in french chalk. This was chosen in preference to d.p.p.h. as it obeys Curie's law, whereas d.p.p.h. has been found in some instances, depending on the preparation, to be antiferromagnetic.[14, 15, 16].

Around the cavity was wrapped a 5Ω heater coil, which in turn was enveloped by a corrugated teflon sheath, shown in figure 5.3. The temperature of the sample was controlled by a Euratherm thyristor temperature controller (DHS/PID/SCR), with a gallium doped germamium thermometer (T.I. type RT-106) acting as the sensing element. The temperature controller incorporated three term control (proportional, derivative and integral), and by adjustment of the time constants of the derivative and

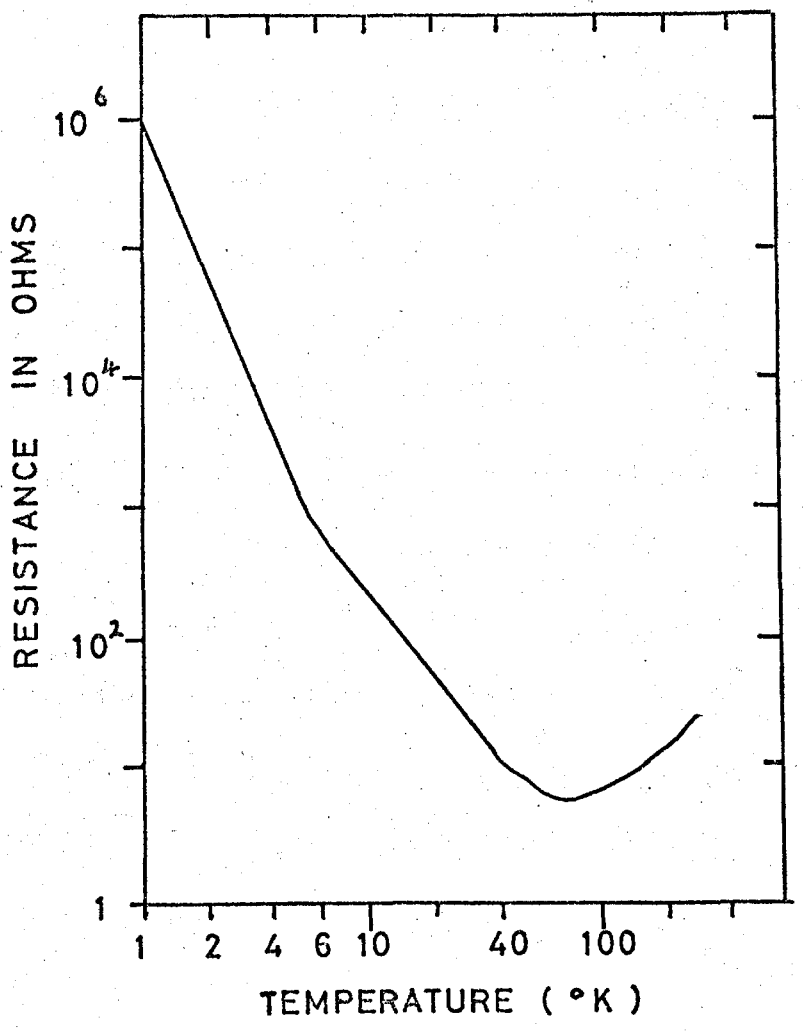

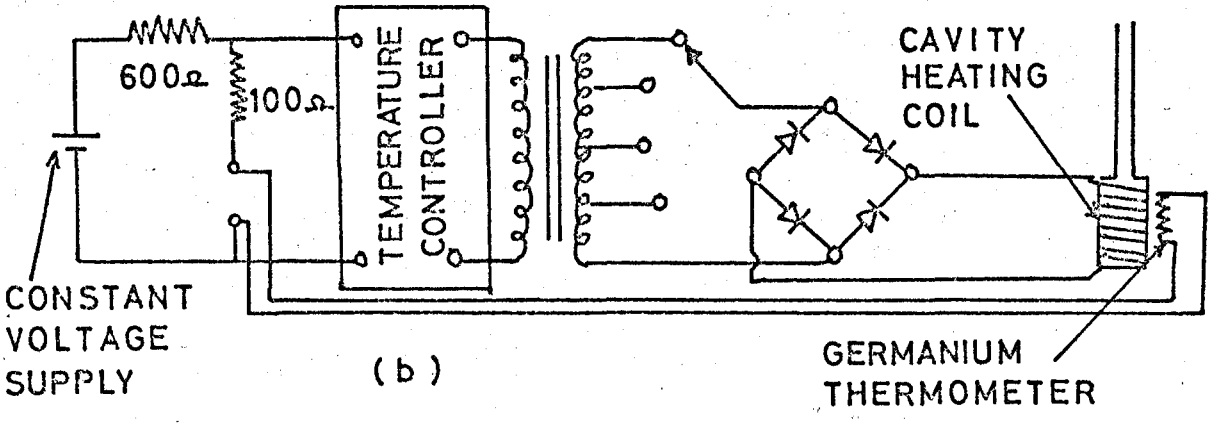

FIG. 5·13 (a) RESISTIVITY CHARACTERISTIC OF A GERMANIUM THERMOMETER

(b) TEMPERATURE CONTROL SYSTEM

and integral damping it was possible to maintain the temperature of the cavity within $\pm$ 0.2° C. A germanium thermometer was fixed to the top of the cavity with one lead, that was in good thermal contact with the germanium element, attached to the cavity by a sout copper wire. The copper wire was araldited to the top of the cavity to ensure good thermal contact, and the thermometer and lead were encapsulated in expanded polystyrene.

Using the circuit shown in figure 5.13, the variation in resistance of the thermometer between 4°K and 40°K produced an e.m.f. variation across the input of the temperature controller of 10 mV, thus utilising the full range of the controller. The sensitivity was therefore far greater than could be achieved using a thermocouple, since the most sensitive couple at these temperatures[17] (gold-chromel) only has an average thermoelectric output of about 15μV $^{o}K^{-1}$.

The magnet was rotated until the maximum g-value position was found. Assuming the system to be axial, the magnetic field was then in the $g_{\perp}$ plane. Three successive sweeps were made of the $g_{\perp}$ = 6 signal of myoglobin, and also of the carbon signal at g = 2. The temperature was raised from 4.2°K up to 30°K in 2° intervals, and the myoglobin and carbon signals were recorded at each temperature.

5.9. Zero Field Splitting Measurements

To determine zero field splittings from temperature variation studies of myoglobin it was necessary to calculate the

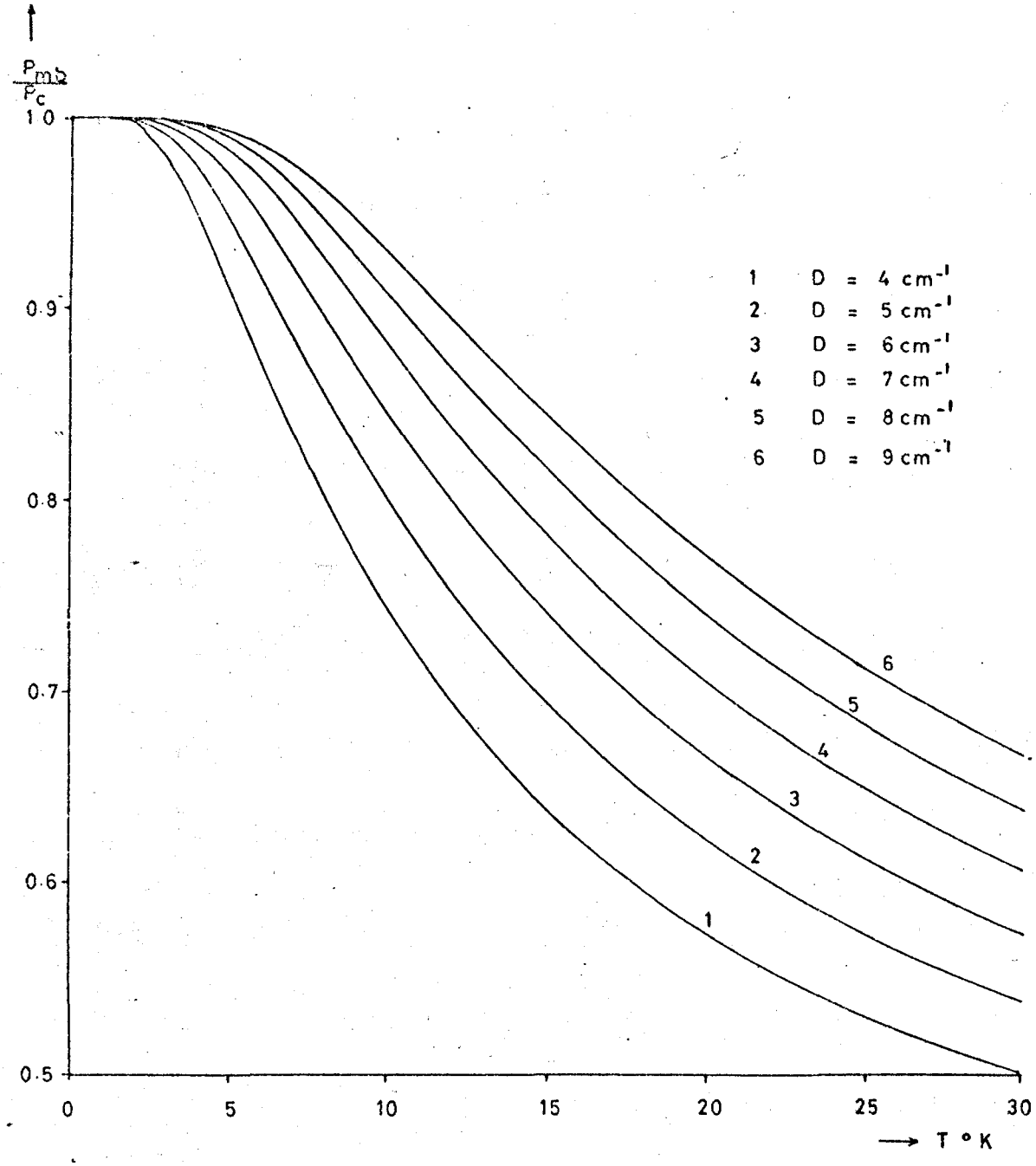

FIG. 5.14 VARIATION OF INTENSITY OF $g_\perp = 6$ SIGNAL WITH TEMPERATURE FOR DIFFERENT ZERO FIELD SPLITTINGS.

intensity of the signals from the first derivative of the absorption tracings. Several approximation methods[18, 19] have been devised for determining the intensity of an absorption from the first derivative signal for both Gaussian and Lorentzian lineshapes. The intensity is usually taken as being proportional to hw^2 or to D^2/h where h is the peak to peak height, $2w$ is the peak to peak width, and D is the total area under the first derivative envelope. The validity of these approximations is discussed by McLintoch and Orr.[20]

In these studies a double integration was performed on each first derivative signal. The coordinates of the line envelope were put on to paper tape using a DMac machine, and integration was performed numerically on a computer. The results for the acid-met derivative are shown in figure 5.15. It is seen that the results are scattered, even though the average of three readings at each temperature was taken. The results were too scattered to obtain a least squares fit to them, but, as shown, by measuring the mean deviation, and mean square deviation, of the experimental points from various computed lines, using different values of D, a significant result was obtained. For the acid-met derivative the best fit obtained was for $D = 5\ cm^{-1}$, whilst in the fluoride derivative the best fit was for $D = 4\ cm^{-1}$! These values are lower than those obtained by Kotani et al,[21] these being 9.6 ± 0.5 for acid-met, and 6.5 ± 0.5 for fluoride derivatives. Kotani used the variation of magnetic susceptibility with temperature to determine this parameter. The discrepancy

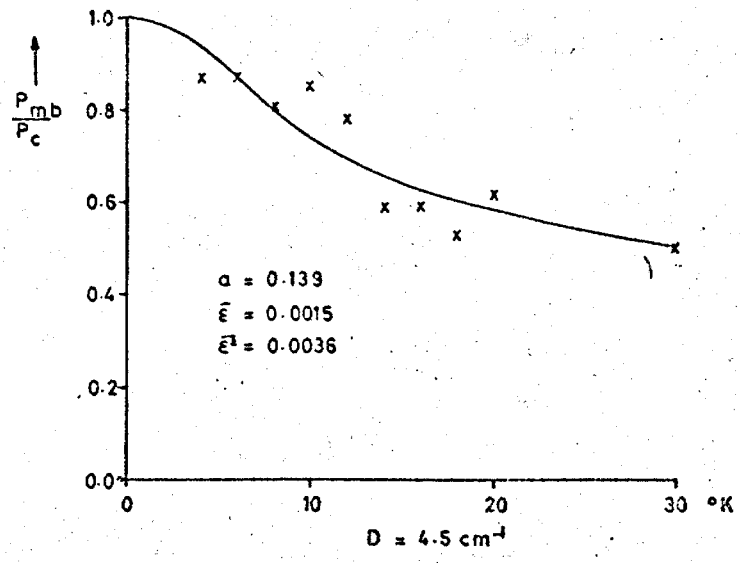
$\frac{P_{mb}}{P_c}$
1.0
0.8
0.6
0.4
0.2
0.0
0
10
20
30 °K
a = 0.139
$\bar{\epsilon}$ = 0.0015
$\bar{\epsilon}^2$ = 0.0036
D = 4.5 cm^{-1}

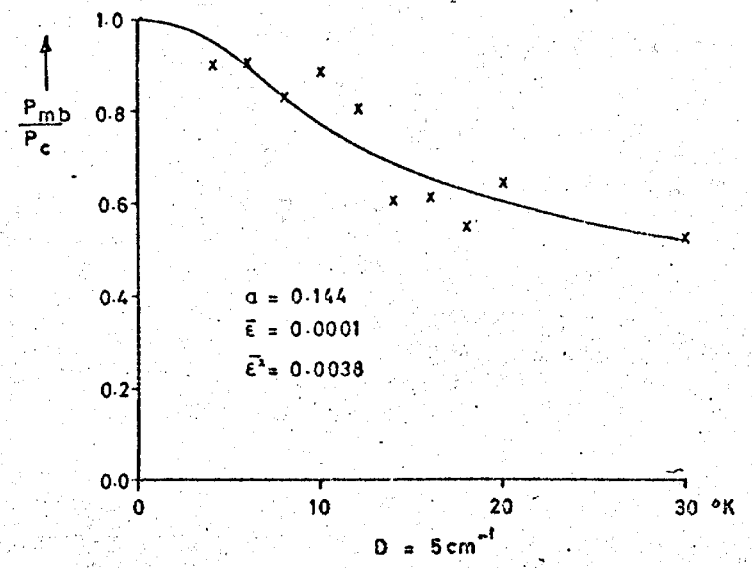
$\frac{P_{mb}}{P_c}$
1.0
0.8
0.6
0.4
0.2
0.0
0
10
20
30 °K
a = 0.144
$\bar{\epsilon}$ = 0.0001
$\bar{\epsilon}^2$ = 0.0038
D = 5 cm^{-1}

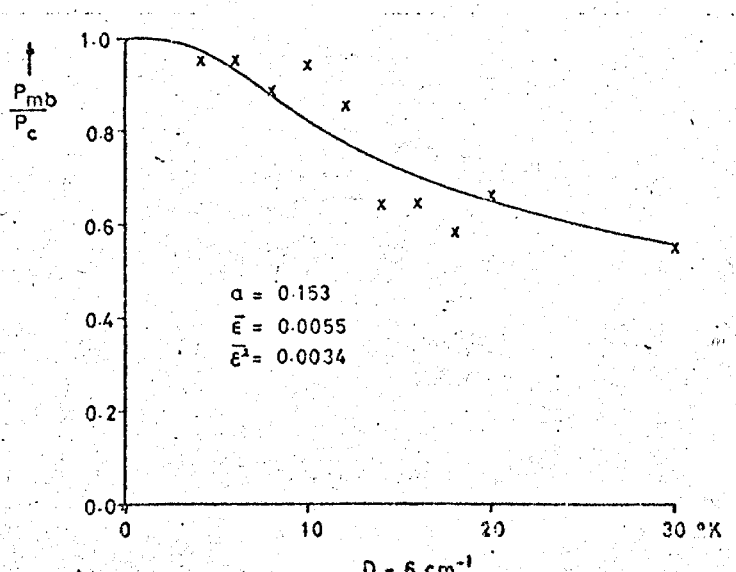
$\frac{P_{mb}}{P_c}$
1.0
0.8
0.6
0.4
0.2
0.0
0
10
20
30 °K
a = 0.153
$\bar{\epsilon}$ = 0.0055
$\bar{\epsilon}^2$ = 0.0034
D = 6 cm^{-1}

between these two sets of results will be discussed in Chapter 7.

In section 5.5. it was found that from single crystal measurements on the fluoride derivative the ratio $\lambda = {}^{E}/_{D} = 0.0027$. Therefore using the estimated value of the tetragonal component D (4 cm^{-1}) the rhombic distortion E is found to be 0.011 cm^{-1}. This compares with the value 0.025 cm^{-1} determined by Kotani.[21,22].

REFERENCES

1. J.C. Kendrew, R.G. Parrish, J.R. Marrack, E.S. Orlans, Nature 174, p.946, 1954.
2. J.C. Kendrew, R.G. Parrish, Proc. Roy. Soc. A238, p.305, 1956.
3. B. Chance, Watson. "Hemes and Hemoproteins" Edited by B. Chance 1967.
4. F.R.N. Gurd, pp 221-38, "Hemes and Hemoproteins" Edited by B. Chance 1966.
5. F. Quiocho, F. Richards, Proc. Nat. Acad. Sci. U.S. 57, No.3. pp 525-37, 1967.
6. F.N.H. Robinson, J.S.I. 42 p.653, 1965.
7. H. Zeldes, R. Livingston, J. Chem. Phys., 34 No.1. Jan. 1961.
8. G.A. Helcke, D.J.E. Ingram, E.F.Slade. Proc. Roy. Soc. B169 pp 275-288, 196[illegible].
9. J.E. Bennett, J.F. Gibson, D.J.E. Ingram. Proc. Roy. Soc. A240, p67, 1957.
10. Private communication.
11. W. Scheler, G. Schoffa, F. Jung. Biochem. Z. 329, p.232 1957.
12. E.S. Kirkpatrick, K.A. Muller, R.S. Rubins, Physical Review, 135, No 1A, July 1964.

REFERENCES

13. G. Feher, P.L. Richards, "Magnetic REsonance in Biological Systems", Ed. A. Ehresberg, pp.141-144, 1966.

14. Edelstein, J.Chem. Phys., 40, p.488, 1965.

15. Turkevitch, J.A.C.S. 63, p.1077, 1941.

16. Duffy, J. Chem. Phys. 36, p.490, 1962.

17. A.C. Rose-Innes, "Low Temperature Techniques".

18. S.J. Wyard, J.S.I., 42, pp 769-70, 1965.

19. McLintoch et al.
Phys. Status Solidi 29, k.157, 1968.

20. McLintoch

21. H. Venogama, T. Iizuka, H. Morimoto, M. Kotani, Biochemica et Bioph. Aita, 160 pp.159-166, 1968.

22. M. Kotani, H. Morimoto, "Magnetic Resonance in Biological Systems". Edited by A. Fhrenberg et al, pp.135-140, 1966.

CHAPTER 6.

RESULTS FROM MYOGLOBIN SOLUTIONS.

6.1. Introduction

It is often assumed that X-ray data obtained from a single crystal is directly applicable to a solution. A comparison of the optical spectra of single crystals and solutions of sperm-whale myoglobin has been made by Day et al.[1]. They found a slight difference between the two spectra which was initially ascribed to a small conformational change in the molecule between the two states causing the spin equilibrium position to move towards high spin in the crystal. An alternative explanation[23] not involving any change in the haem environment has been proposed, but the doubt still remains. It is therefore important to ascertain whether e.p.r. results from solutions correspond with those from single crystals. It is extremely difficult to produce single crystal forms of certain derivatives, and in such cases one is forced to study them in solution form. Since preparation of solutions is simple it is worthwhile making preliminary studies on solutions anyway, especially as one can compute g-values and linewidth from the solution spectrum.

Several myoglobin derivatives were investigated and the g-values have been determined at 35 GHz (Q-band), and at 70 GHz (4 mm). From the two measurements the zero field splitting for each derivative has been calculated.

The optical absorption spectra of haem-proteins, in the visible region, consists of five distinct bands. Two of these are characteristic of high spin Fe^{3+}, and two are prominent in low spin Fe^{3+}. Each myoglobin derivative has a characteristic absorption spectrum, and therefore optical spectra offer information concerning the spin state of the iron, and indicate which derivative is predominant in a given solution. Optical spectra may be observed at room temperature and above, where it is virtually impossible to see e.p.r. in haem-proteins. Therefore valuable information on the spin state equilibrium at these higher temperatures can be determined. The optical absorption spectra for several myoglobin derivatives were measured in the wavelength region 340-700 mμ. From these results a measure of the spin state was obtained and this was compared with the results obtained from e.p.r. measurements.

6.2. E.P.R. of Solutions at Q-band.

Solutions of myoglobin were prepared by adding a saturated solution of a salt (e.g. Na HCO_2) to freeze dried myoglobin until the protein concentration was 20 m M. The solution was buffered to a slightly alkaline pH value around 8. Alternatively sufficient myoglobin was added to form a paste. The solution was put into a hollow peg by means of a hyperdermic syringe. A small amount of d.p.p.h. was placed on the side of the peg and, as before, the microwave frequency was determined from the magnetic field strength at which resonance in d.p.p.h. occurred. The microwave

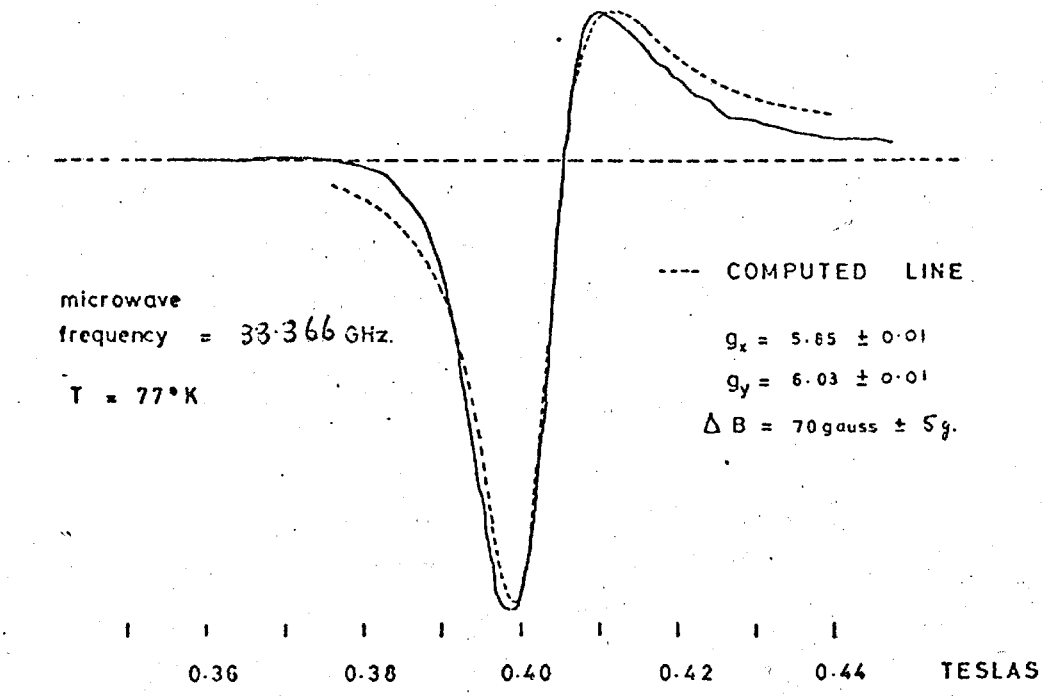

MYOGLOBIN FLUORIDE (Q BAND)

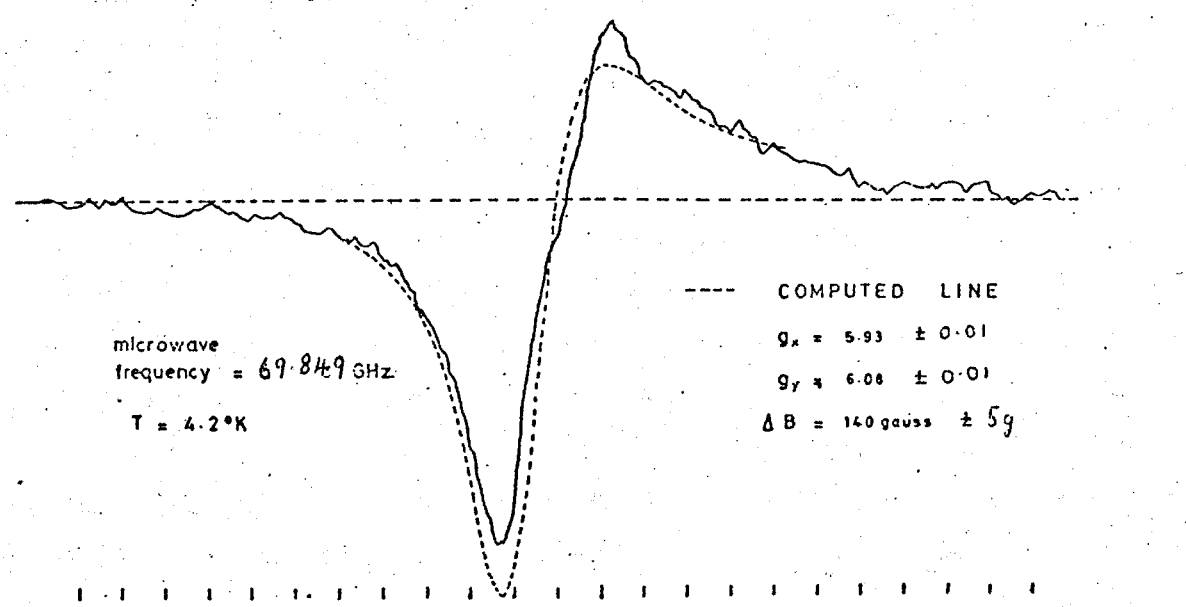

MYOGLOBIN FLUORIDE (4mm.)

FIG. 6·1

cavity (see Fig. 5.3.) was placed into a sealed stainless steel tube which was immersed in a glass dewar containing liquid nitrogen. Magnetic field strength was measured with a proton resonance unit.

Investigations were made to discover whether or not the concentration of the solution affected the e.p.r. spectra, but no significant change was detected. It is obviously preferable to have the solution as dense as possible to increase the number of paramagnetic ions within the same volume. Using a thick paste it was not possible to determine the pH and hence some experimental control was lost. The effect of variation of pH on the e.p.r. spectra was also investigated. It was found that a change in the shape of the acetate derivative (axial ligand $CH_3\ CO_2^-$) spectrum occurred with change of the solution pH between 6.0 and 10.0. Although no quantitative analysis was undertaken a possible explanation for this effect is that competition occurred between the acetate and acid-met forms, this having a pH dependance. The intensity of the acid met signal diminished as the pH was increased, due to conversion from high spin form (acid-met) to low spin form (hydroxide), with increasing pH.

The e.p.r. spectra of a solution is the envelope of transitions arising from ions whose magnetic axes have completely random orientations. In the case of high spin myoglobin the spectrum consists of a broad line around $g_{eff} = 6$, and a weak line at $g = 2$. Analysis of such spectra is outlined in Appendix 4, where it is seen that allowance must be made for the change in

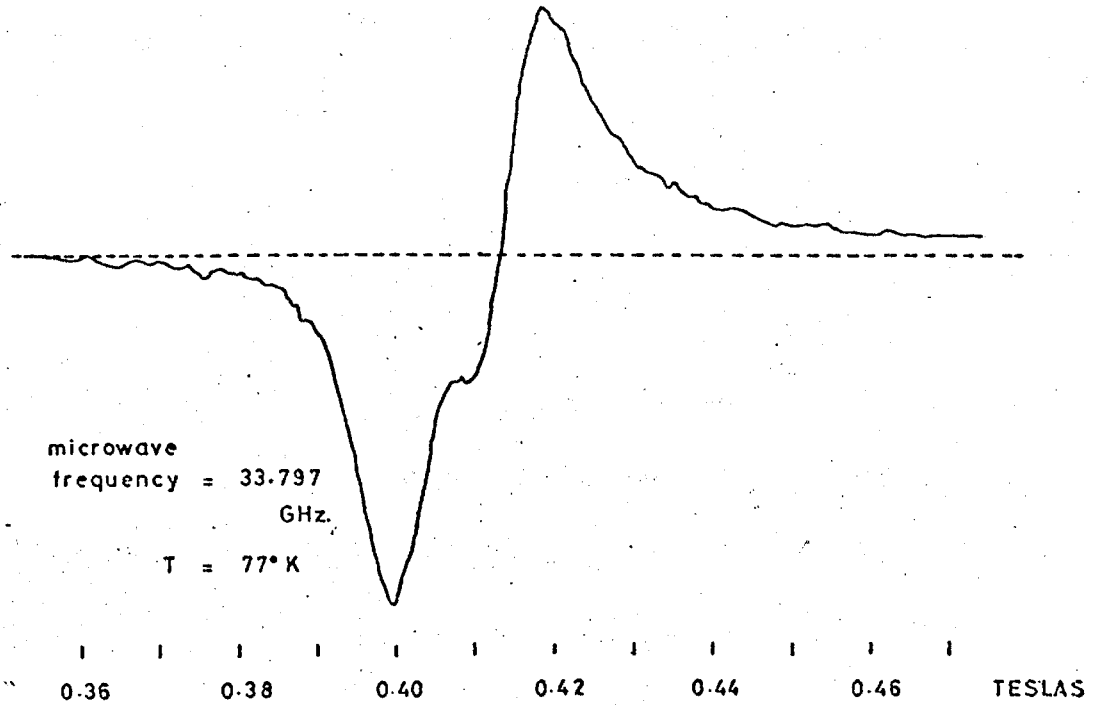

MYOGLOBIN FORMATE (Q BAND)

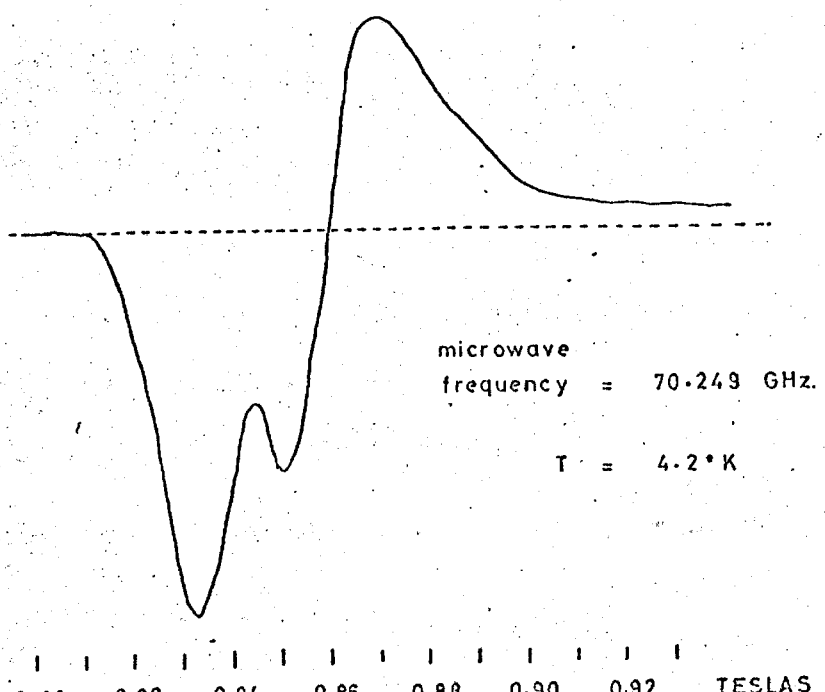

MYOGLOBIN FORMATE (4 mm.)

transition probability with orientation. This is because the transition probability depends on the precise relationship of the oscillatory magnetic field B_1 to the principal axes of the g-tensor. The spectra of each derivative was analysed by superimposing a synthesised spectrum on to the experimentally derived spectrum, and then by re-adjusting the parameters (linewidth, g-values) in the synthesis programme until a good fit was obtained. The spectra and computed g-values are given in figures 6.1 - 6.5.

The best computed fit to the fluoride spectrum was using $g_x = 5.85$, $g_y = 6.03$, and a Lorentzian linewidth $\Delta B = 7$ Milli Teslas (70 gauss). This compared with the single crystal results of $g_x = 5.85$, $g_y = 5.98$. Thus the effective g-value, g_y, for the solution has marginally increased from the value determined for the single crystal. This difference could be accounted for by an increase in the parameters D and E between single crystal and paste forms.

For the formate derivative (axial ligand HCO_2^-) the best fit requires a rather more anisotropic g-value than usual, which could be explained by a large rhombic distortion of the crystalline electric field, as has been used to explain similar spectra elsewhere.[24] However subsequent measurements on single crystals revealed that two high spin forms exist for this derivative. Therefore the spectrum shown in figure 5.6. is the superposition of two overlapping spectra and unfortunately it was not possible to synthesise this result.

Pastes were prepared by adding concentrated solutions,

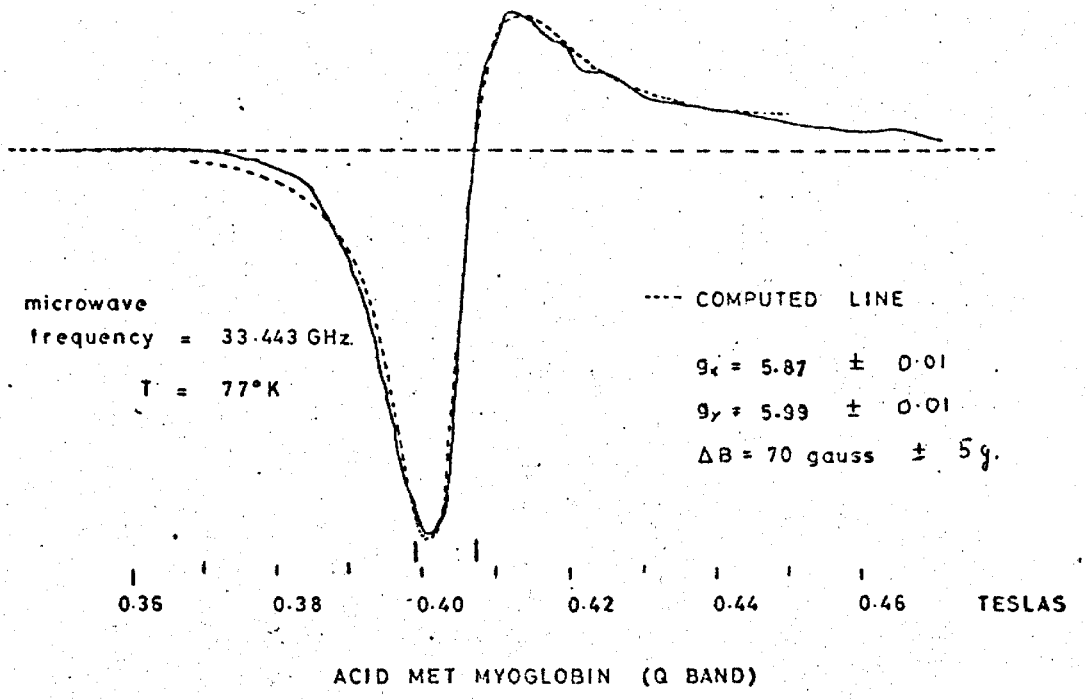

ACID MET MYOGLOBIN (Q BAND)

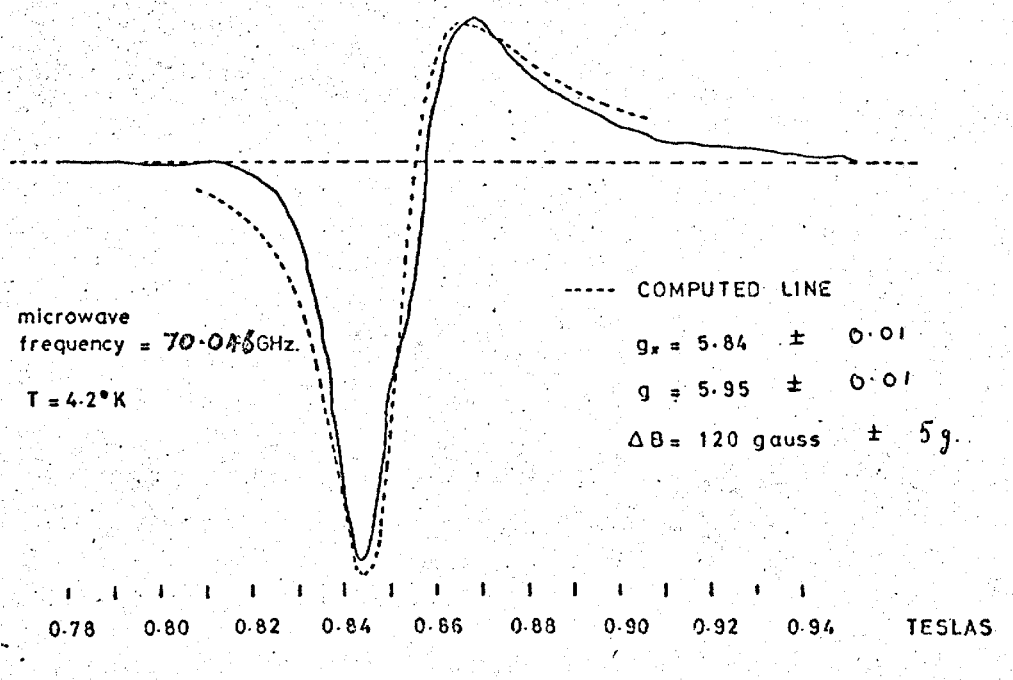

ACID MET MYOGLOBIN (4mm.)

FIG. 6·3

buffered to pH 8.0, of the sodium salts chloride, bromide and Iodide to freeze dried myoglobin. No signal was observed in the case of the 'Iodide' paste, whereas the spectra shown in figure 6.5. were observed from the other pastes. The best fit to these spectra were found to be with g-values very close to those found for the acid-met derivative. In section 6.6. the optical absorption measurements made on solutions of these salts indicate that the ions have not complexed with the iron. The ions may have become attached to the molecule somewhere in the vicinity of the haem without complexing with it.

Finally a solution of the cyanate derivative was investigated at 4.2°K. A high spin signal was observed as shown in figure 6.4. The best fit is with $g_x = 5.78$, $g_y = 5.92$, and a Lorentzian linewidth $\Delta H = 6.5$ milli teslas. These values differ from the acid-met results and therefore this signal appears to result from a cyanate derivative rather than from molecules which have not converted to the cyanate form but remain in the acid-met form. This endorses the interpretation of the single crystal results on this derivative that two forms of this derivative exist, one high spin, and the other low spin.

6.3. E.P.R. of Pastes at 4 mm.

A complete description of the 4 mm spectrometer used in these studies has been given elsewhere[2,3] and therefore only a brief outline will be given here. The spectrometer incorporated a magic tee bridge and power was carried from this bridge to the sample cavity via an oversized waveguide. At either end of

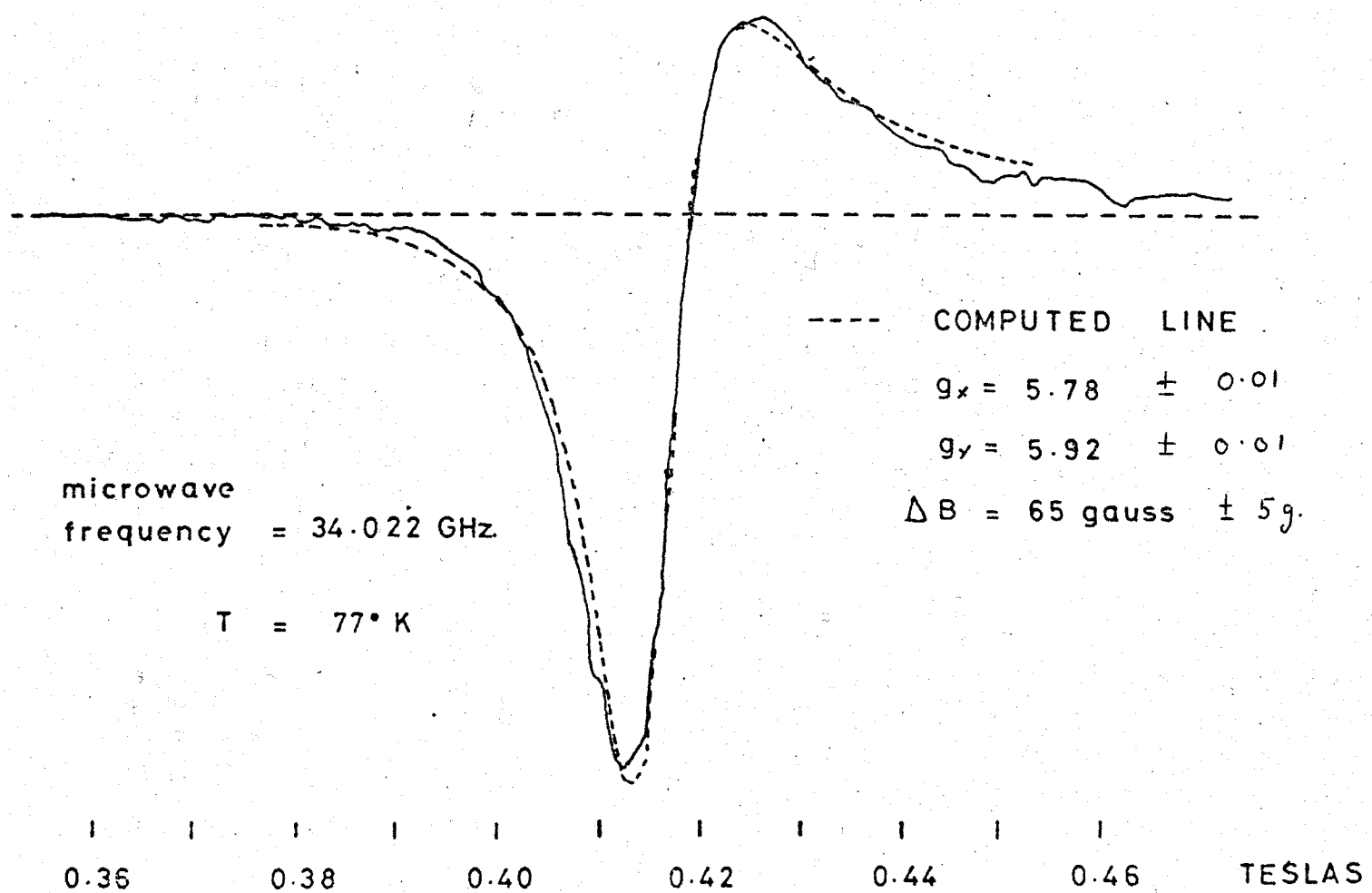

FIG. 6.4 MYOGLOBIN CYANATE (Q BAND)

the oversized waveguide a taper reduced the guide dimensions to those of the 4 mm waveguide. A cylindrical sample cavity, shown in figure 6.6., which operated in the H_{012} mode was used.

Myoglobin samples were prepared in the same way, described in section 6.2., except that sufficient myoglobin was added until a stiff paste was obtained. This paste was extruded from a fine capillary tube and a short length was attached to one end of the microwave cavity by silicon grease.

The cavity was then placed inside a superconducting magnet solenoid. This magnet, manufactured by Oxford Instruments, has also been described in reference 2 and therefore details will not be given here. The field in the superconducting solenoid was determined by accurate measurement of the current through the solenoid. This current was found by measuring the p.d. developed across a standard resistor (0.01Ω) connected in series with the solenoid. The standard resistor was immersed in an oil bath to maintain a constant temperature, and the p.d. across the resistor was measured using a potentiometer. As the field was swept either up or down the potentiometer was set to a certain voltage, and when this voltage was balanced by the p.d. developed across the standard resistor. the recorder tracing was marked by an event marker. A series of marks at different intervals of current were put on to the chart for each experimental run.

For each derivative studied the magnetic field was swept both up and down several times, with recordings of the spectra taken each time, to allow for any inertia in the process

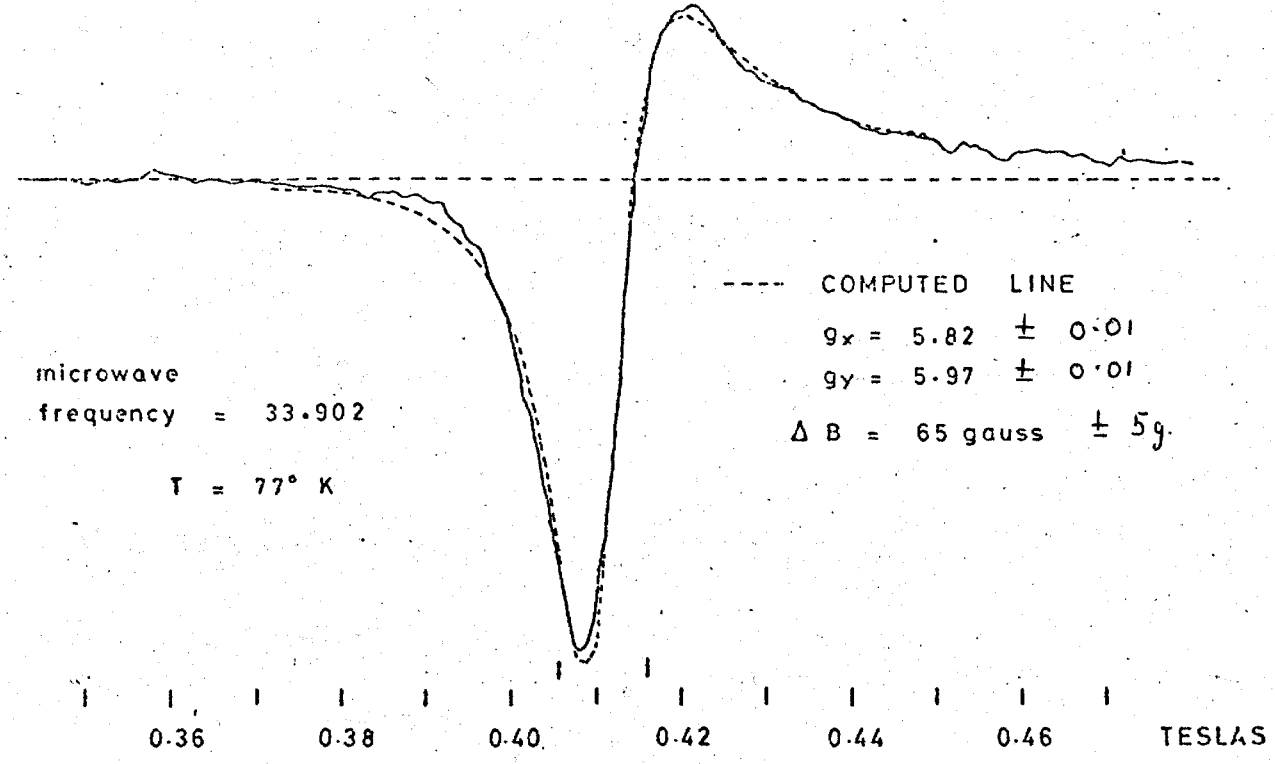

MYOGLOBIN CHLORIDE (Q BAND)

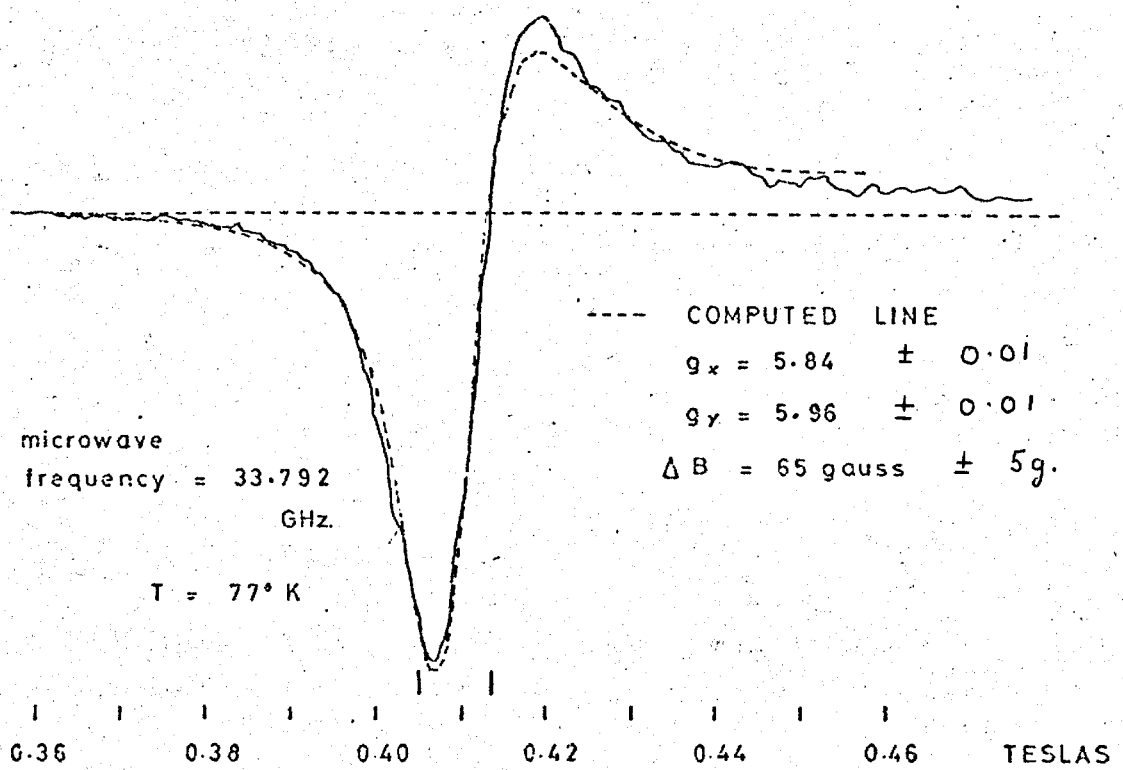

MYOGLOBIN BROMIDE (Q BAND)

FIG. 6·5

of marking the field. The magnet had already been calibrated and was found to produce 0.2641 Teslas/amp. at the centre of the solenoid. This value was adopted in these studies, since any error in the calibration would only have a small effect upon the results. This is because the g-values were determined by a direct comparison between the solenoid current values at resonance, and at the resonance of d.p.p.h. ($g_{d.p.p.h.} = 2.0035$)

Analysis of the results is the same as given above for the Q-band spectra. Three derivatives were investigated at 4 mm, these being acid-met, fluoride, formate, and their spectra are shown in figures 6.3.

It is interesting to note that to obtain a reasonable fit to the experimental spectra an intrinsic linewidth double that found at Q-band, needed to be used in the synthesis programme. This frequency dependance of the linewidth confirms the results obtained from single crystals at 4 mm^4 in which the minimum linewidth was found to have this dependance. A poor fit to the fluoride derivative spectrum was achieved, and the computed mean g-value had increased from the value found at Q-band frequency, which, as will be seen in section 6.4., contradicts theory. Analysis of the spectrum of the formate derivative was not achieved for the same reasons as given in the previous section.

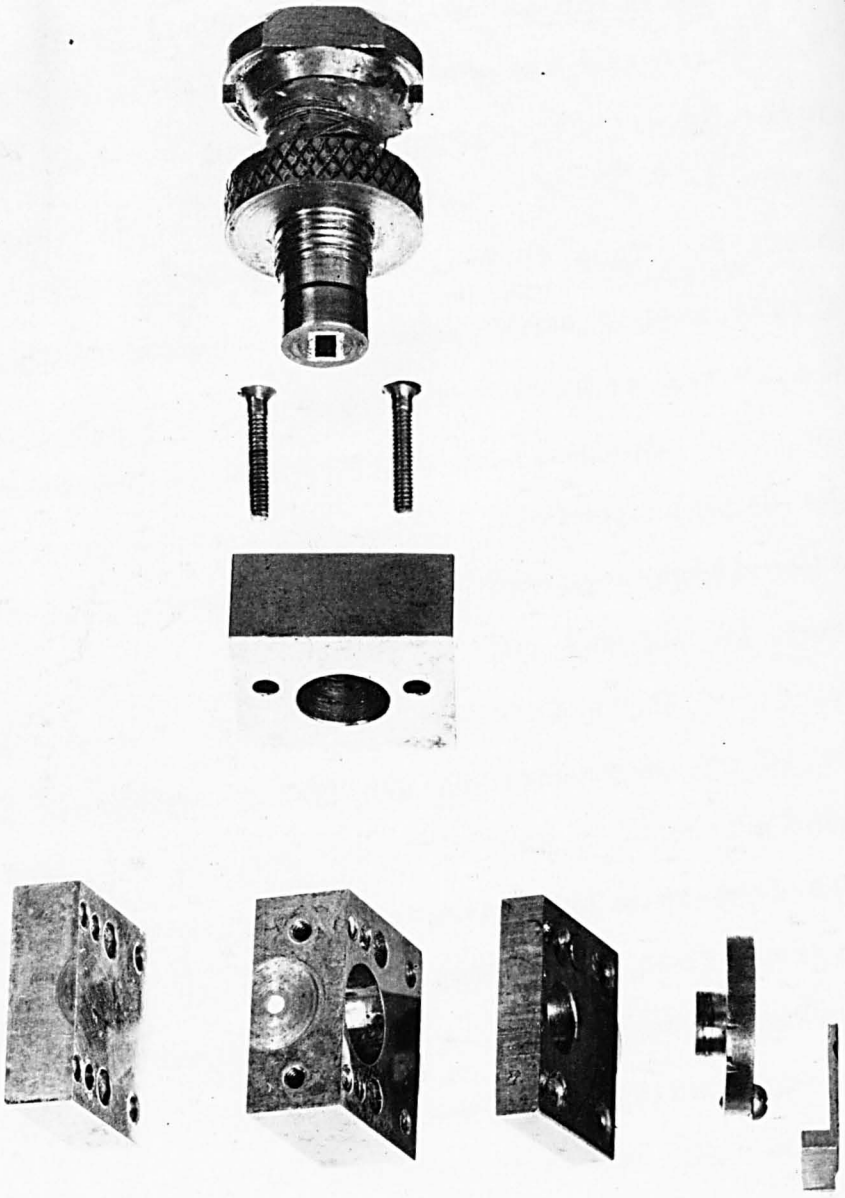

Figure 6.6 4mm Cavity

6.4. Estimations of Zero Field Splittings

A paramagnetic ion with spin $S = \frac{5}{2}$ situated in an axial crystal field can be described by a spin Hamiltonian.

$$= D(Sz^2 - \frac{35}{12}) + g_{\parallel} Bz\ Sz + g_{\perp} (Bx\ Sx + By\ Sy) \quad 6.1.$$

The eigenvalues of this Hamiltonian may be evaluated, as outlined in section 3.7., numerically, using a computer, or perturbation theory may be applied. If we consider the term involving D first (assuming this to be larger than the Zeeman terms), then this will lift the 2S + 1 degeneracy of the ground state into three doubly degenerate levels. These levels will be characterised by $m_s = \pm \frac{1}{2}$, $m_s = \pm \frac{3}{2}$, $m_s = \pm \frac{5}{2}$, and the splittings will be 2D and 4D, as shown in figure A.2. Applying the Zeeman interaction as a perturbation, up to third order, it is only necessary to consider the $S_z = \pm \frac{1}{2}$, and $S_z = \pm \frac{3}{2}$ levels since there are no matrix elements between $S_z = \pm \frac{5}{2}$ and $S_z = \pm \frac{1}{2}$. Third order perturbation calculations[5] yield;

$$\text{for} \quad \theta = 0, \quad g_{\parallel}\ \text{eff} = g_{\parallel} \qquad 6.2.$$

$$\text{and} \quad \text{for} \quad \theta = 90^{\circ}, \quad g_{\perp}\ \text{eff} = 3g_{\perp} \left[1 - 2 \frac{g_{\perp} \beta B^2}{(2D)^2}\right] \qquad 6.3.$$

where $g_{\parallel}$ eff and $g_{\perp}$ eff are the effective g-values defined by

$$h\nu = g_{eff} \beta B$$

Therefore by measuring $g_{\perp}$ eff at two microwave frequencies, and

ZERO FIELD SPLITTINGS AS DETERMINED FROM PASTE SPECTRA.

Acid-met

Q-band $g_x = 5.87$ $g_{av} = 5.93$

$g_y = 5.98$ $B_1 = 0.4031$ Teslas

4mm $g_x = 5.84$ $g_{av} = 5.90$

$g_y = 5.95$ $B_2 = 0.8489$ Teslas

$g_\perp = 1.978$ $D = 6.65\ cm^{-1}$

Formate 1.

Q-band $g_1 = 6.04$ 4mm $g_2 = 6.01$

$B_1 = 0.3996$ Teslas $B_2 = 0.8350$ Teslas

$g_\perp = 2.000$ $D = 6.72\ cm^{-1}$

Formate 2.

Q-band $g_1 = 5.91$ 4mm $g_2 = 5.87$

$B_1 = 0.4085$ Teslas $B_2 = 0.8545$ Teslas

$g_\perp = 1.974$ $D = 6.19\ cm^{-1}$

TABLE 6.1.

hence at two different resonance magnetic fields, B_1 and B_2, $g_\perp$ and $|2D|$ can be found.[6,7] Using equation 6.2. and 6.3. we find

$$g_\perp = \frac{g_{\perp\ \mathrm{eff}}}{3} \quad \frac{1}{\alpha} \quad \frac{(\alpha - \delta)}{(1 - \delta)} \qquad 6.4.$$

$$|2D| = g_\perp \beta \left| 2 \frac{(\alpha B_2^2 - B_1^2)}{\alpha - 1} \right|^{\frac{1}{2}} \qquad 6.5.$$

where $\alpha = \dfrac{g_{\perp\ \mathrm{eff}\ (1)}}{g_{\perp\ \mathrm{eff}\ (2)}}$ and $\delta = \dfrac{B_1^2}{B_2}$

Using these equations $g_\perp$ and 2D are calculated for the acid-met and two formate derivatives. The results are listed in Table 6.1. Analysis of the acid-met paste spectrum shows that there is a rhombic component in the Hamiltonian giving rise to two g values, g_x and g_y (5.866 and 5.988 at Q-band) instead of just $g_\perp$. If a rhombic term $E(Sx^2 - Sy^2)$ is included in the Hamiltonian it is found that the eigenvalues are now dependant on the angle ϕ, giving two transitions characterised by g_x and g_y. For small values of $\lambda = \frac{E}{D}$ ($\sim$0.01) it is found that g_x and g_y diverge linearly with λ at the same rate. Thus the mean of these two readings is the value of $g_\perp$ that would exist in an axial system with the corresponding value of D. Therefore for the acid-met derivative the values for $g_\perp$ at Q-band and 4mm were taken to be 5.927 $\pm$ 0.005 and 5.895 $\pm$ 0.005, these being the average values of g_x and g_y at the two microwave frequencies. Using these figures we arrive at a value of 6.65 $\pm$ 1.5 cm^{-1} for the

VISIBLE ABSORPTION SPECTRA OF MYOGLOBIN

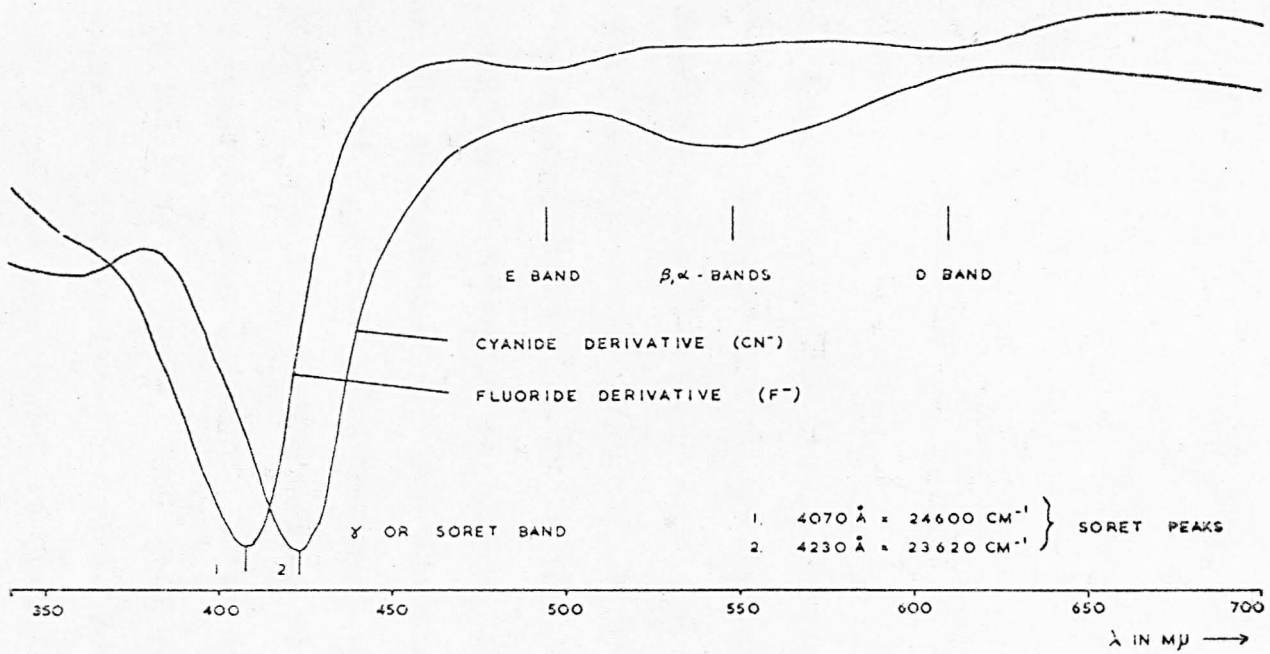

SORET BAND OCCURS IN ALL PORPHYRINS INCLUDING METAL FREE ONES

D & E BANDS ARE CHARACTERISTIC OF HIGH SPIN DERIVATIVES

α, β BANDS ARE MORE INTENSE IN LOW SPIN DERIVATIVES

THE SORET BAND IS SEEN TO SHIFT TO LONGER WAVELENGTHS AS THE SPIN STATE OF A SYSTEM MOVES FROM HIGH TO LOW

CONSIDER 1 AND 2 AS TWO GAUSSIAN FUNCTIONS

$\varepsilon_1 = 14{\cdot}6\ \mathrm{EXP}-(\nu - 24600)^2 / h_1^2$ $\qquad$ $\varepsilon_2 = 11{\cdot}6\ \mathrm{EXP}-(\nu - 23620)^2 / h_2^2$

THEN FOR ANY MYOGLOBIN DERIVATIVE THE SORET BAND CAN BE ANALYSED AS A COMBINATION OF ε_1 AND ε_2 GIVING THE SPIN STATE EQUILIBRIUM AT T°K

FIG. 6.7

zero field splitting parameter D. The large error in 2D is caused by its dependance on the small difference between $g_{\perp 1}$ and $g_{\perp 2}$. Therefore this result is nearer to the results obtained by temperature variation studies than the susceptibility measurements of Kotani, and the two measurements of D made in these studies indicate that D is considerably less than 9.6.

As already mentioned, the formate spectra were not analysed so the effective axial g-value $g_\perp$ was taken to be the turning point at the peak of the signal. This was found to be approximately true in the other derivatives. The estimated values of D for the two formate derivatives, 6.7 cm^{-1} and 6.2 cm^{-1}, are very close to the value found for the acid-met derivative.

In the fluoride derivative it was found, contrary to the theory, that the mean g-value $g_\perp$ increased with increasing microwave frequency from 5.938 at Q-band (35 GHz) to 6.002 at 4 mm (70 GHz). The lineshape was scanned several times at both frequencies, and the same results were obtained each time. This strange result and difficulty of producing a good fit to the lineshape suggest some other mechanism is altering the lineshape.

6.5. Optical Absorption Spectra of Haem-proteins.

The spectra of ferrous haems and haem-proteins are now reasonably understood[8-11], but the ferric compounds are more complicated due to extra ligand to metal charge transfer bands, and also due to the existence of an equilibrium between the high spin and low spin forms, each with distinct spectra. The

CHANGE OF SPIN STATE WITH CHANGE OF pH IN Mb

ACID MET ⟶ HYDROXIDE

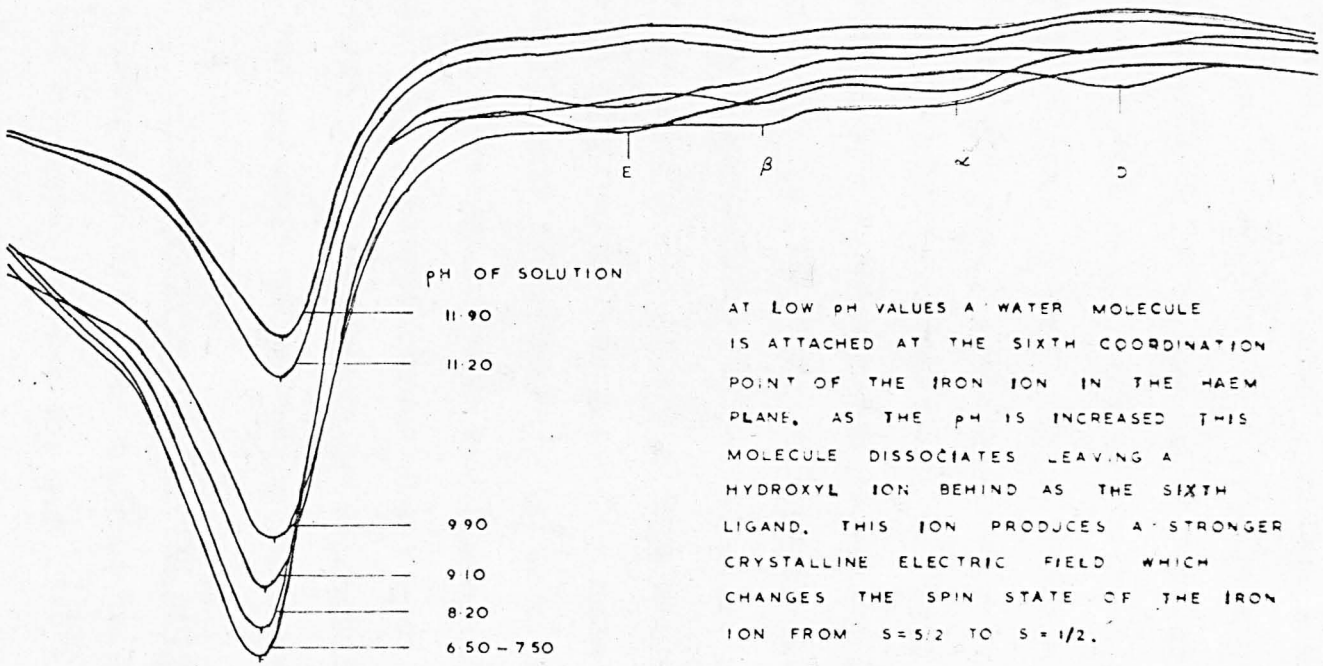

AT LOW pH VALUES A WATER MOLECULE IS ATTACHED AT THE SIXTH COORDINATION POINT OF THE IRON ION IN THE HAEM PLANE. AS THE pH IS INCREASED THIS MOLECULE DISSOCIATES LEAVING A HYDROXYL ION BEHIND AS THE SIXTH LIGAND. THIS ION PRODUCES A STRONGER CRYSTALLINE ELECTRIC FIELD WHICH CHANGES THE SPIN STATE OF THE IRON ION FROM S = 5/2 TO S = 1/2.

pH OF SOLN.	ν MAX	% LOW SPIN
6·50	24480	9
8·20	24450	12
9·10	24340	23
9·90	24200	38
11·20	24180	42
11·90	24160	44

FIG. 6·8

spectra of ferric haem-proteins in the visible region consists of five distinct bands, as shown for the case of acid-met myoglobin in figure 6.9. The bands are :

(i) The intense Soret band (24,000 cm^{-1}) appears in all haem-protein derivatives, as well as in metal free porphyrins. It is nearly independant of the axial ligand, but it shifts in frequency according to the spin state of the iron. This band is due to a porphyrin $\pi - \pi^*$ transition accurring in a region remote from the metal ion. It was found that the Soret band peak shifted from 23,700 cm^{-1} in the cyanide derivative to 24,600 cm^{-1} in the fluoride derivative. This shift is thought[12] to be due to mixing of this band with the charge transfer band (E band) in the high spin form.

As all derivatives, except the cyanide[13, 14], are mixtures of the two spin states, the observed Soret band must be the envelope of the Soret bands of the high and low spin forms superimposed. Therefore the spin equilibrium situation of any temperature T may be determined by analysing the Soret band. This is demonstrated in figure 6.8. where the increase in the low spin form (hydroxide) is observed as the pH of the aqueous solution is increased.

(ii) The D and E bands at 16,000 cm^{-1} and 20,000 cm^{-1} are found to be characteristic of high spin derivatives, and are thought to be due to a mixture of $\pi - \pi^*$ and ligand to metal charge transfer bands.

(iii) The α and β bands at 17,000 cm^{-1} and 18,500 cm^{-1} respectively were present in all ferrimyoglobin derivatives

studied, but they were more intense in the derivatives known to be low spin. The transition responsible for this band is the result of charge excitation from the t_{2g} orbitals of Fe^{3+} to the π system of the ligand.

Spectroscopic studies of other metalloporphyrins have shown that the β band is relatively unaffected in wavelength or intensity by substitution of any of the ligands at the metal ion, whereas the intensity of the α band is strongly dependant on the identity of the sixth ligand.[15] Therefore, one would expect a linear relationship between the intensity of the β band and the corresponding magnetic susceptibility for a series of derivatives of a given haem-protein. D.W. Smith and R.J.P. Williams[14] plotted the intensity of the β band against the magnetic susceptibility for a range of derivatives of horse myoglobin and found they all fell in a straight line except for the cyanate derivative.

It can be seen that optical absorption is a simple technique that can provide valuable information concerning the balance between high and low spin states. Measurements can be made at room temperature where it is virtually impossible to observe e.p.r. in haem-proteins. It is important to remember that oxygenated myoglobin or haemoglobin is in the ferrous state, and is diamagnetic so that no information can be obtained using e.p.r., whereas optical absorption is applicable.

Several papers[16-20] have recently been published on optical and e.p.r. spectra of isolated chains of haemoglobin. R. Banerjee et al [21, 22] discovered that the α and β absorption

bands of the isolated β helix are more intense than in ferri-haemoglobin. This indicates a shift towards low spin which was confirmed by e,p,r, studies. This optical absorption serves well as a complimentary technique to e.p.r. for investigations of haem-proteins.

6.6. Optical Absorption Measurements.

A 1mM stock solution of myoglobin was prepared by adding 0.425 gms of freeze dried Mb to a 25 mls aqueous solution. A sample of the required derivative was prepared by adding 9 mls of a solution, saturated with the appropriate sodium or potassium salt, to 1 ml. of the stock myoglobin solution. The sample was poured into a one centimetre square cross-section quartz cell, and a reference cell was filled with the saturated salt solution. The spectra were determined at room temperature in the region 340 mμ to 700 mμ using a Hitachi Perkin Elmer spectrophotometer (Type EPR 3).

Optical absorption in myoglobin obeys Beer's law whether it is in solution or in crystalline form[23]. Beer's law states that the decrease in intensity of radiation incident on an absorbing solution, with distance l, is proportional not only to the intensity I, but also to the concentration of the solution c; that is

$$-\frac{dI}{dl} = \varepsilon' Ic \qquad 6.6.$$

where ε' is the absorption coefficient.

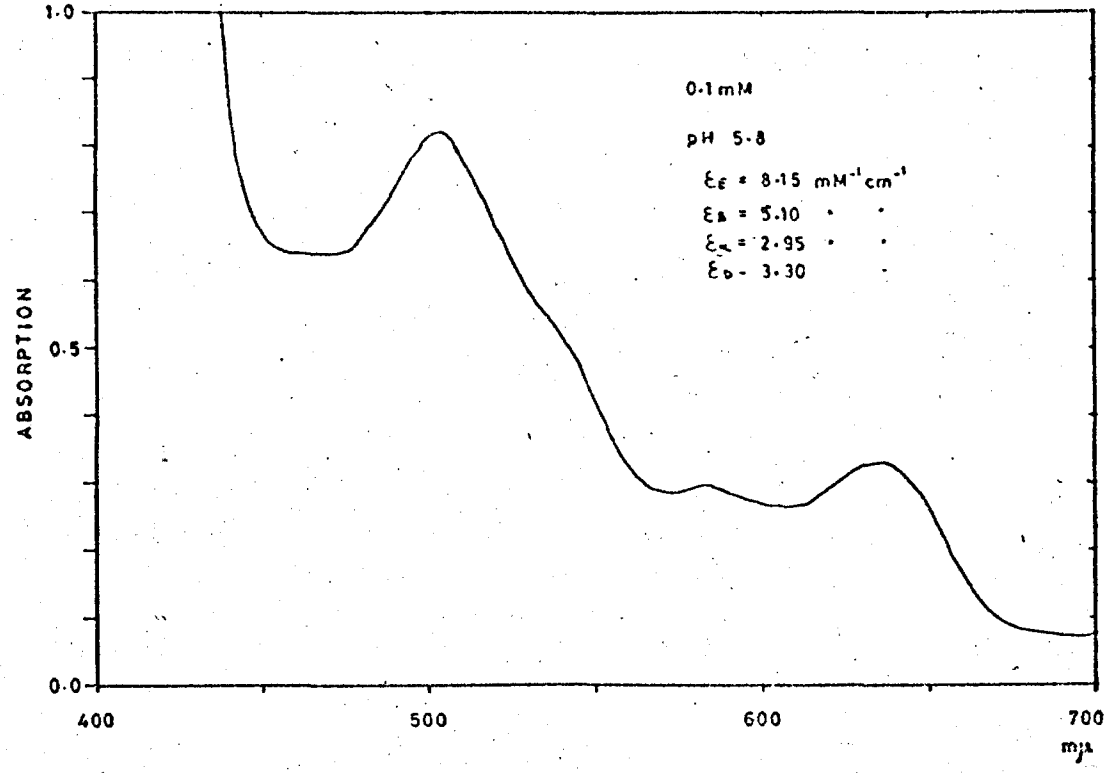

ACID MET MYOGLOBIN

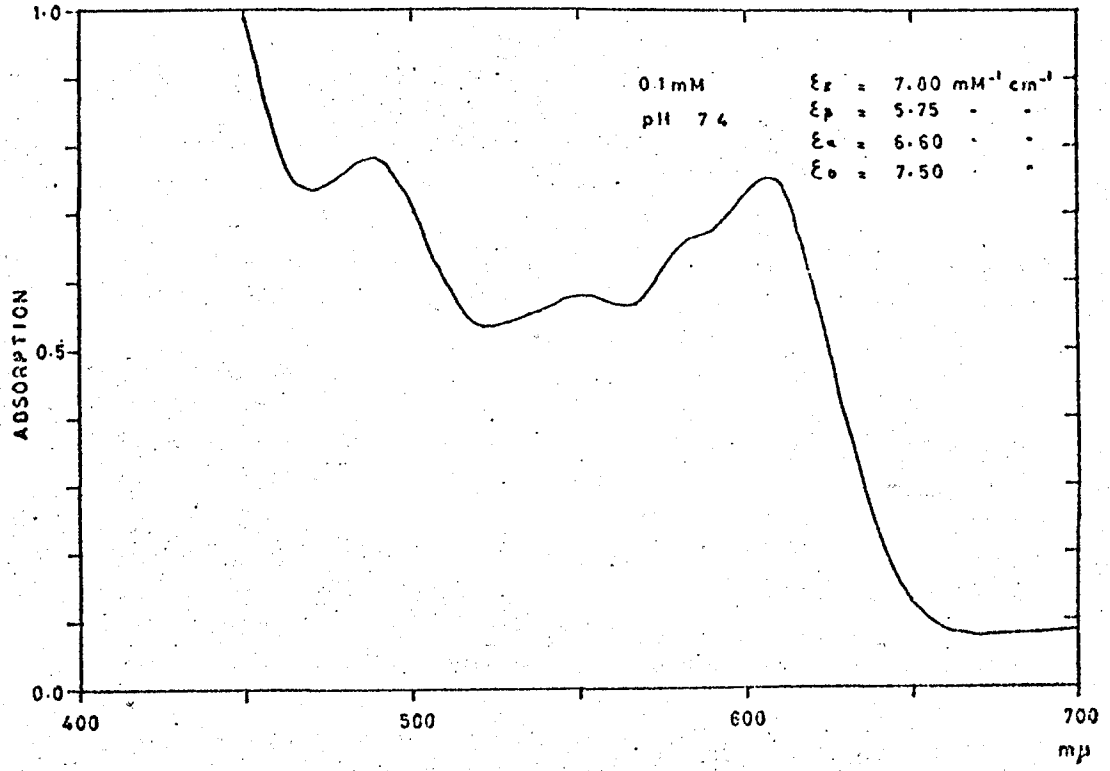

MYOGLOBIN FLUORIDE

FIG. 6·9

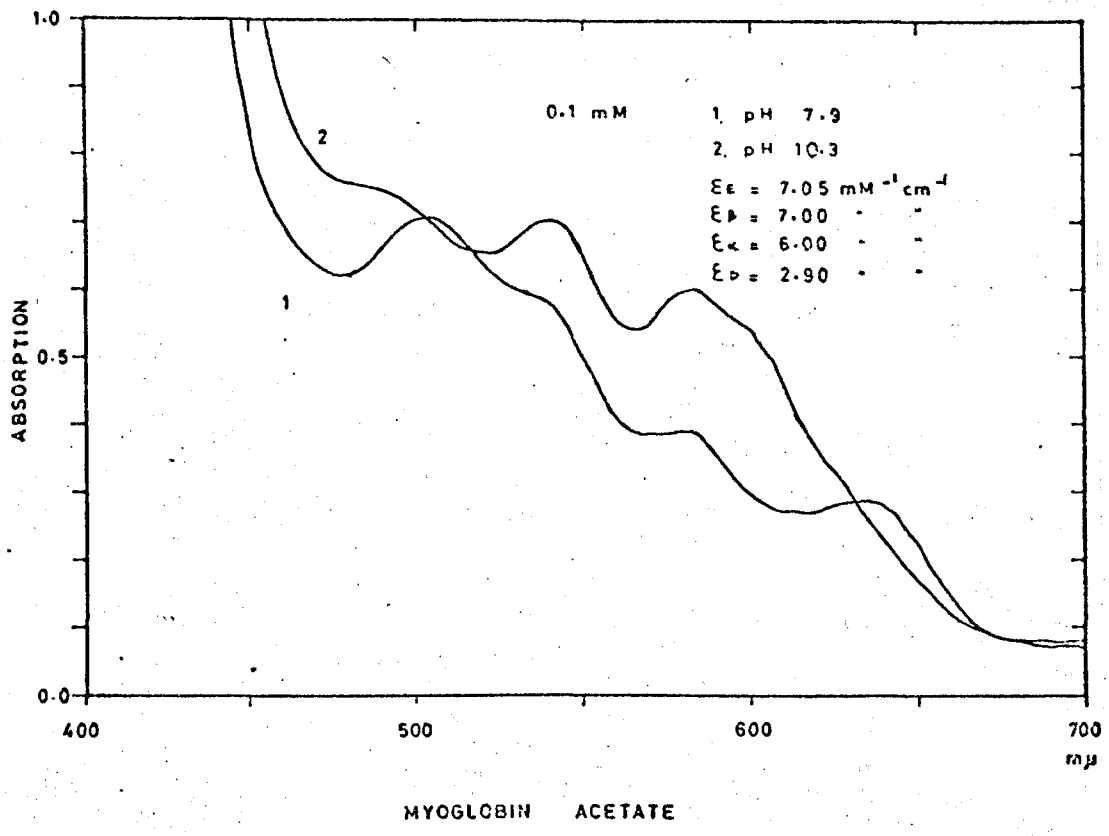

MYOGLOBIN ACETATE

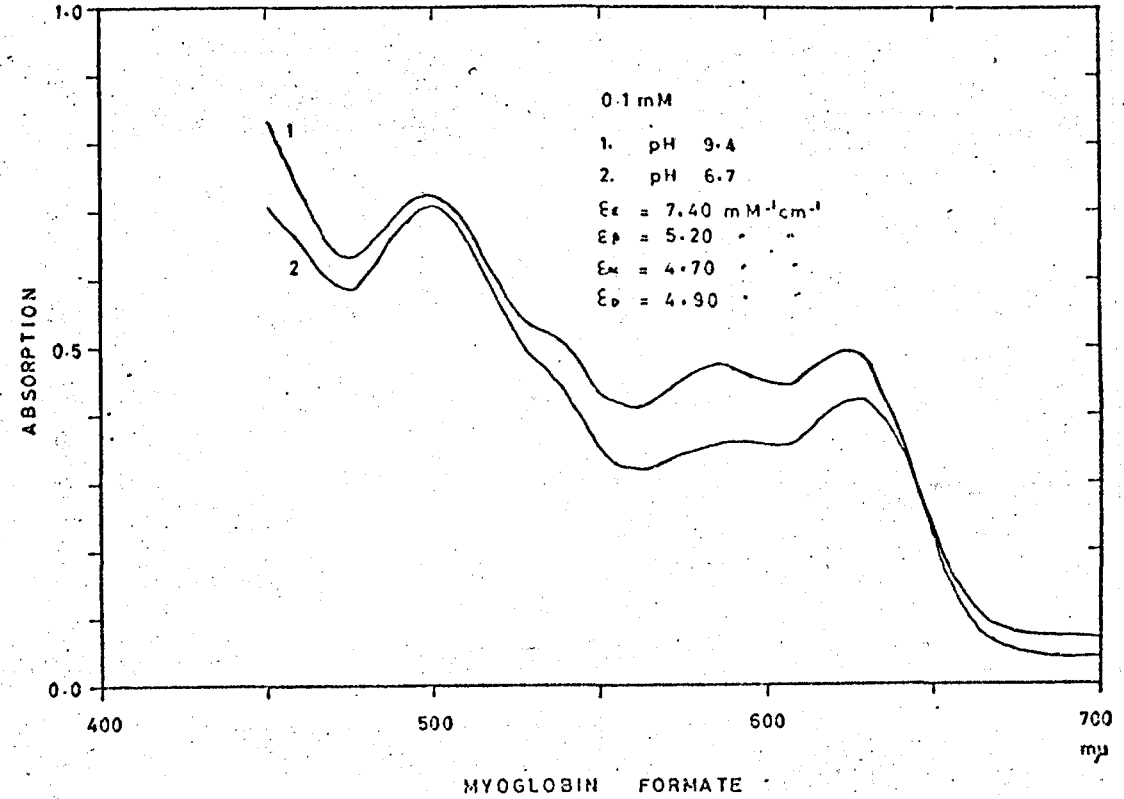

MYOGLOBIN FORMATE

FIG. 6.10

Then if the incident intensity is Io, integration of equation 6.6. gives

$$I_t = Io \exp(-\varepsilon cl) = Io\ 10^{-\varepsilon cl} \qquad 6.7.$$

where ε is the extinction coefficient. The spectra were measured in absorbance and the corresponding expression for the absorbancy A is

$$A = \log(Io/I_t) = \varepsilon cl$$

Since l = 1 cm and c = 0.1 mM the extinction coefficient can be read directly from the charts in units of $mM^{-1}\ cm^{-1} \times 10$.

For accurate values of extinction coefficient the absorbance spectra should be analysed into several Gaussian components[14] and the extinction coefficient determined for each component. The absorbance value at the peaks in the spectrum were considered in this study and therefore the results must be considered as being approximate.

The results for the derivatives studied are shown in figures 6.9 - 6.13. It can be seen that from the intensity of the β band, the predicted low spin derivatives at room temperature are hydroxide, azide, cyanide, cyanate and acetate pH.10.3. The first three agree with susceptibility and e.p.r. measurements made at lower temperatures, whilst the final two do not. The cyanate derivative has an optical spectra almost identical to that of the cyanide form, yet it definitely has a strong high spin component at 77°K to produce the e.p.r. signal at g = 6.

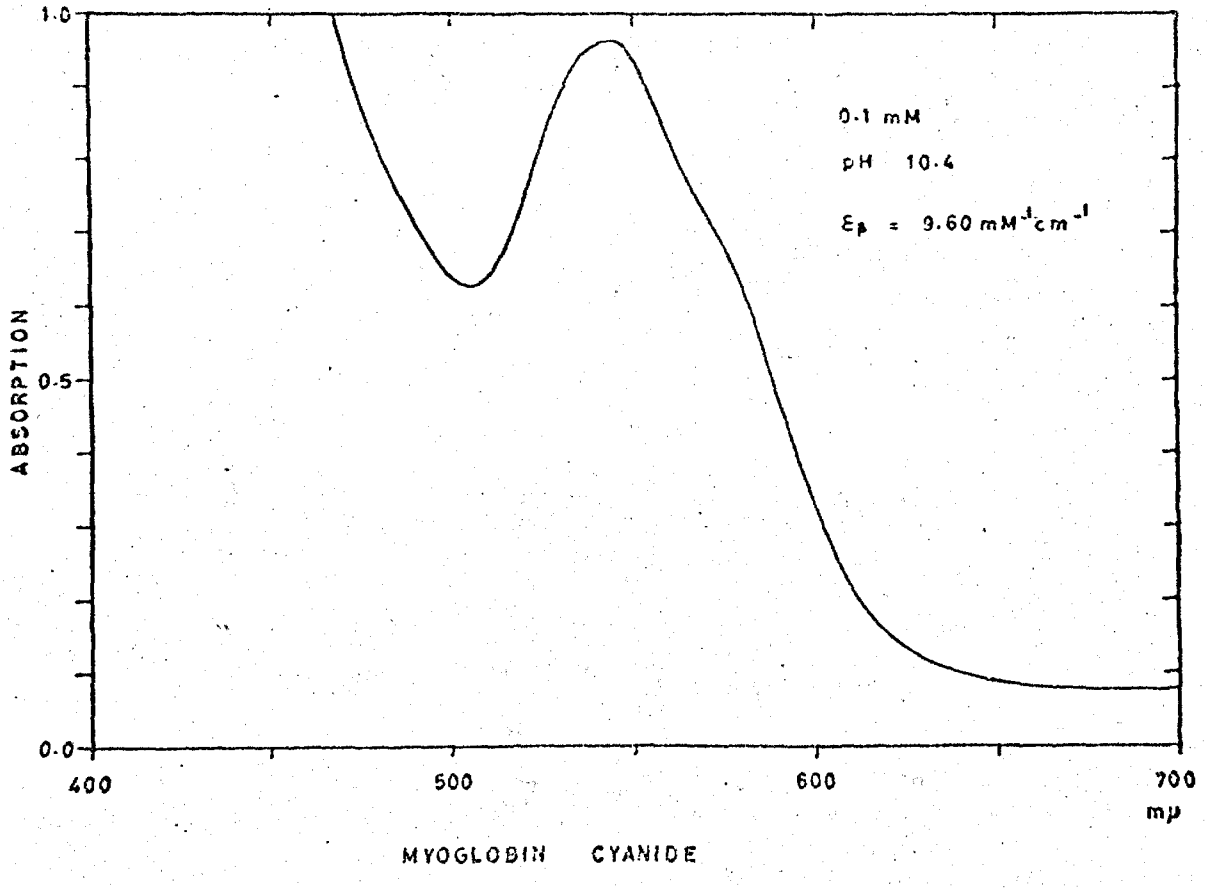

MYOGLOBIN CYANIDE

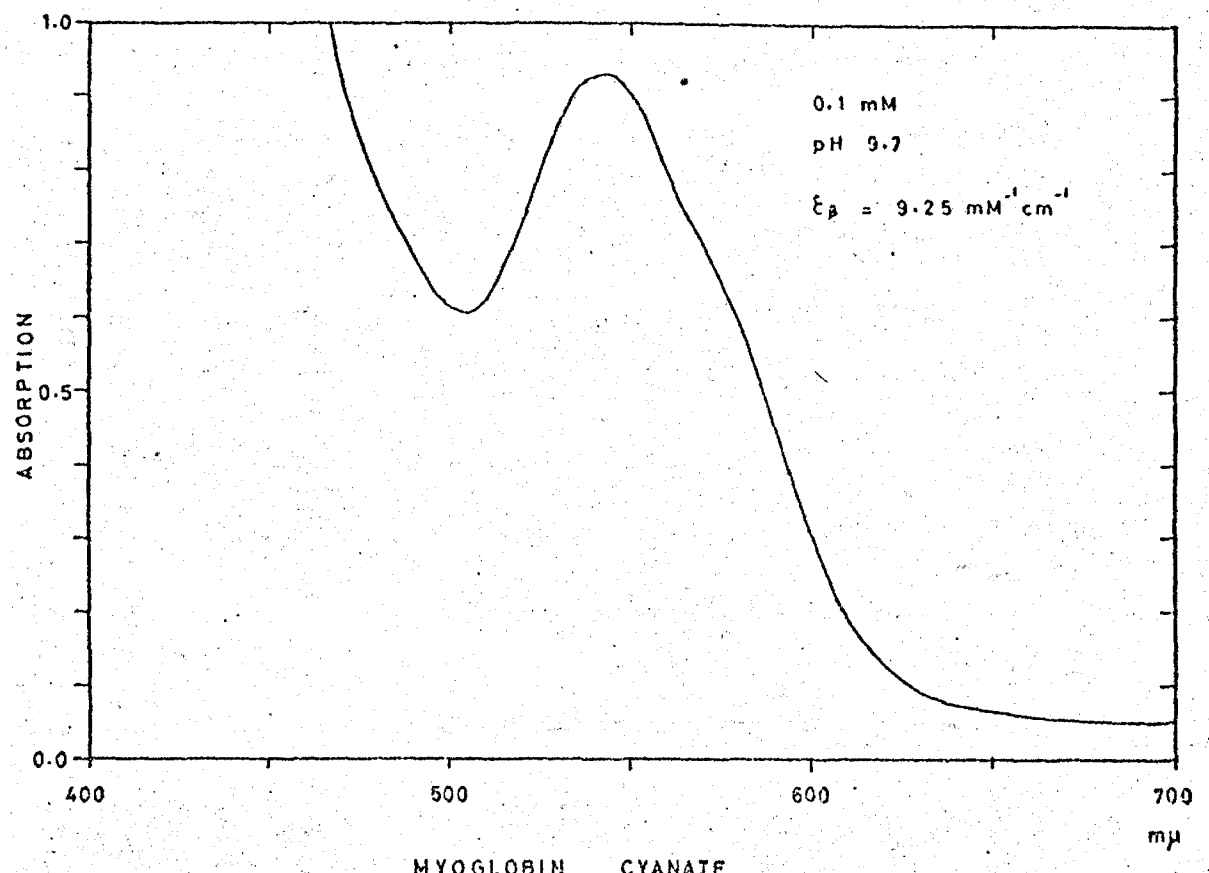

MYOGLOBIN CYANATE

FIG. 6.11

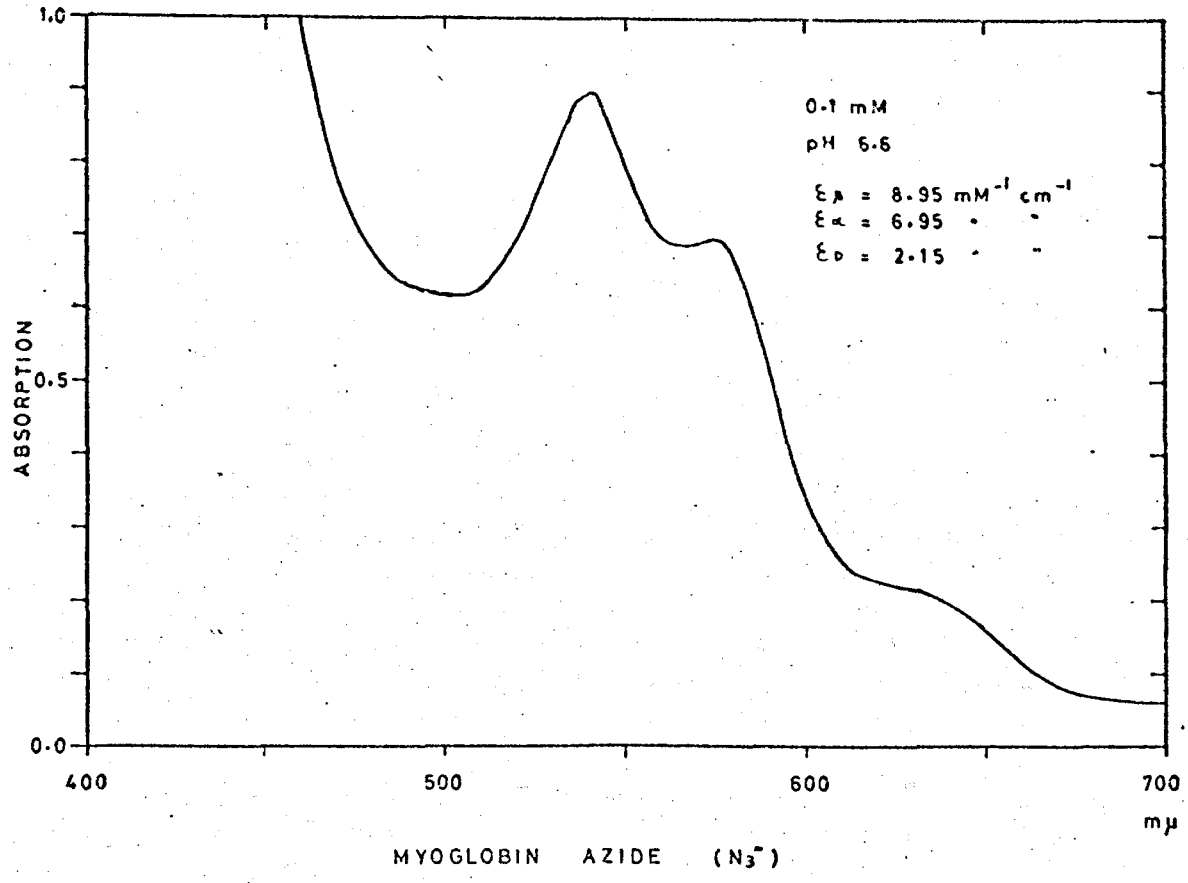

MYOGLOBIN AZIDE (N_3^-)

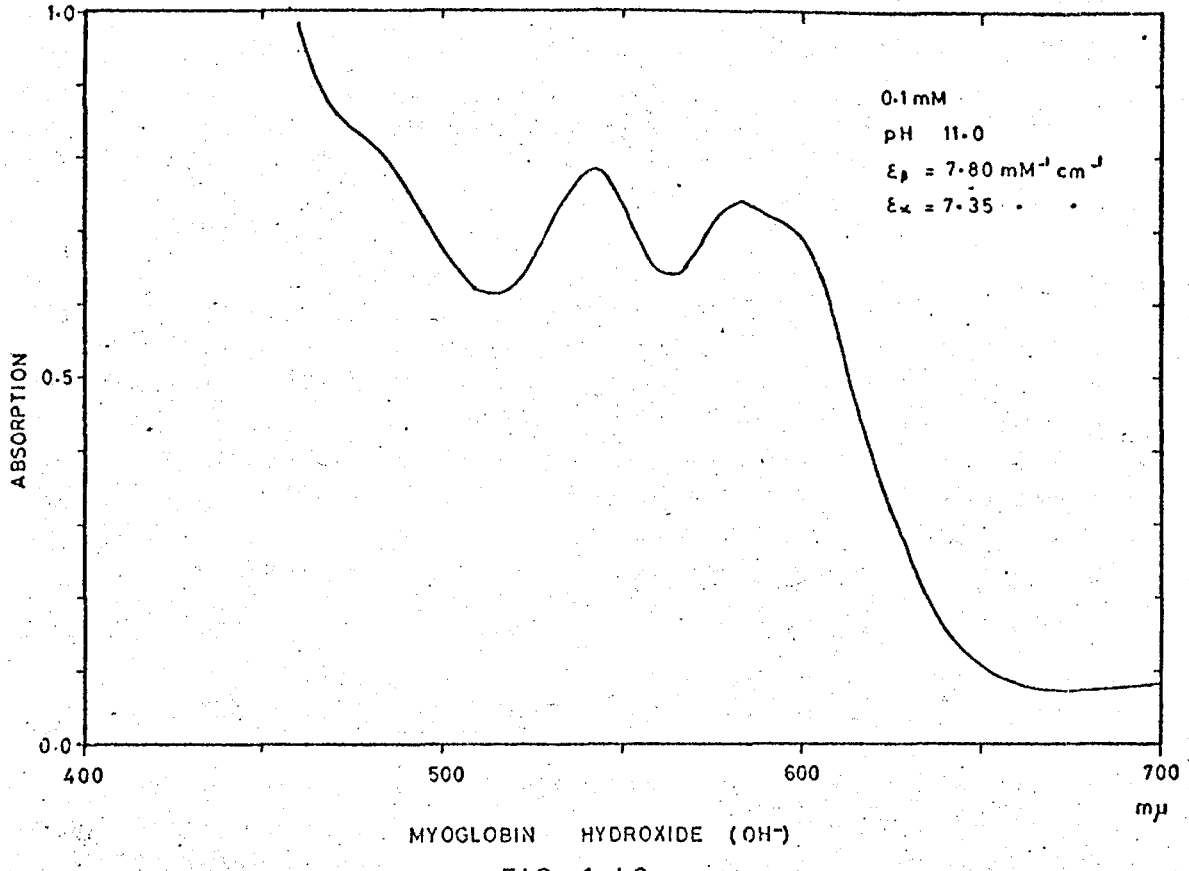

MYOGLOBIN HYDROXIDE (OH^-)

FIG. 6·12

This derivative is anomalous in its magnetic properties and needs investigating further. At the higher pH value the acetate spectra appears similar to that of the hydroxide derivative. This situation would confirm the interpretation made earlier concerning the pH dependance of the e.p.r. spectra. The formate spectra also shows a slight increase in the intensity of the α and β bands with increasing pH which is also possibly due to attachment of hydroxyl ions in place of the formate ions.

In the two solutions containing sodium chloride and sodium bromide the spectra are essentially that of the acid-met derivative, and hence from the optical spectra it seems that these haloger ions do not complex with the haem group, but they may attach themselves to the myoglobin molecule close to the haem group. This would explain the change in g-values detected, and this would not necessarily change the spin state equilibrium, and hence the optical spectra. From figure 6.13 it appears that introducing myoglobin into a solution of sodium iodide causes the molecule to denature in some way. No e.p.r. signal was observed from a paste of myoglobin in a sodium iodide solution, which suggests a change of spin state or denaturation.

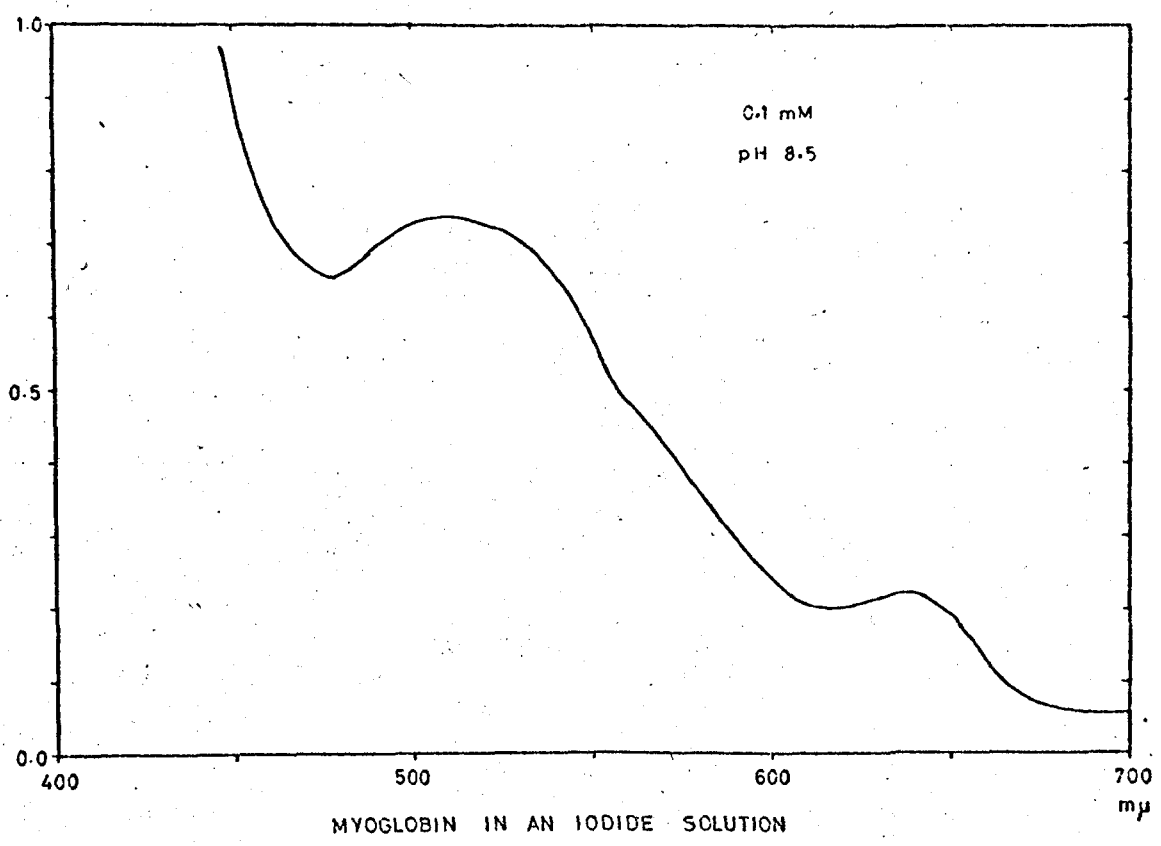

MYOGLOBIN IN AN IODIDE SOLUTION

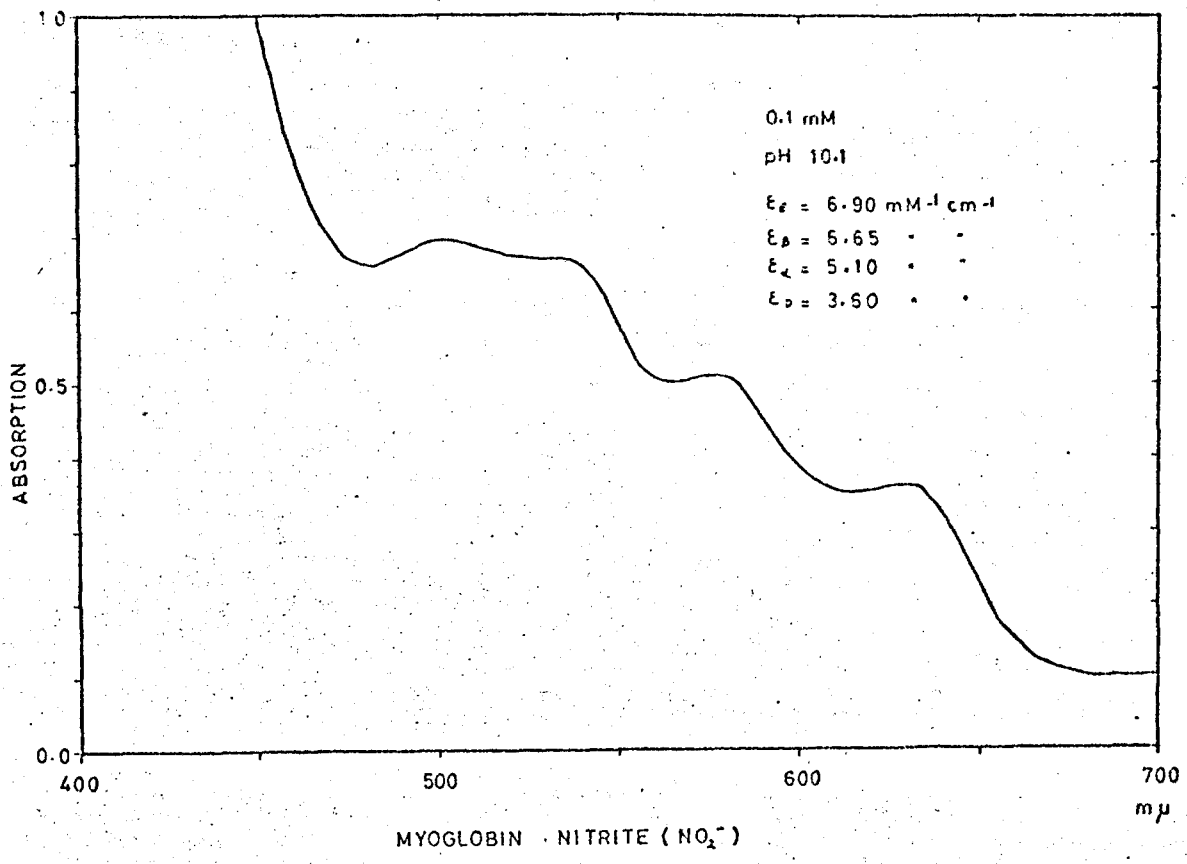

MYOGLOBIN - NITRITE (NO_2^-)

FIG. 6.13

REFERENCES

1. P. Day, D.W. Smith, R.J.P. Williams, Biochim. Biophys. Acta. pp 1563-1566, 6, No 5, May 1967.
2. E.F. Slade, Ph.D. Thesis, Keele University, 1968.
3. E.F. Slade, D.J.E. Ingram, Proc. Roy. Soc. A 313, pp 85-98,1969
4. E.F. Slade, D.J.E. Ingram, Nature, 220, p.785, November 23, 1968.
5. E.S. Kirkpatrick, K.A. Muller, R.S. Rubins, Physical Review, 135, No 1A, July 1964.
6. P. Eisenberger, P.S. Pershan, Journal of Chemical Physics, 45, No 8, pp 2832-2835, October 1966.
7. G.J. Troup, D.R. Hutton, Brit. J. App. Phys. 15, pp 1493-1499, 1964.
8. M. Gouterman, Journal of Mol. Spect., 6, pp 138-163, 1961.
9. M. Gouterman, G.H. Wagniere, Journal of Mol. Spect., 11 pp 108-127, 1963.
10. C. Weiss, H. Kobayashi, M. Gouterman, Journal of Mol. Spect., 16, pp 415-450, 1965.
11. M. Zerner, M. Gouterman, Theoret. Chim. Act, 4, pp 44-63, 1966.
12. W. Scheler, G. Schoffa, F. Jung, Biochem. 2. 329, p 232, 1957.
13. P. George, J. Beetlestone, J.S. Griffith, Haematin Enzymes, part 1. p 142 Ed. by J.E. Falk et al.
14. D.W. Smith, R.J.P. Williams, Biochem. J. 110, pp 297-301, 1968.
15. P.S. Braterman, R.C. Davies, R.J.P. Williams, Advances Chem. Phys. 7, p 359, 1964.
16. T.K. Li, B.P. Johnson, Biochemistry, 8, No.9, pp 3638-3643, September 1969.

17. G.E. Willick, G.R. Schonbaum, C.M. Kay, Biochemistry 8 No 9, pp 3729-3734, September 1969.

18. S. McCoy, W.S. Caughey, Biochemistry, 9, No.12, pp 2387-2393, June 1970.

19. R.W. Briehl, J.F. Hollo, Journal Biol. Chem. 245, pp 544-54, 1970.

20. Journal Biol. Chem. pp 555-8, 1970

21. R. Banerjee, Y. Alpert, F. Leterrier, R.J.P. Williams, Biochemistry, 8 No. 7. July 1969.

22. Y. Henry, R. Banerjee, J. Mol. Biol. 50, pp 99-110, 1970.

23. P. Day, D.W. Smith, R.J.P. Williams, Biochemistry, 6, No. 12, pp.3747-3750, December 1967.

24. W.E. Blumberg, Magnetic Resonance in Biological Systems.

CHAPTER 7.

DISCUSSION AND SUGGESTIONS FOR FUTURE WORK

7.1. Fluoride Derivative (F^-)

Angular variation measurements in three planes of single crystals of the fluoride derivative yielded principal g-values $g_x = 5.85$, $g_y = 5.98$, $g_z = 2.00$. The computed fit to the paste spectrum of this derivative determined effective g-values, $g_x = 5.85$ and $g_y = 6.03$ which are in close agreement with the 'single crystal' g-values. The increase in the value of g_y from single crystal to paste form could be accounted for by an increase in the rhombic and tetragonal components of the crystal electric field, as respresented in the spin Hamiltonian by D and E. Such a change could be effected by a conformational change in the myoglobin molecule between the two forms. Haem-proteins are highly susceptible to conformational changes when the extremities of the molecule are disturbed. In haemoglobin it is found, as was discussed in Chapter 4, that separation of the four chains resulted in a change in the haem environment. Such conformational changes have now been confirmed by Perutz[1] as the mechanism responsible for co-operative ligand binding.

No sign of splitting of the resonance line around $g = 6$ was observed in studies on single crystals of myoglobin fluoride. Splittings have been observed by other workers[2] using X-band microwave frequencies which have been ascribed to

hyperfine structure due to interaction of the 3d wave-functions with the nuclear moment of the fluorine ion. However the width of the resonance line was found to be frequency dependant. The linewidth, therefore, had increased in proportion to the ratio of the microwave frequencies, whilst the splitting which is independant of frequency had remained the same. Therefore the 50 gauss splitting had been lost in the broadened lineshape.

It is perhaps significant that a poor fit was obtained to the paste spectra of the fluoride derivative at both 35 GHz and 70 GHz. This may well be the result of nuclear interaction with the fluorine ion which had not been taken into account in the lineshape analysis. If this nuclear interaction is included in the analysis of the paste spectra it may well uncover the reason for the results in which the mean g-value increased with frequency.

7.2. Formate Derivative (HCO_2^-)

A peculiar e.p.r. spectrum was produced by a paste of myoglobin formate (axial ligand HCO_2^-) as shown in figure 6.2. This signal could be due either to the presence of two high spin derivatives existing together in thermal equilibrium, or to a large rhombic distortion causing g_x and g_y to become resolved. However, subsequent measurements made on single crystals of this derivative showed the former explanation to be the correct one. Investigations on single crystals revealed two distinct pairs of resonance lines, thus proving the existence of two

high spin derivatives within the same crystal. Two possible explanations remain concerning the presence of these two high spin derivatives. Either the haem in myoglobin has approximately equal affinities for a formate ion or a water molecule, or, alternatively, the formate ion is able to complex with the haem group in two distinct ways. Measurements on single crystals of the acid-met derivative at Q-band have determined g-values $g_x = 5.98$, $g_y = 5.92$. These results do not coincide with the g-values of either of the 'formate' lines ($g_x = 5.52$, $g_y = 5.94$, $g_x = 5.87$, $g_y = 6.06$), and therefore it is concluded that the formate ion produces two separate derivatives.

The orientation of the formate ion in the haem pocket needs to be determined by X-ray diffraction. Such X-ray information would enable one to elucidate the reasons for the rotation of principal axes between the two derivatives, and also to determine a molecular orbital model for the haem-formate complex.

7.3. Cyanate Derivative (OCN^-)

The paste form of this derivative produced at 4.2^oK a high spin derivative spectrum plus a broad line similar to that found in the cyanide derivative. The g-values associated with the high spin signal were found to be $g_x = 5.78$, $g_y = 5.92$, which are far from coincident with the acid-met g-values. Hence this signal is not an acid-met component due to incomplete conversion of myoglobin to the cyanate form. It is possible

that again two derivatives are existing together in equilibrium with one being a high spin form and the other low spin at 4.2°K.

The optical absorption spectrum is almost identical to that of the cyanide derivative at room temperature. Therefore at room temperature the low spin form is dominant, and it is possible that between 4.2°K and room temperature the high spin form is thermally excited into the low spin state, but this is purely speculative since optical measurements could not be made at lower temperatures. It would be interesting to follow the absorption spectrum as the temperature is reduced to see if such a process does occur. Such an effect could account for the anomalous behaviour of this derivative mentioned in section 5.7.

7.4. Linewidths

Analysis of the paste spectra showed that the intrinsic linewidth of the signal at Q-band frequency was between 6 and 7 milli Teslas (60 and 70 gauss). This linewidth is due to various mechanisms. There is homogeneous broadening caused by dipolar interaction between the electronic spins of neighbouring iron atoms. A maximum value of 14 milli Teslas (14 gauss) has been calculated for this effect in single crystals where the neighbouring iron atoms are between 20 Å and 35 Å apart. This separation precludes any significant contribution from exchange interaction. Also the linewidth is found to be concentration independent, which means the above mechanisms are not the dominant ones.

Inhomogeneous broadening of the intrinsic linewidth may result due to unresolved hyperfine structure caused by interaction between the 3d electrons and the neighbouring nitrogen nuclei, but Endor studies have failed to confirm this.

Measurements at 70 GHz microwave frequency show that the intrinsic linewidth has increased linearly with frequency. Such an effect is uncommon since most broadening mechanisms are frequency independant. This effect implies that there is a scatter in the g-values from different paramagnetic centres within a crystal or solution.

7.5. Zero Field Splitting

Zero field splitting values have been determined by two methods. Firstly, by measuring the variation of g-values with microwave frequency, and, secondly, from measurements of the signal intensity variation with temperature. For the acid-met derivative a value of 6.65 $\pm$ 1.5 cm^{-1} was determined by the first method, whilst a value of 5 cm^{-1} was determined by the second technique. Obviously these methods are not sufficiently sensitive, but they nevertheless are much lower than values determined by other workers[3,4]. Susceptibility measurements by Kotani produced values of 9.6 $\pm$ 0.5 for acid-met and 6.5 $\pm$ 0.5 for fluoride derivatives. Mossbauer measurements by Lang[5] produced similar figures of 10.0 cm^{-1} and 6.3 cm^{-1} for the acid-met and fluoride derivatives respectively. It appears that a comparison of samples used by different workers is needed.

In Mossbauer studies the porphyrin group is removed and Fe^{57} enriched porphyrin is substituted. It is found that crystallization of the protein after this process will not occur, and therefore it is possible that the haem environment has been disturbed.

7.6. Suggestions for Future Work.

It is clear that an alternative technique is desirable for the accurate determination of the large zero field splittings found in the different myoglobin derivatives. Consideration should be given to the possibility of observing a transition between the middle Kramer's doublet. Such a transition will be extremely weak. It will also be broad since the effective g-value, for this transition, varies between 0 and 10, the linewidth being proportional to the rate of change of g-value. However, it may be possible to find an orientation at which the linewidth and transition probability are such as to enable the observation of this signal.

It may be necessary to have the oscillatory magnetic field parallel to the static magnetic field in order to select $\Delta m = 2$ transition components.

If such a transition was observed and its intensity was measured with increasing temperature a sharp hump would occur in the variation in the same way that the Schattky anomaly arises in specific heats. A dramatic increase in intensity would occur at a temperature around $15^{\circ}K$ dependant on the value of D.

The method of analysis of the paste spectra was tedious and inefficient. A least squares fitting procedure needs to be

developed for fitting a computed absorption line to the empirical one.

Such a computation has been undertaken by other workers[6], although their calculations of the variation of transition probability with orientation are incorrect[7]. With improved computation it should be possible to determine the g-values of the two formate derivatives from the paste spectra. Such an analysis would also determine the ratio of the two derivatives in a given solution or crystal.

As single crystals of proteins are difficult to grow, and are destroyed on warming up after an experimental run, it is desirable to undertake as many measurements in any one experiment as possible. Therefore, for future studies a goniometer arrangement needs to be constructed so that angular variation measurements can be made in three planes using one myoglobin crystal only.

As already mentioned, it would be interesting to follow the optical absorption spectra of various derivatives down to low temperatures in the hope of observing a change in the spin state of iron. It should be possible to construct a glass dewar for this purpose.

REFERENCES

1. M.F. Perutz, Nature, 228, pp 726-739, November 1970.

2. H. Morimoto, M. Kotani, Biochim. Biophys. Acta, 126, pp 176-178, 1966.

3. H. Uenoyama, T. Iizuka, H. Morimoto, M. Kotani, Biochim. Biophys. Acta, 160, p 159, 1968.

4. A. Tasaki, J. Otsuka, M. Kotani, Biochim. Biophys. Acta, 140, p 284, 1967.

5. G. Lang, W. Marshall, Proc. Phys. Soc. 87, pp 3.34, 1966.

6. T.S. Johnston, H.G. Hecht, Journ. Mol. Spect., 17, pp 98-107, 1965.

7. J.R. Pilbrow, Mol. Phys. 16, No.3, pp 307-309, 1969.

APPENDIX 1

Splitting of Orbital Levels in T_i^{3+} by a Crystal Electric Field

Assume we have a T_i^{3+} ion situated in a crystal electric field with octahedral symmetry. The crystal field potential due to this crystal field was found to be (equation 3.8) :

$$V(x, y, z) = \frac{6q}{a} + \frac{35q}{4a^5}\left[(x^4 + y^4 + z^4) - \frac{3}{5} r^4\right] + \ldots \qquad 3.8$$

In order to determine the splitting of the orbital ground state of the $3d^1$ ion we need to calculate the matrix elements of the Hamiltonian $= e|V|$. The wavefunctions for the degenerate states within the ^2D ground level are the one-electron orbitals given in equation 3.10. Only matrix elements between wavefunctions with the same L_z quantum number will be finite.

The first term in the potential operator merely raises the energy of each orbital level equally and therefore may be ignored. However consider the second term in which, for the sake of simplicity, $x^4 + y^4$ has been ignored. To calculate the diagonal matrix elements all that is required is to write the operator as $Ar^4 \left|\frac{5}{3}\cos^2\theta - 1\right|$, and evaluate the integrals :

$$\langle 20|v|20\rangle = A\int_0^\infty |f(r)|^2 r^4 r^2 \, dr$$

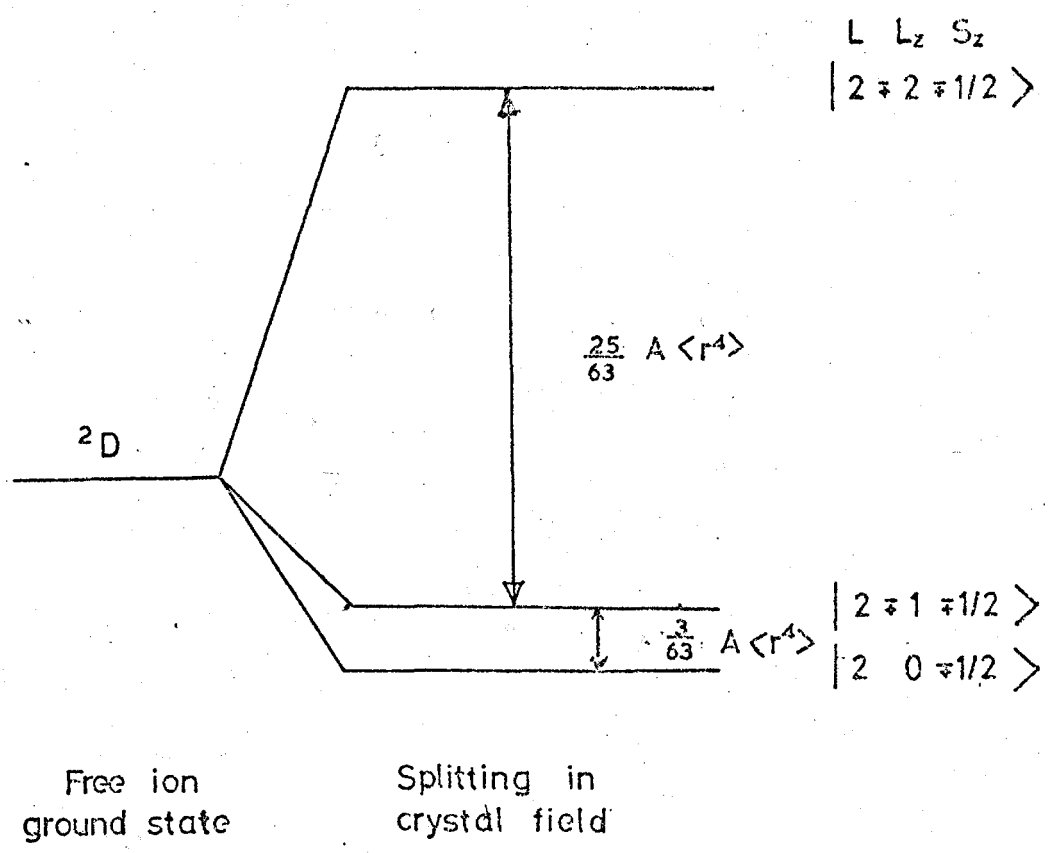

FIG. A1 SPLITTING OF ORBITAL GROUND STATE OF AN $3d^1$ ION

$$\int_0^{\pi} \frac{10}{16} (3\cos^2\theta - 1)^2 \left(\frac{5}{3}\cos^4\theta - 1\right) \sin\theta \, d\theta$$

$$\int_0^{2\pi} \frac{1}{2\pi} \, d\phi$$

putting $\langle r^4 \rangle = \int_0^{\infty} |f(r)|^2 r^4 . r^2 \, dr$

and leaving as an undetermined coefficient we obtain

$$\langle 20 \mid v \mid 20 \rangle = -\frac{10}{21} A \langle r^4 \rangle$$

similarly it can be shown that

$$\langle 2 \pm 1 \mid v \mid 2 \pm 1 \rangle = -\frac{38}{63} A \langle r^4 \rangle$$

$$\langle 2 \pm 2 \mid v \mid 2 \pm 2 \rangle = -\frac{58}{63} A \langle r^4 \rangle$$

where $A = \frac{21q}{4a^5}$

The splitting of these orbital levels are shown in Figure A.1.

APPENDIX 2.

Least Squares Fit Upon g-tensor Components.

In the ab plane the effective g-value is equated to the G tensor components by equation 5.5.

$$g^2 = G_{aa} \cos^2 \theta + G_{bb} \sin^2 \theta + 2 G_{ab} \cos \theta \sin \theta \qquad (1)$$

For each data point g (θ) we can obtain a set of residuals

$$r_i = G_{aa} \cos^2 \theta + G_{bb} \sin^2 \theta + 2G_{ab} \sin \theta \cos \theta - g^2 \qquad (2)$$

We require that Σr_i^2 be a minimum

$$\begin{aligned}\Sigma r_i^2 = \Sigma \; (&G_{aa}^2 \cos^4 \theta + G_{bb}^2 \sin^4 \theta + 4G_{ab}^2 \sin^2 \theta \cos^2 \theta + g^4 \\ &+ 2G_{aa} G_{bb} \cos^2 \theta \sin^2 \theta + 4G_{ab} G_{bb} \sin^3 \theta \cos \theta \\ &+ 4G_{aa} G_{ab} \cos^3 \theta \sin \theta - 2G_{aa} g^2 \cos^2 \theta - 2G_{bb} \sin^2 \theta g^2 \\ &- 4G_{ab} \sin \theta \cos \theta g^2)\end{aligned}$$

Σr_i^2 has a minimum value when all its partial derivatives with respect to G_{aa}, G_{bb}, G_{ab} are simultaneously zero.
Taking these three partial derivatives we arrive at three simultaneous equations :

$$\begin{aligned} AG_{aa} + BG_{bb} + 2CG_{ab} - D &= 0 \\ BG_{aa} + EG_{bb} + 2FG_{ab} - H &= 0 \\ CG_{aa} + FG_{bb} + 2BG_{ab} - K &= 0 \end{aligned} \qquad (3)$$

where $A = \Sigma \cos^4 \theta$ $\quad E = \Sigma \sin^4 \theta$

$B = \Sigma \cos^2 \theta \sin^2 \theta$ $\quad F = \Sigma \sin^3 \theta \cos \theta$

$C = \Sigma \cos^3 \theta \sin \theta$ $\quad H = \Sigma g^2 \sin^2 \theta$

$D = \Sigma g^2 \cos^2 \theta$ $\quad K = \Sigma g^2 \sin \theta \cos \theta$

A direct solution of the simultaneous equations (4) can be found for the tensor components G_{aa}, G_{bb}, G_{ab}. A similar analysis can be made of the angular variation of g-values in the bc* and c*a crystal planes, and hence all nine components of the tensor G_{ij} can be determined. A check on the values of the diagonal components is provided from analysis of the three planes since each diagonal element value is determined from measurements in two planes.

A computer programme for performing this least squares fit upon the g-values was provided by P. Weightman.

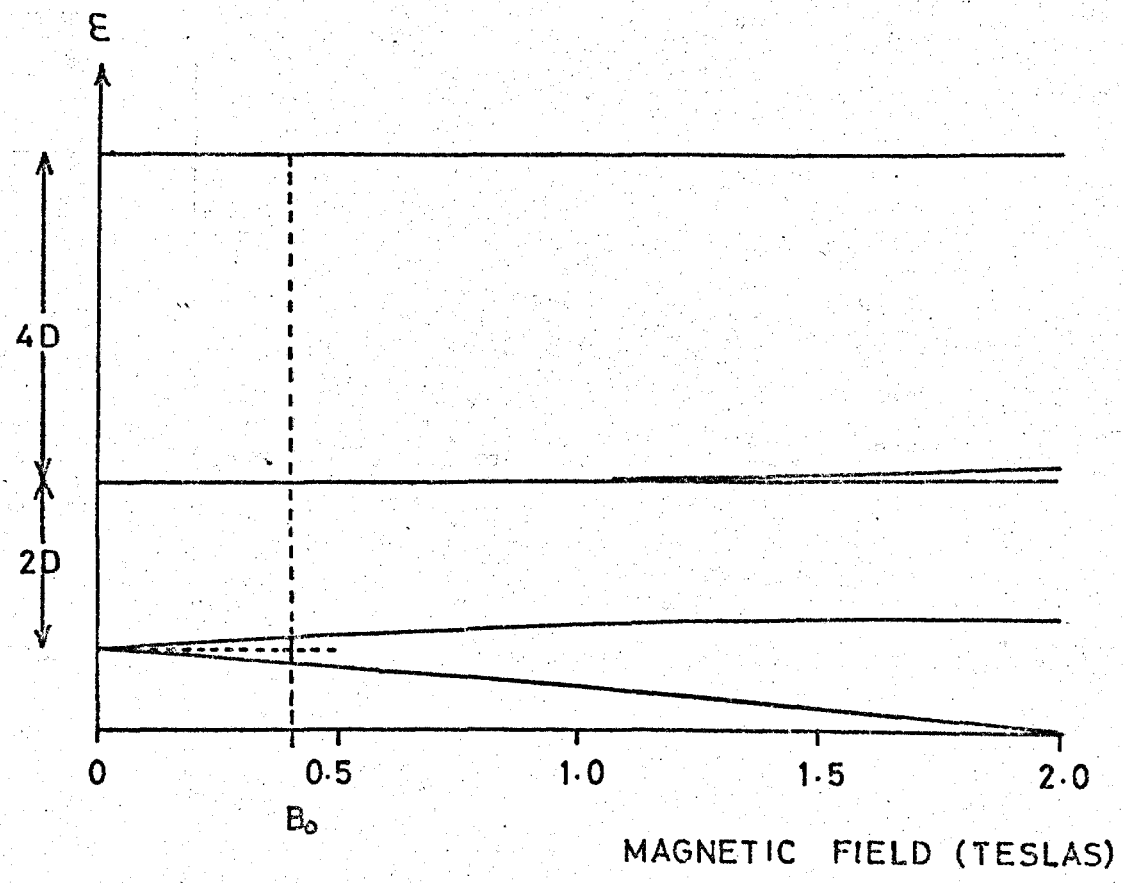

FIG. A2 MYOGLOBIN ENERGY LEVELS WHEN B IS ⊥ TO Z

APPENDIX 3.

Intensity Variation of g = 6 signal with temperature.

From equation 2.52 the rate of absorption of microwave energy is seen to be

$$\frac{dE}{dt} = n\ h\nu\ W \qquad (1)$$

where W is the transition probability as given by equation 2.34. The population distribution between the Zeeman levels of myoglobin, shown in figure A2, is according to the Boltzmann function

$$n_i = \frac{N \exp(-Ei/kT)}{\Sigma j \exp(-Ej/kT)} \qquad (2)$$

where n_i is the population of the ith level and N is the total number of systems present

The intensity of the absorption due to a transition between the lowest Kramers doublets is

$$P_{MB} = \left(\frac{dE}{dt}\right)_{MB} (n_1 - n_2)\ h\nu_{21}\ W_{21} \qquad (3)$$

Therefore the power absorbed, due to this g = 6 transition, at resonance will be, from equations (2) and (3)

$$P_{MB} = \frac{N_{MB}\ (1 - \exp(-h\nu/kT))\ h\nu_{21}\ W_{21}}{A} \qquad (4)$$

where $A = 1 + \exp(-h\nu/kT) + 2\exp(-(2D + \frac{1}{2}h\nu)/kT) + 2\exp(-(6D + \frac{1}{2}h\nu)/kT)$

Carbon is an $S = \frac{1}{2}$ system and hence the power absorbed at resonance due to a transition between the two Zeeman levels is

$$P_c = \frac{dE}{dt}_c = \frac{N_c\,(1 - \exp(-h\nu/kT))}{1 + \exp(-h\nu/kT)}\; h\nu_{21}\, W \qquad (5)$$

Therefore if myoglobin and carbon signals are compared using the same microwave frequency the ratios of the intensities will be

$$\frac{P_{MB}}{P_c} = \frac{N_{MB}}{N_c}\;\frac{(1 + \exp(-h\nu/kT))}{A}\;\frac{W_{MB}}{W_c} \qquad (6)$$

If we put $\dfrac{N_{MB}\,W_{MB}}{N_c\,W_c} = a$

Then $$\frac{P_{MB}}{P_c} = a\,\frac{(1 + \exp(-h\nu/kT))}{A} \qquad (7)$$

This expression is plotted as a function of temperature for a range of values of the zero field splitting parameter D in figure 5.14. These results are calculated for a = 1.

APPENDIX 4

Synthesis of Paste Spectra

Assume that the zero field splitting is sufficiently large so the system may be described by a simple Hamiltonian

$$= \beta \bar{B}.g.\bar{S} \qquad (1)$$

which can be written as

$$= g(\theta, \phi)\ \beta\ B\ S_z \qquad (2)$$

where $g(\theta, \phi) = (g_z^2 \cos^2\theta + g_x^2 \sin^2\theta \cos^2\phi + g_y^2 \sin^2\theta \sin^2\phi)^{\frac{1}{2}}$ (3)

where θ and ϕ are the polar angles of the magnetic field with respect to the magnetic axes and g_x, g_y, g_z are the effective g-values of the transition.

The energy of a transition is given by

$$h\nu = g(\theta, \phi)\ \beta\ B \qquad (4)$$

For a paste the molecules will be randomly orientated and the fraction of the molecules with their magnetic axes in the angular range

$$\phi^1 \rightarrow \phi^1 + \Delta\phi$$

and $$\theta^1 \rightarrow \theta^1 + \Delta\theta$$

is proportional to $\Delta\phi \sin\theta\ \Delta\theta$ which becomes $d\phi \sin\theta d\theta$ in the limit as $\Delta\theta, \Delta\phi \rightarrow o$.

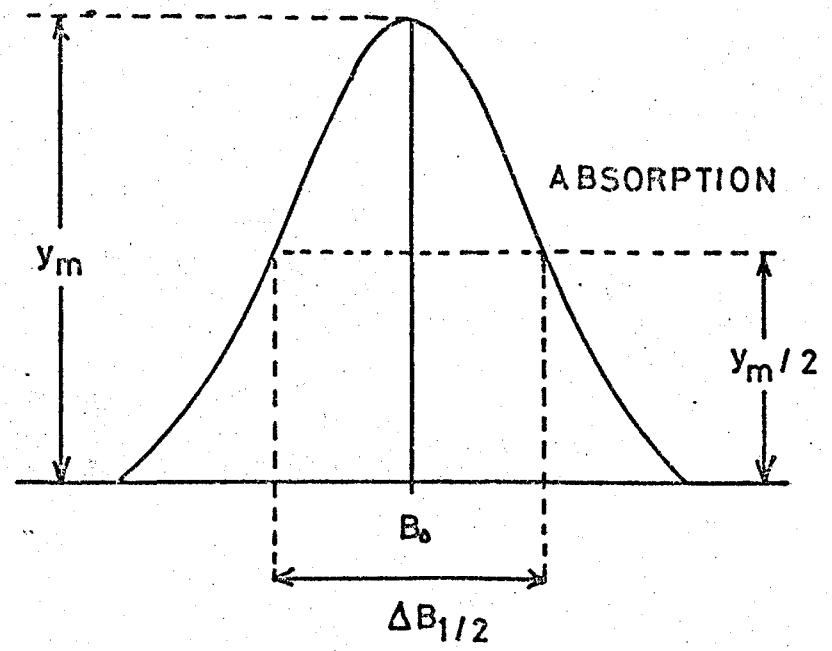

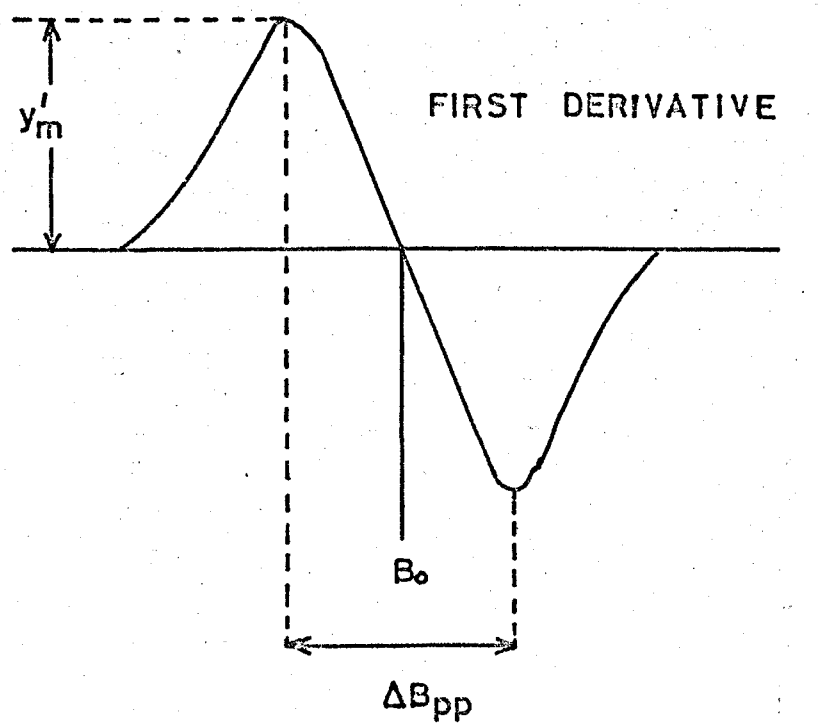

FIG. A3 LORENTZIAN LINESHAPE

At a magnetic field B^1 a transition occurs when

$$B^1 = \frac{h\nu}{\beta g^1(\theta,\phi)} \qquad (5)$$

The intensity of the absorption at field B^1 is given by the sum over all angles of

$$F(B^1) = \sum_{\theta}\sum_{\phi} \frac{h\nu}{\beta g^1(\theta\ \phi)} \Delta\phi \sin\theta\ \Delta\theta \qquad (6)$$

However the energy levels have a finite width so that transitions occur over a range of field strengths around B^1. We assume that the lineshape function is Lorentzian so the intensity of the intrinsic absorption line will be described by

$$Y(B) = \frac{y_m}{1 + |\ (B - B_o)/\tfrac{1}{2}\ \Delta B_{\frac{1}{2}}|^2} \qquad (7)$$

where B_o is the field at the centre of the resonance line and y_m and $\Delta B_{\frac{1}{2}}$ are as shown in figure A3. As the spectrometer detects the first derivative of the absorption it is neccesary to differentiate (7) with respect to B.

$$Y^1(B) = \frac{16\ y_m^1\ |(B-B_o)/\tfrac{1}{2}\ \Delta B_{pp}\ |}{|3 + (B-B_o/\tfrac{1}{2}\ \Delta B_{pp})^2|}\ 2 \qquad (8)$$

where B_o is a fn of θ and ϕ.

Bleaney[1] and Kneubuehl and Natterer[2] have indicated that the lineshape function should include a term for the variation of

transition probability $P(\theta,\phi)$ with respect to the orientation of the static and oscillatory magnetic fields. The expression $P(\theta, \phi)$ has been explicitly given for the case of complete assymmetry by Pilbrow[3] as

$$P(\theta, \phi) = g_x^2 g_y^2 \sin^2\theta + g_y^2 g_z^2 (\sin^2\phi + \cos^2\theta \cos^2\phi) + g_z^2 g_x^2 (\cos^2\phi + \cos^2\theta \sin^2\phi) \quad (9)$$

The intensity of the absorption due to a single transition in one paramagnetic ion is

$$F(B) = P(\theta, \phi)\, Y^1(B) \quad (10)$$

Hence for a collection of ions, with random orientations, the intensity due to a single transition at a field B is given by

$$F(B) = \int_0^{\pi} \int_0^{\pi/2} P(\theta, \phi)\ Y^1(B)\, d\phi \sin\theta\, d\theta \quad (11)$$

This function cannot be integrated analytically but may be evaluated numerically. A computer programme for the synthesis of paste spectra was written by B.J. Munday for use on the Keele University I.C.L. 4130 computer.

1. B. Bleaney, Proc. Phys. Soc. p621, 75, 1960.

2. F.K. Knuebuehl, B. Natterer, Helv. Phys. Acta. p 710, 34, 1961.

3. J.R. Pilbrow, Molecular Phys. p.307, Vol. 16, No.3. 1969.